Stress Relaxation by Addition-fragmentation Chain Transfer in Glassy Polymer Networks

A Thesis Submitted to the

Faculty of

The University of Colorado

by

Hee Young Park

B.S., Pusan National University, 2000

M.S., Pusan National University, 2002

In Partial Fulfillment of the

Requirements for the Degree

of

Doctor of Philosophy

May, 2011

This thesis entitled:
Stress Relaxation by Addition-fragmentation Chain Transfer in Glassy Polymer Networks
written by Hee Young Park
has been approved for the Department of Chemical and Biological Engineering

Christopher N. Bowman

Jeffrey W. Stansbury

*Date*_____

The final copy of this thesis has been examined by the signatories, and we
Find that both the content and the form meet acceptable presentation standards
Of scholarly work in the above mentioned discipline.

Abstracts

Park, Hee Young (Ph.D., Chemical and Biological Engineering)

Stress Relaxation by Addition-fragmentation Chain Transfer in Glassy Polymer Networks Thesis directed by Patten Professor Christopher N. Bowman

Since polymer materials have come to dominate our life by replacing many other, more traditional materials, any endeavors to improve their performance have heightened importance. Here, we have strived to develop methodologies to reduce and understanding of the processes relevant to the origins of polymerization-induced shrinkage stress. In this thesis, addition-fragmentation chain transfer (AFCT) was utilized to reduce the shrinkage stress through network relaxation and adaptation by radical-mediated bond rearrangement that occurs throughout the polymerization. In previous studies, the presence of the allyl sulfide functional group was shown to reduce the final stress in thiol-ene resins via AFCT. Unfortunately, thiol-ene polymerizations often yield elastomeric materials with low glass transition temperatures (T_gs) that are ill-suited for structural applications. To extend the utility of AFCT into structural applications, AFCT-capable monomers have been incorporated into many systems to achieve both low stress and excellent mechanical properties by designing chemical structure of monomers and by exploration of the polymerization and relaxation mechanisms. In particular, incorporation of AFCT-capable monomers into conventional dental resins was investigated to generate novel low stress dental composites. This thesis has demonstrated the development and implementation of thiol-ene and thiol-yne based monomers that are capable of undergoing AFCT to reduce polymerization stress further in a glassy polymer and its application for the conventional glassy methacrylate-based

dental resins. Additionally, novel monomers that undergo AFCT were developed and implemented in methacrylate-based resins that undergo propagation exclusively through chain growth mechanisms. Since direct incorporation of the allyl sulfide in methacrylate-based systems was not effective for stress relaxation with large amounts of methacrylate, trithiocarbonates were used in place of allyl sulfides in dimethacrylate monomers, where the trithiocarbonate enables reversible reactions with the methacrylic radicals. The trithiocarbonate-based dimethacrylate demonstrated 65 % stress reduction compared with the standard BisGMA-TEGDMA composite while demonstrating fracture toughness which was slightly higher than the control BisGMA-TEGDMA composite indicating that TTCDMA and related monomers represent excellent candidates for reactive diluents in BisGMA-based dental materials. The improved understanding of the trithiocarbonate functional group will broadly expand its utility for a wide range of applications such as coatings, microelectronics, photoresists, and dental materials.

Table of Contents

List of Tables

Tables

List of Figures

Chapter 1

Introduction

1.1 Overview

Polymerization of multifunctional monomers yields crosslinked polymeric networks (i.e., thermosets) that are extensively utilized in applications ranging from coatings and adhesives to microelectronics[1-3]. Especially, polymer-based dental restorative composites have largely replaced more traditional amalgams since not only the clinical use of mercury is avoided but also they possess several advantageous properties such as rapid reactions, high strength, and durability. Nevertheless, these polymerizations are typically accompanied by significant amounts of volumetric shrinkage[4], and the associated stress that arises from the combination of shrinkage and the formation of a crosslinked polymer. Polymerization shrinkage results from the decrease in molecular spacing between monomers as the van der Waals interactions present in the monomer are replaced with covalent bonds that bring the monomer units together more closely. Polymerization shrinkage stress is a deleterious phenomenon that plagues numerous polymer material applications[1-3] and results in warping, microcracks, and material failure.

Mitigation of this polymerization-induced shrinkage and/or the associated stress has been the focus of extensive research efforts over the past several decades. Traditional polymer resins generally undergo a chain-growth polymerization mechanism, typically gelling at low conversion before vitrifying at higher conversions and thus developing shrinkage stress early on and

throughout the polymerization[5]. To overcome this phenomena, several polymerization mechanism including ring-opening polymerization[6-7], thiol-ene polymerizations [8], and polymerization-induced phase separation [9] have been reported.

Recently, a novel mechanism for stress relaxation in a polymer network has been shown via photo-induced bond rearrangement of a polymeric network[10,11-12], i.e., the formation of a "covalent adaptable network" (CAN). This mechanism has been utilized in thiol-ene systems and led to significant stress relaxation. However, the thiol-ene has limited mechanical properties not appropriate for many structural applications of thermosets [13].

Thus, counteracting this limitation for structural materials by designing monomers and exploring novel polymerization mechanisms has been a focus of great interest. Specifically, demonstration of new materials which possesses low stress and good mechanical properties by incorporation of addition-fragmentation chain transfer is industrially relevant and also has the potential for leading to fundamental information regarding polymer network formation and structure.

1. 2 Background

1.2.1 Stress Relaxation by Addition-fragmentation Chain Transfer

The mechanism for stress relaxation in a polymer network via radical-induced bond rearrangement of a polymeric network was first demonstrated as photoinduced plasticity in 2005 [11-12]. The mechanism for this stress relaxation utilizes radical-mediated addition-fragmentation chain transfer events through allyl sulfide functionalities incorporated within the crosslinking strands of the polymer network, allowing crosslinking strand rearrangement in the presence of radicals (Figure 1.1(A)). The addition-fragmentation rearrangement reaction typically preserves the concentration of both the allyl sulfide and radical reactants, which subsequently participate in further chain transfer events. This cascading rearrangement of the network connectivity results in a global reduction in stress without any concomitant degradation of mechanical properties. When incorporated in thiol-ene networks, the allyl sulfide addition-fragmentation was shown to reduce the shrinkage stress relative to an analogous network incapable of addition-fragmentation chain transfer (AFCT) (Figure 1.1 (B)). However, the low, sub-ambient T_g of that material (~ –20°C) precludes it from use in nearly all structural applications.

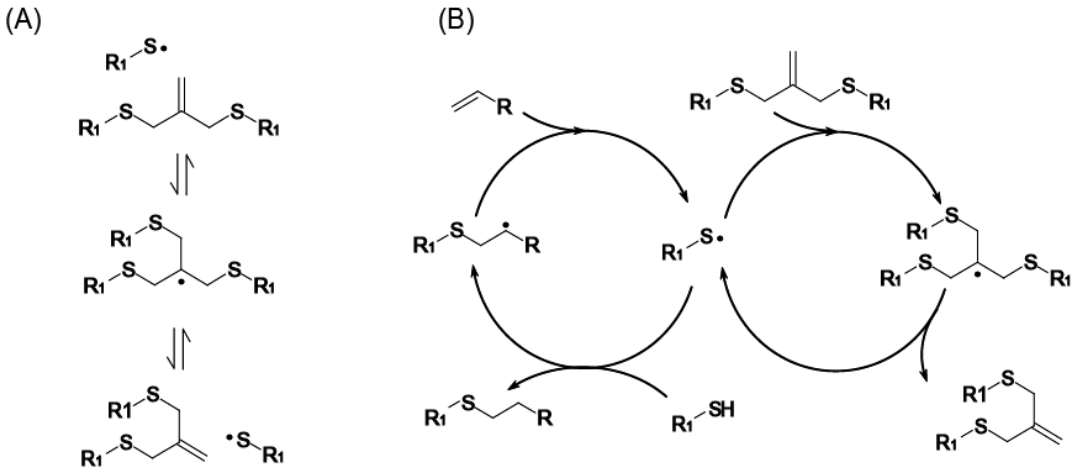

Figure 1.1. (A) Schematic of allyl sulfide addition-fragmentation chain transfer mechanism that promotes network relaxation and polymerization shrinkage stress. (B) The thiol-ene polymerization mechanism with addition-fragmentation chain transfer of allyl sulfide

1.2.2 Polymer-based Dental Composites

Dental restorative materials are specially fabricated materials which are designed for restoration of tooth structure loss usually resulting from dental caries. Amalgam, which is a metallic filling material composed from a mixture of mercury and alloy, has been one of the most commonly used dental restorative materials since the early 19th century because of its cost effectiveness, excellent strength and longevity. Polymer-based dental composites possess several advantageous properties, such as rapid reactions, high strength, and durability [2]. These composites are considered a favorable alternative to the more traditional amalgams as the clinical use of mercury is avoided. Moreover, the matching of aesthetically pleasing natural tooth colors is readily accomplished using polymer composite materials.

Nevertheless, the shrinkage stress that accompanies the polymerization of these composite materials is a primary concern for dental clinicians since it can initiate microcracking of restorative materials, leading to bacterial microleakage and secondary caries [14-15]. While dimethacrylate-based composites are the most common material used as dental restoratives, they are also accompanied by substantial polymerization-induced shrinkage stress [16-17].

Dental polymer-based composites are most commonly composed of 10 to 30 wt% of BisGMA or its analog monomers, 70 to 90 wt% of filler material such as silica, and initiating system like photoinitiator. TEGDMA are also commonly added to achieve flowability to make manipulation easier. The properties of an ideal dental restorative material are low thermal conductivity and expansion, resistance to forces and chemical erosion, and biocompatibility. Development of a low stress polymer that simultaneously achieves other properties of an ideal dental restorative material is highly in demand. In particular, the demonstration of stress reduction in multimethacrylate or multiacrylate systems will be most relevant.

1.3 Experimental Section

1.3.1 Synthesis of Monomers

Throughout the project, all allyl sulfide-containing monomers are synthesized from 3-mercapto-2-(mercaptomethyl)-1-propene and a halide-bearing polymerizable functional group to form the desired monomer structure. Additionally, propyl sulfide-containing monomers, which do not undergo addition-fragmentation chain transfer, are synthesized from 1,3-dimercapto-2-

methylpropane to isolate the effect of AFCT for stress relaxation. Both dithiols are synthesized by a procedure found in the literature [18-19]. Synthetic schemes of each monomer are shown in Figure 1.2. Detailed procedures are presented in later chapters.

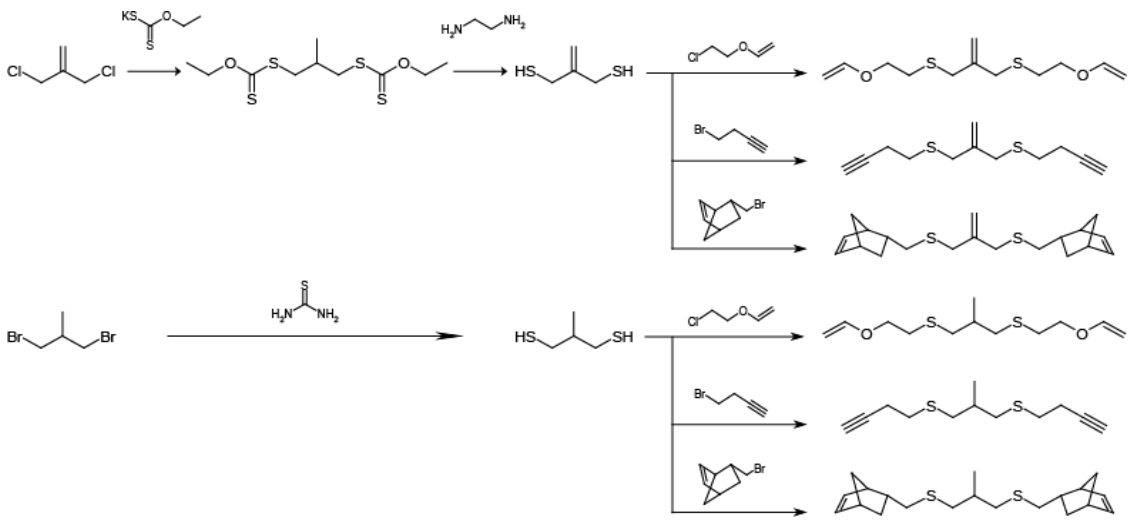

Figure 1.2. Synthetic scheme for the allyl (top) and propyl (bottom) sulfide-containing monomers.

Trithio carbonate-containing dimethacrylate was synthesized from S,S'-bis(α,α'-dimethyl-α''-acetyl chloride)-trithiocarbonate and 2-hydroxyethyl methacrylate (HEMA) following the procedure in the literature [20]. Detailed synthetic procedure will be described in later chapters.

1.3.2 Simultaneous Shrinkage Stress and Functional Group Conversion Measurements

Simultaneous shrinkage stress and functional group conversion measurements were performed during polymerization using a cantilever-type tensometer (Paffenbarger Research Center, American Dental Association Health Foundation) coupled with a Nicolet 670 FTIR spectrometer

via near-infrared transmitting optical fiber patch cables; a detailed description of this measurement technique is presented in the literature [8, 21]. A tensometer utilizes the cantilever beam deflection theory to evaluate how much the beam deflects under the generated stress. Since the cantilever beam deflection theory is valid only in the linear elastic region of the beam, different compliance beams were necessary to measure very different shrinkage stress levels due to the limitation of each beam. Since the obtained stress value decreases in low compliance configurations as the beam accommodates deformation of the polymer specimen during stress measurement [21], the stress values obtained with lower compliance configurations need to be considered higher. Therefore, if the stresses are obtained in different compliances, the stress difference between systems is even larger than what it is reported. Care is taken to report compliance configurations for all stress measurements.

The infrared spectrometer was equipped with an indium gallium arsenide (InGaAs) detector and collected spectra at a rate of approximately 2 scans/sec and a resolution of 2 cm^{-1}. Samples 6 mm in diameter and 1 or 2 mm thick were irradiated *in situ* by a mercury arc lamp (Acticure, EXFO) equipped with a bandpass filter to isolate the desired spectral line. The evolution of the functional group concentrations was determined by monitoring the corresponding infrared absorption peaks.

1.4 References

(1) Drury, C. J.; Mutsaers, C. M. J.; Hart, C. M.; Matters, M.; de Leeuw, D. M. *Applied Physics Letters* **1998,** *73,* 108-110.

(2) Stansbury, J. W.; Bowman, C. N.; Newman, S. M. *Physics Today* **2008,** *61,* 82-83.

(3) Yoffe, A. D. *Advances in Physics* **2001,** *50,* 1-208.

(4) Sanda, F.; Takata, T.; Endo, T. *Macromolecules* **1994,** *27,* 1099-1111.

(5) Bowman, C. N.; Kloxin, C. J. *Aiche Journal* **2008,** *54,* 2775-2795.

(6) Ge, J. H.; Trujillo-Lemon, M.; Stansbury, J. W. *Macromolecules* **2006,** *39,* 8968-8976.

(7) Stansbury, J. W. *Polymers of Biological and Biomedical Significance* **1994,** *540,* 171-183.

(8) Lu, H.; Carioscia, J. A.; Stansbury, J. W.; Bowman, C. N. *Dent Mater* **2005,** *21,* 1129-1136.

(9) Lee, T. Y.; Cramer, N. B.; Hoyle, C. E.; Stansbury, J. W.; Bowman, C. N. *J Polym Sci Pol Chem* **2009,** *47,* 2509-2517.

(10) Kloxin, C. J.; Scott, T. F.; Adzima, B. J.; Bowman, C. N. *Macromolecules* **2010,** *43,* 2643-2653.

(11) Scott, T. F.; Draughon, R. B.; Bowman, C. N. *Advanced Materials* **2006,** *18,* 2128-+.

(12) Scott, T. F.; Schneider, A. D.; Cook, W. D.; Bowman, C. N. *Science* **2005,** *308,* 1615-1617.

(13) Kloxin, C. J.; Scott, T. F.; Bowman, C. N. *Macromolecules* **2009,** *42,* 2551-2556.

(14) Kleverlaan, C. J.; Feilzer, A. J. *Dent Mater* **2005,** *21,* 1150-1157.

(15) Burke, F. J. T.; Cheung, S. W.; Mjor, I. A.; Wilson, N. H. F. *Quintessence International* **1999,** *30,* 234-242.

(16) Labella, R.; Lambrechts, P.; Van Meerbeek, B.; Vanherle, G. *Dent Mater* **1999,** *15,* 128-137.

(17) Walls, A. W. G.; Mccabe, J. F.; Murray, J. J. *Journal of Dentistry* **1988,** *16,* 177-181.

(18) Evans, R. A.; Rizzardo, E. *Macromolecules* **2000,** *33,* 6722-6731.

(19) Evans, R. A.; Rizzardo, E. *J Polym Sci Pol Chem* **2001,** *39*, 202-215.

(20) Pavlovic, D.; Linhardt, J. G.; Kunzler, J. F.; Shipp, D. A. *J Polym Sci Pol Chem* **2008,** *46,* 7033-7048.

(21) Lu, H.; Stansbury, J. W.; Dickens, S. H.; Eichmiller, F. C.; Bowman, C. N. *Journal of Materials Science-Materials in Medicine* **2004,** *15*, 1097-1103.

Chapter 2

Objectives

Previous approaches used to combat polymerization stress have focused on minimizing the volume change, using materials that exhibit low polymerization shrinkage, such as ring-opening polymerizations or polymerization induced phase separation. Additionally, strategies that delayed the gel-point conversion, such as thiol-ene and thiol-yne polymerizations, have been used to enable the material to shrink in the later stages of the reaction without leading to any significant stress accumulation. Here, prior to the gel-point, a material is capable of dissipating shrinkage via the viscous flow of the monomer/oligomer species; however, after gelation, molecular rearrangement is reduced and stress accumulates. To address this issue, addition-fragmentation chain transfer (AFCT) was utilized that enables the radical-mediated repetitive breaking and reforming of polymer network strands throughout the polymerization. The initial demonstrations of reduced polymerization shrinkage stress using AFCT employed the allyl sulfide functional group in thiol-ene materials. Although AFCT was capable of dramatically reducing the polymerization shrinkage-induced stress in rubbery, elastomeric networks, demonstrating a similar effectiveness in glassy materials would vastly broaden its utility. Additionally, the general understanding of the addition-fragmentation chain transfer mechanism in polymer networks is necessary to expand its application.

The overall objective of this project is the investigation of stress relaxation by addition-fragmentation chain transfer in polymer networks which exhibit super ambient glass transition

temperatures. Specific aims to meet this objective are as follows:

Specific Aim #1: Incorporate moieties capable of addition-fragmentation chain transfer into conventional glassy methacrylate-based dental resins to reduce polymerization shrinkage stress;

Specific Aim #2: Develop and implement thiol-ene and thiol-yne based monomers that are capable of undergoing addition-fragmentation chain transfer to reduce polymerization stress further in a glassy polymer; and

Specific Aim #3: Develop and implement monomers that undergo addition-fragmentation chain transfer in resins that undergo propagation exclusively through chain growth mechanisms.

By forming polymeric materials that simultaneously are glassy and exhibit low polymerization shrinkage induced stress, we aim to achieve a better understanding of the molecular rearrangement process and its effect on stress, shape, and other material properties. Therefore, it will be possible to implement these molecularly controlled polymer networks in a number of applications, including dental materials, coatings, photoresists, and optical films.

Chapter 3

Covalent Adaptable Networks as Dental Restorative Resins: Stress relaxation by addition-fragmentation chain transfer in allyl sulfide containing resins

The aim of this chapter is to demonstrate significant polymerization shrinkage stress reduction in model resins through incorporation of addition-fragmentation chain-transfer moieties that promote network stress accommodation by molecular rearrangement. Monomers containing allyl sulfide linkages are incorporated to affect the shrinkage stress that arises during photopolymerization of model resins that contain an initiator and dimethacrylates. Radical-mediated allyl sulfide addition-fragmentation is enabled during polymerization. We hypothesize that allyl sulfide incorporation into methacrylate polymerizations promotes stress relaxation by enabling network adaptation. A 1:2 mixture of tetrathiol and allyl sulfide-containing divinyl ethers is formulated with glass-forming dimethacrylates and compared to controls where the allyl sulfide is replaced with a propyl sulfide that is incapable of undergoing addition-fragmentation. Simultaneous shrinkage stress and functional group conversion measurements are performed. The T_g is determined by DMA. Increasing allyl sulfide concentration reduces the relative stress by up to 75% in the resins containing the maximum amount of allyl sulfide. In glassy systems, at much lower allyl sulfide concentrations, the stress is reduced by up to 20% as compared to propyl sulfide-containing systems incapable of undergoing addition-fragmentation chain transfer.

3.1 Introduction

Traditional dimethacrylate-based dental resins undergo a chain-growth polymerization mechanism, typically gelling at low conversion before vitrifying at higher conversions and thus developing shrinkage stress early on and throughout the polymerization[1]. Conversely, molecular weights and polymer structure build geometrically in a step-growth polymerization, leading to delayed gelation and reduced polymerization shrinkage stress. Thiol-ene photopolymerizations follow a step-growth mechanism and are proposed to reduce polymerization-induced shrinkage stress in dental materials[2-3]. Although organic thiols are frequently malodorous, high molecular weight thiols such as pentaerythritol tetra(3-mercaptopropionate) (PETMP) exhibit very low volatility, alleviating odor concerns. Additionally, thiol-ene resins have been examined in multiple studies as dental restorative materials since they exhibit rapid photopolymerization, necessary for clinical applicability. However, thiol-ene networks typically exhibit relatively low moduli and glass transition temperatures (T_g) when compared with methacrylate–based systems. Ternary mixtures of thiol-ene and methacrylate–based monomers yield a synergistic combination of attributes, blending enhanced mechanical properties with lowered shrinkage stress [4-5].

Recently, a novel mechanism for stress relaxation in a polymer network has been shown via photo-induced bond rearrangement of a polymeric network [6-8], i.e., the formation of a "covalent adaptable network" (CAN). The mechanism for this stress relaxation utilizes radical-mediated addition-fragmentation chain transfer events through allyl sulfide functionalities incorporated within the crosslinking strands of the polymer network, allowing crosslinking strand rearrangement in the presence of radicals (Figure 3.1). The addition-fragmentation reaction

preserves the concentration of both the allyl sulfide and radical reactants, which subsequently participate in further chain transfer events [6, 8]. This cascading rearrangement of the network connectivity effects a global reduction in stress without any concomitant degradation of mechanical properties. When applied to thiol-ene networks, the allyl sulfide addition-fragmentation reduced shrinkage stress relative to an analogous network incapable of addition-fragmentation [6] ; however, the low T_g of that material (~ -20°C) precludes it from use as a dental restorative material. Here, we examine the effect of incorporating a dimethacrylate monomer into an allyl sulfide–containing thiol-ene system and determine its effects on the thermomechanical properties and polymerization-induced shrinkage stress. The effects of allyl sulfide concentration and polymer mobility are evaluated to ascertain under which conditions the addition-fragmentation mechanism is capable of reducing stress in model resins.

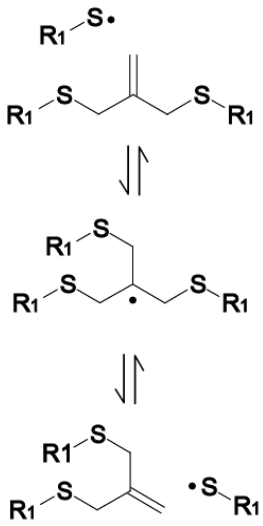

Figure 3.1. Schematic of allyl sulfide addition-fragmentation chain transfer mechanism that promotes network relaxation and polymerization shrinkage stress.

3.2 Materials and Methods

3.2.1 Materials

The monomers and photo-initiator used in this study is shown in Figure 3.2. Resins were comprised of a stoichiometric mixture of 2-methylene-propane-1,3-di(thioethyl vinyl ether) (MDTVE) and pentaerythritol tetrakis(3-mercaptopropionate) (PETMP, Evans Chemetics), which was formulated with ethoxylated bisphenol A dimethacrylate (EBPADMA, Esstech) in various ratios. 2-methyl-propane-1,3-di(thioethyl vinyl ether) (MeDTVE), a MDTVE analogue that replaces the allyl sulfide with a propyl sulfide moiety that is incapable of stress relaxation, was employed as a molecular control to isolate the effect of the allyl sulfide functionality on the stress evolution during polymerization. These monomers, with nearly identical molecular weight and structure, attempt to vary only the shrinkage stress while leaving all other properties of the resin the same. 1-Hydroxycyclohexylphenylketone (HCPK, Ciba Specialty Chemicals), an ultraviolet (UV)-active photoinitiator, was utilized at 1 wt%. Although visible light irradiation, in conjunction with camporquinone as photoinitiator, is the prevalent clinical approach to curing dental materials, HCPK is used in the current study as a model radical generator as it possesses low molar absorptivity. This approach ensures uniform irradiation intensity throughout the sample thickness and eliminates spurious effects owing to uneven cure rates. Although not the focus of this study, a potential advantage to UV irradiation is the prospect of initiatorless photopolymerization as achievable in thiol-ene based systems [9]. Since the goal of these studies is the demonstration of shrinkage stress behavior in model compounds rather than clinically relevant systems, the use of this combination of initiator and UV light is appropriate as it enables

a more accurate assessment of the effects of allyl sulfide concentration on the stress development. MDTVE and MeDTVE were synthesized from 2-chloroethyl vinyl ether with 3-mercapto-2-(mercaptomethyl)-1-propene and 1,3-dimercapto-2-methylpropane, respectively, according to a method described in the literature [6].

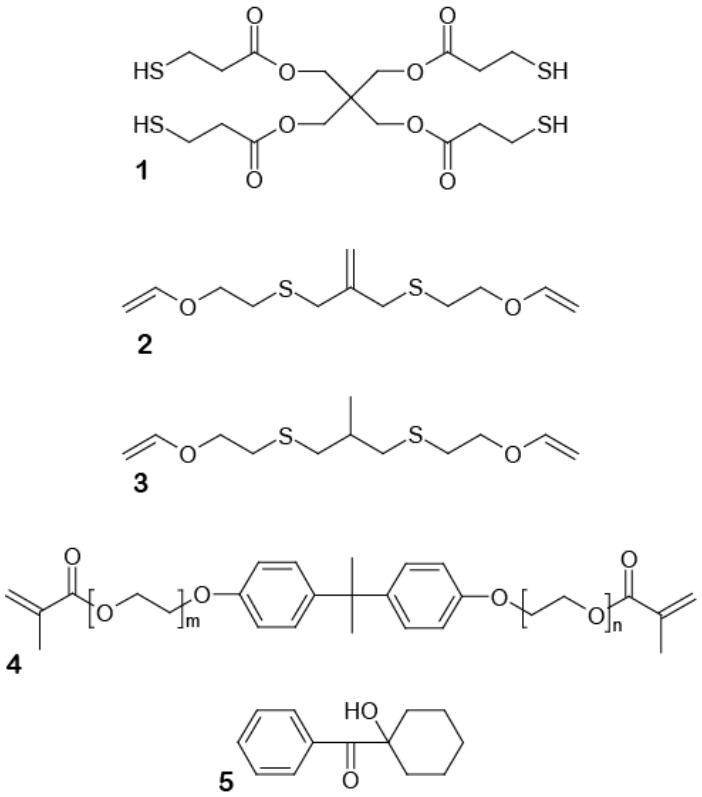

Figure 3.2. Materials used : (1) PETMP (2) MDTVE (3) MeDTVE (4) EBPADMA (5) HCPK

3.2.2 Methods

Simultaneous shrinkage stress and functional group conversion measurements were performed during polymerization using a cantilever-type tensometer (Paffenbarger Research Center, American Dental Association Health Foundation) coupled with a Nicolet 670 FTIR spectrometer via near-infrared transmitting optical fiber patch cables; a detailed description of this measurement technique is presented in the literature [3, 10].The infrared spectrometer was equipped with an indium gallium arsenide (InGaAs) detector and collected spectra at a rate of approximately 3 scans/sec and a resolution of 2 cm^{-1}. Samples 6 mm in diameter and 1 mm thick were irradiated *in situ* for 20 minutes at an intensity of 3 mW/cm^2 by a mercury arc lamp (Acticure, EXFO) equipped with an interference filter isolating the 365 nm Hg spectral line. The evolution of the methacrylate, vinyl ether and allyl sulfide double bond concentrations were determined by monitoring the infrared absorption peaks centered at 6166 cm^{-1} (C=**C-H** stretching, overtone), 6189 cm^{-1} (C=**C-H** stretching, overtone), and 6121 cm^{-1} (C=**C-H** stretching, overtone), respectively. As the methacrylate peak is overlapped with the vinyl ether and allyl sulfide peaks, Gaussian fitting was used to deconvolute the peak areas. This deconvolution technique was validated by comparing known model resin compositions with the spectrum deconvolution output and the error associated with deconvolution based on this validation was determined to be less than 4% conversion.

Dynamic mechanical analysis (DMA) was performed using a TA Instruments Q800 DMA to determine the elastic moduli (E′) and glass transition temperatures of polymerized samples. Samples were prepared by sandwiching the material between two glass slides separated by a 1

mm thick spacer and irradiating under condition identical to those employed in the tensometer. Experiments were performed at a strain and frequency of 0.1% and 1 Hz, respectively, scanning the temperature from -50°C to 140°C twice at 1°C/minute; the temperature scan was repeated to ensure the absence of dark polymerization at temperatures greater than the glass transition temperature (T_g). The T_g was assigned as the temperature at tan δ maximum of the second scan [11]. Analysis of variance (ANOVA), using a 95% confidence interval, was conducted to determine the significance in the differences between mean values.

3.3. Results

Formulations of PETMP-MDTVE-EBPADMA (allyl sulfide containing) and PETMP-MeDTVE-EBPADMA (identical but replacing the allyl sulfide with the propyl sulfide that is incapable of addition-fragmentation) were created and evaluated to ascertain differences in the polymerization kinetics, polymer network structure, and polymerization-induced shrinkage stress associated with the presence of the allyl sulfide functionalities that enable polymer network adaptation and the hypothesized stress reduction. Photopolymerization kinetics as measured by changes in the functional group conversions during the photopolymerization of PETMP-MDTVE-EBPADMA and PETMP-MeDTVE-EBPADMA ternary systems are shown in Figure 3.3. The ternary monomer systems are formulated with a 3:3:4 thiol:vinyl ether:methacrylate stoichiometric ratio for the results presented in Figure 3.3. While the methacrylate conversions of both systems develop similarly, both the polymerization rate and the final conversion of the vinyl ether are reduced in the MDTVE-based ternary system when compared with the equivalent MeDTVE-based system. The allyl sulfide moiety exhibited only 26% conversion, the lowest of the reactive

functionalities.

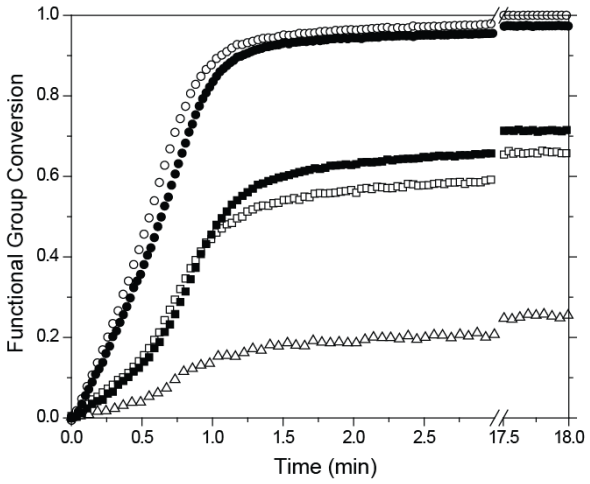

Figure 3.3. Methacrylate (circle), vinyl ether (square), and allyl sulfide (triangle) conversion versus time for allyl sulfide (open symbols) and propyl sulfide (closed symbols) containing materials in a 3:3:4 thiol:vinyl ether:methacrylate mol ratio. Samples contain 1 wt% HCPK, irradiated at 3 mW/cm^2 using 365 nm light.

A comparison of the stress evolution during polymerization of allyl and propyl sulfide-containing resins with 3:3:2 thiol:vinyl ether:methacrylate stoichiometric ratios is shown in Figure 3.4. The allyl sulfide-containing ternary system exhibits lower final shrinkage stress than in the analogous propyl sulfide-containing system. Moreover, stress relaxation is observed in the latter stages of polymerization of the allyl sulfide-containing system.

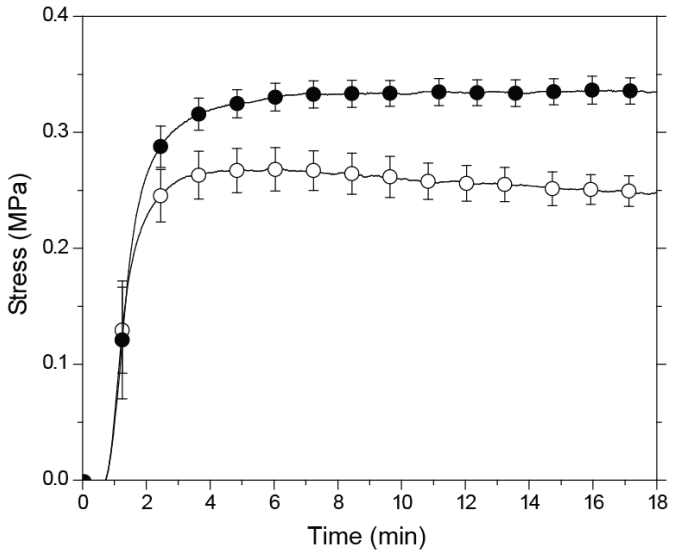

Figure 3.4. Polymerization shrinkage stress versus time of a 3:3:2 stoichiometric mixture of thiol:vinyl ether:methacrylate (PETMP-MDTVE-EBPADMA (○) and PETMP-MeDTVE-EBPADMA (●)). Samples contain 1 wt% HCPK, irradiated at 3 mW/cm^2 using 365 nm light.

The observed final stresses for both the allyl and propyl sulfide-containing materials were non-dimensionalized via division by the modulus in the linear rubbery regime, which is directly related to the crosslink density through rubbery elasticity theory [12]. Here, we denote the ratio of dimensionless stresses in allyl to propyl sulfide-containing materials as the relative shrinkage stress (Figure 3.5). This approach further minimizes the difference in crosslink density between the allyl sulfide-containing networks and their propyl sulfide-containing analogues. The relative shrinkage stress decreases with increasing allyl sulfide concentration (Figure 3.5A) and decreasing T_g of the material (Figure 3.5B). The two resins containing the highest allyl sulfide concentrations demonstrated reduced shrinkage stress relative to the propyl sulfide-containing analogues at the 95% confidence interval. A ternary resin consisting of an off-stoichiometric thiol-ene mixture with an excess of thiol functional groups relative to the vinyl ether (2:1:2 thiol:vinyl ether:methacrylate) also exhibited a relative shrinkage stress less than one.

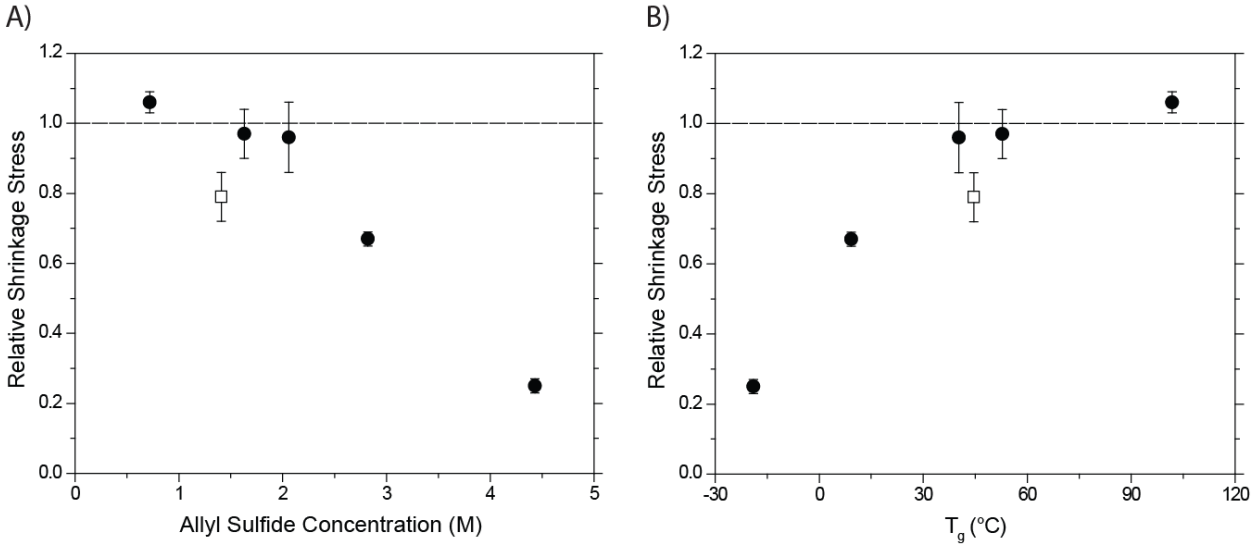

Figure 3.5. (A) Relative polymerization shrinkage stress versus allyl sulfide concentration and (B) versus glass transition temperature. The experiments were conducted using stoichiometric thiol-ene mixture (●) and off-stoichiometric 2:1 thiol-ene mixture (□). Samples contain 1 wt% HCPK, irradiated at 3 mW/cm^2 using 365 nm light.

The glass transition temperature, E′/RT (proportional to the crosslink density, as discussed later, R: gas constant and T: temperature at T_g+30°C), and E′ (at 25°C) all increase with increasing methacrylate and decreasing allyl sulfide proportion (Table 3.1). Additionally, while increasing the methacrylate molar ratio (from 3:3:2 to 1:1:6 – thiol:vinyl ether:methacrylate) yields only a slight decrease in the final methacrylate conversion (from approximately 100 to 84%), significant variation is observed in the final vinyl ether and allyl sulfide conversions (from approximately 99 to 54% and 8 to 62%, respectively).

Table 3.1. Summary of final conversion, T_g, E′/RT, and elastic modulus.

Vinyl ether monomer used in the ternary system (thiol:vinyl ether:methacrylate ratio)	Allyl sulfide concentration (mol/L)	Final functional group conversion [%]			T_g (°C)	E′/RT at $T = T_g + 30°C$ (Mol/m^3)	Elastic modulus at T = 25°C before heating (MPa)
		Methacrylate	Vinyl ether	Allyl sulfide			
MDTVE (1:1:0)	4.43	-	96	8	-20.0 ± 0.8	5040 ± 40	0.12 ± 0.001
MeDTVE (1:1:0)	-	-	99	-	-28.0 ± 0.2	4440 ± 40	0.11 ± 0.002
MDTVE (3:3:2)	2.80	100	85	14	9.2 ± 0.9	6500 ± 700	0.18 ± 0.002
MeDTVE (3:3:2)	-	98	88	-	5 ± 0	6100 ± 400	0.15 ± 0.001
MDTVE (3:3:4)	2.10	100	67	26	40 ± 2	9200 ± 700	0.4 ± 0.04
MeDTVE (3:3:4)	-	98	72	-	43.8 ± 0.6	9800 ± 100	0.6 ± 0.07
MDTVE (1:1:2)	1.60	99	62	33	52.8 ± 0.6	9700 ± 700	1.4 ± 0.02
MeDTVE (1:1:2)	-	98	61	-	55 ± 1	10100 ± 700	1.2 ± 0.1
MDTVE (1:1:6)	0.72	84	56	62	102 ± 2	17600 ± 900	2.7 ± 0.2
MeDTVE (1:1:6)	-	87	54	-	108 ± 2	20000 ± 1000	2.3 ± 0.1
MDTVE (2:1:2)	1.40	98	88	41	44.6 ± 0.3	7800 ± 300	1.0 ± 0.1
MeDTVE (2:1:2)	-	97	95	-	39 ± 1	6880 ± 70	0.6 ± 0.02

3.4 Discussion

Carbon-carbon double bond conversion profiles for analogous allyl and propyl sulfide-containing ternary systems (3:3:4 – thiol:vinyl ether:methacrylate) are shown in Figure 3.3. Two conversion regimes are apparent during the polymerization as indicated by the inflection point in the vinyl ether conversion profile occurring after approximately 40 seconds irradiation. The first regime is dominated by methacrylate homopolymerization as well as chain transfer to thiol, whereas after the inflection point the rate of vinyl ether incorporation into the polymer network,

relative to the methacrylate, progressively increases. Similar trends have been observed previously in thiol-allyl-methacrylate ternary systems and have been attributed to the propensity of the methacrylate to homopolymerize, rather than copolymerize with other electron rich carbon-carbon double bonds such as the vinyl ether [4-5].

While both the vinyl ethers and allyl sulfides constitute enes that can engage in the overall thiol-ene polymerization process, the radical addition to the allyl sulfide, unlike the vinyl ether, regenerates both the allyl sulfide and thiyl radical species [8, 13]; thus, the allyl sulfide consumption during irradiation (Figure 3.3) indicates side reactions by hydrogen abstraction from thiol and/or copolymerization with methacrylate, leading to additional crosslinking [6]. A previous study has shown negligible copolymerization between the vinyl ether and allyl sulfide and is therefore discounted as a potential side reaction in the present work [6]. As the polymerization regime transitions towards thiol-ene incorporation, loss of the allyl sulfide is compounded by hydrogen abstraction. The effect of reduced thiol concentration through this side reaction is observed in the lower final vinyl ether conversion of the allyl sulfide-containing resin as compared to that of the propyl sulfide-containing resin (Figure 3.3). As the proportion of methacrylate is increased in the system, the allyl sulfide consumption is correspondingly raised, somewhat reducing the capacity for stress relaxation via the addition-fragmentation pathway (Table 3.1); however, this does not preclude the allyl sulfide from undergoing multiple addition-fragmentation chain transfer events prior to irreversible consumption.

Glassy polymer networks have been shown to be well suited as excellent dental restorative materials as they are capable of withstanding intraoral mechanical stresses. The T_g of a polymer

network is dependent on its crosslink density and network strand flexibility [14-15]. According to the theory of rubbery elasticity, the crosslink density is proportional to E′/RT and increases as the proportion of methacrylate is raised (Table 3.1). Moreover, the bisphenol-A core of EBPADMA is a particularly inflexible functionality [16], leading to an increase in the overall chain stiffness. Thus, the increased T_g associated with higher methacrylate proportion is attributed to a combination of these two effects.

Polymerization shrinkage stress is the superposition of that stored by network formation and dissipated by stress relaxation. Typically, stress relaxation is achieved via the viscous flow of low molecular weight species in the early stages of polymerization. Incorporation of the allyl sulfide functionality provides an alternative avenue for stress relaxation by network rearrangement, both throughout and after the polymerization, as observed in the reduced polymerization shrinkage stress developed by the allyl sulfide-containing material versus the propyl sulfide analogue (Figure 3.4). The stress relaxation associated with the allyl sulfide incorporation into methacrylate-based polymerizations conclusively demonstrates the capability of addition-fragmentation chain transfer to reduce stress build up during polymerizations of multimethacrylates. Thus, this novel mechanism is actively occurring during conventional chain growth free-radical polymerizations.

The allyl sulfide-containing material demonstrates a maximum in the stress evolution and, at extended irradiation, undergoes stress relaxation whereas the propyl sulfide-containing material does not (Figure 3.4). The reduction in molecular mobility, associated with vitrification in highly crosslinked systems, effectively traps radical species [17] and increases their lifetime on the order

of several months [18-19]. These species are able to react over extended time periods, suggesting the potential for further stress relaxation via addition-fragmentation chain transfer in allyl sulfide-containing systems subsequent to the polymerization reaction.

Polymerization shrinkage-induced stress is a consequence of the polymer network crosslinking, as the ultimate magnitude of the stress is related, in part, to the crosslink density. Thus, the relative shrinkage stress, which accounts for crosslink density via division by the elastic modulus, was used as the metric for comparison to compensate for the relatively small differences in the network crosslink density. The decrease in relative shrinkage stress as the allyl sulfide concentration in the active network is increased is attributed to a higher probability of addition-fragmentation chain transfer events (Figure 3.5). As the polymerizations are carried out under ambient conditions, vitrification occurs at lower conversions for high methacrylate proportions. The rate of stress relaxation during the polymerization owing to addition-fragmentation in the vitrified regime appears slow, likely associated with the reduced molecular mobility; however, the ternary mixture with an off stoichiometric ratio of 2:1 thiol:vinyl ether (open square symbol in Figure 3.5) has a glass transition temperature greater than the cure temperature and exhibits more than 20% reduction in the relative stress during the polymerization. This behavior suggests that, despite vitrification, reduced polymerization stress is achievable and that the increased thiol promotes a relatively greater number of addition-fragmentation chain transfer events and ultimately a faster rate of network relaxation. Based upon these findings, we speculate that increasing the allyl sulfide content while increasing or maintaining the methacrylate concentration would produce a material exhibiting both low polymerization stress accompanied by a further increased in T_g. One approach to achieve this outcome would be to incorporate the

allyl sulfide moiety directly into a methacrylate-functionalized monomer. Alternatively, one could synthesize allyl sulfide-based monomers capable of producing a similar crosslink density as methacrylate-based materials. For example, one could synthesize an alkyne-functionalized allyl sulfide monomer to be used in thiol-yne polymerizations [20].

3.5 Conclusions

In conclusion, allyl sulfide addition-fragmentation chain transfer reduces the final stress in ternary thiol-ene-methacrylate polymerizations by as much as 75% at high allyl sulfide concentrations. Although this effect is mitigated by lower allyl sulfide concentration as well as decreased mobility in the ternary systems presented here, stress reduction is observed in systems possessing super-ambient T_gs. This behavior indicates that the utilization of the allyl sulfide functionality and network adaptation in dental materials represents a new paradigm for polymerization stress reduction concurrent with and subsequent to the polymerization in these materials. Great opportunities exist for creating dental resins that simultaneously incorporate higher allyl sulfide concentrations into resins that achieve appropriate mechanical and thermal properties.

3.6 Acknowledgments

This investigation was supported by NIDCR 2 R01 DE-010959-11 from the National Institute of Health.

3.7 References

(1) Bowman, C. N.; Kloxin, C. J. *AIChE Journal* **2008,** *54,* 2775-2795.

(2) Carioscia, J. A.; Lu, H.; Stanbury, J. W.; Bowman, C. N. *Dental Materials* **2005,** *21,* 1137-1143.

(3) Lu, H.; Carioscia, J. A.; Stansbury, J. W.; Bowman, C. N. *Dental Materials* **2005,** *21,* 1129-1136.

(4) Lee, T. Y.; Carioscia, J.; Smith, Z.; Bowman, C. N. *Macromolecules* **2007,** *40,* 1473-1479.

(5) Lee, T. Y.; Smith, Z.; Reddy, S. K.; Cramer, N. B.; Bowman, C. N. *Macromolecules* **2007,** *40,* 1466-1472.

(6) Kloxin, C. J.; Scott, T. F.; Bowman, C. N. *Macromolecules* **2009,** *42,* 2551-2556.

(7) Scott, T. F.; Draughon, R. B.; Bowman, C. N. *Advanced Materials* **2006,** *18,* 2128-+.

(8) Scott, T. F.; Schneider, A. D.; Cook, W. D.; Bowman, C. N. *Science* **2005,** *308,* 1615-1617.

(9) Cramer, N. B.; Reddy, S. K.; Cole, M.; Hoyle, C.; Bowman, C. N. *J Polym Sci Pol Chem* **2004,** *42,* 5817-5826.

(10) Lu, H.; Stansbury, J. W.; Dickens, S. H.; Eichmiller, F. C.; Bowman, C. N. *Journal of Materials Science-Materials in Medicine* **2004,** *15,* 1097-1103.

(11) Li, G.; Lee-Sullivan, P.; Thring, R. W. *Journal of Thermal Analysis and Calorimetry* **2000,** *60,* 377-390.

(12) Flory, P. J. *Principles of Polymer Chemistry*; Cornell University Press, Ithaca, NY, 1953.

(13) Meijs, G. F.; Rizzardo, E.; Thang, S. H. *Macromolecules* **1988,** *21,* 3122-3124.

(14) Ueberreiter, K.; Kanig, G. *J Chem Phys* **1950,** *18,* 399-406.

(15) Young, R. J.; Lovell, P. A. *Introduction to Polymers*; 2nd ed.: Chapman & Hall, London, 1991; p 443.

(16) Peutzfeldt, A. *European Journal of Oral Sciences* **1997,** *105,* 97-116.

(17) Scott, T. F.; Cook, W. D.; Forsythe, J. S.; Bowman, C. N.; Berchtold, K. A. *Macromolecules* **2003,** *36,* 6066-6074.

(18) Zhu, S.; Tian, Y.; Hamielec, A. E.; Eaton, D. R. *Macromolecules* **1990,** *23,* 1144-1150.

(19) Kloosterboer, J. G. *Advances in Polymer Science* **1988,** *84,* 1-61.

(20) Fairbanks, B. D.; Scott, T. F.; Kloxin, C. J.; Anseth, K. S.; Bowman, C. N. *Macromolecules* **2009,** *42,* 211-217.

Chapter 4

Stress Relaxation by Addition-Fragmentation Chain Transfer in Highly Crosslinked Thiol-Yne Networks

Radical mediated addition-fragmentation chain transfer of mid-chain allyl sulfide functional groups was utilized to reduce polymerization-induced shrinkage stress in thiol-yne step-growth photopolymerization reactions. In previous studies, the addition-fragmentation of allyl sulfide during the polymerization of a step-growth thiol-ene network demonstrated reduced polymerization stress; however, the glass transition temperature of the material was well below room temperature (~ -20°C). Many applications require super-ambient glass transition temperatures, such as microelectronics and dental materials. Polymerization reactions utilizing thiol-yne functional groups have many of the advantageous attributes of the thiol-ene-based materials, such as possessing a delayed gel-point, resistant to oxygen inhibition, and fast reaction kinetics, while also possessing a high glass transition temperature. Here we incorporate allyl sulfide functional groups into a highly crosslinked thiol-yne network to reduce polymerization-induced shrinkage stress. The resulting networks were highly crosslinked, possessed super-ambient glass transition temperatures, and exhibited significantly reduced polymerization-induced shrinkage stress when compared with analogous propyl sulfide-containing materials that are incapable of addition-fragmentation.

4.1 Introduction

Our previous work exploiting AFCT-mechanisms to reduce polymerization stress utilized thiol-ene networks, whereby multifunctional thiol and vinyl monomers were copolymerized via a radical-mediated step-growth reaction mechanism to incorporate an allyl sulfide functionality[12] in the crosslinking strands.[3] Thiol-ene polymerizations possess many desirable attributes, such as extraordinary resistance to oxygen inhibition (owing to the facile abstractability of the thiol hydrogen)[4-5] and rapid polymerization kinetics; moreover, its step-growth nature produces a homogeneous, crosslinked material with uniformly distributed allyl sulfide functional groups throughout the network. Unfortunately, thiol-ene polymerizations often yield elastomeric materials with low glass transition temperatures (T_gs) that are ill-suited for structural applications. Utilization of the thiol-yne polymerization mechanism (i.e., replacing the vinyl-based monomer with an ethynyl-based monomer) preserves the desirable characteristics of the thiol-ene mechanism while effectively doubling the crosslink density, yielding a concomitant increase in the T_g[6-9]. Here, we incorporate allyl sulfide functional groups into thiol-yne networks to effect stress relaxation in super-ambient T_g materials. Simultaneous shrinkage stress and functional group conversion measurements were performed during polymerization using a cantilever-type tensometer coupled with a FTIR spectrometer.

4.2 Materials and Methods

4.2.1 Materials

The allyl sulfide AFCT functionality was incorporated in a thiol-yne system via the formulation of an allyl sulfide-based diethynyl monomer (2-methylene-propane-1,3-di(thiobut-1-yne) – MDTBY – Figure 4.1A) with a tetrathiol (pentaerythritol tetrakis(3-mercaptopropionate) – PETMP – Figure 4.1C) at a 1:2 ethynyl/thiol stoichiometric ratio, as each ethynyl group is capable of reacting with two thiol groups. For comparison, an analogous thiol-yne network was fabricated utilizing a propyl sulfide-based diethynyl monomer (2-methyl-propane-1,3-di(thiobut-1-yne) – MeDTBY – Figure 4.1B), where the propenyl sulfide is incapable of undergoing the AFCT-mediated relaxation mechanism, in place of MDTBY. These resins were additionally formulated with 3 wt% UV photoinitiator (1-hydroxycyclohexylphenylketone – HCPK – Figure 4.1D) to initiate the thiol-yne polymerization upon UV irradiation.

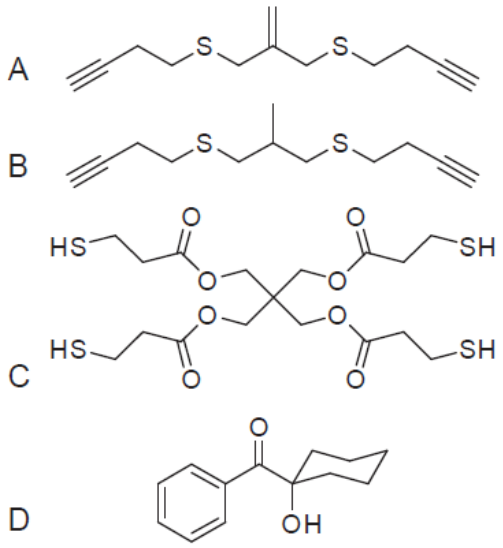

Figure 4.1. Materials used: (A) MDTBY, (B) MeDTBY, (C) PETMP, and (D) HCPK.

4.2.2 Methods

Simultaneous shrinkage stress and functional group conversion measurements were performed during polymerization using a cantilever-type tensometer (Paffenbarger Research Center, American Dental Association Health Foundation) coupled with a Nicolet 670 FTIR spectrometer via near-infrared transmitting optical fiber patch cables[10-11]. Samples 6 mm in diameter and 1 mm thick were irradiated for 30 minutes at 10 mW/cm^2 intensity by a UV lamp (Acticure, EXFO) equipped with a 365 nm interference filter. The conversions of the yne and allyl sulfide functional group were determined by monitoring the infrared absorption peaks centered at 6483 cm^{-1} (C≡**C-H** stretching, overtone) and 6121 cm^{-1} (C=**C-H** stretching, overtone), respectively.

To estimate mechanical properties of the materials, the elastic moduli (E′) and glass transition temperatures of polymerized samples were determined by dynamic mechanical analysis (DMA) (TA Instruments Q800). Rectangular samples (length*width*thickness : 8mm*5mm*1mm, sample size was varied slightly for each experiment) were prepared by sandwiching the material between 2 glass slides with 1mm thickness spacer and irradiating with same condition of a tensometer experiment. Experiments were performed at a strain and frequency of 0.1% and 1 Hz, respectively, scanning the temperature twice at 1 ºC/minute. The T_g was assigned as the temperature at tan delta maximum [12-13] of the second scan to ensure the absence of dark polymerization at temperatures greater than the glass transition temperature.

4.3 Results and Discussion

The thiol-ene reaction follows an elegant mechanism of sequential propagation and chain transfer events, whereby addition of a thiyl radical to a vinyl functional group yields a carbon-centered radical that subsequently abstracts a thiol hydrogen, regenerating the thiyl radical and producing a thioether (Figure 4.2, cycle B). Utilization of an ethynyl-based monomer (i.e., thiol-yne) increases the polymerization reaction complexity as the mechanism proceeds via two sequential thiol addition reactions (Figure 4.2, cycles A and B). Incorporation of the allyl sulfide further increases the reaction complexity and provides a route for network connectivity rearrangement via the AFCT reaction, whereby a thiyl radical adds to an allyl sulfide functional group to yield an unstable carbon-centered radical intermediate, the fragmentation of which regenerates both the allyl sulfide functional group and the thiyl radical (Figure 4.2, cycle C). Whereas MeDTBY participates exclusively in the thiol-yne polymerization reaction (i.e., Figure 4.2, cycle A and B), MDTBY participates in both the thiol-yne polymerization and AFCT network connectivity rearrangement reactions concurrently (i.e., Figure 4.2, cycles A, B, and C). Thus, MeDTBY acts as a negative control monomer possessing similar chemical structure and molecular weight.

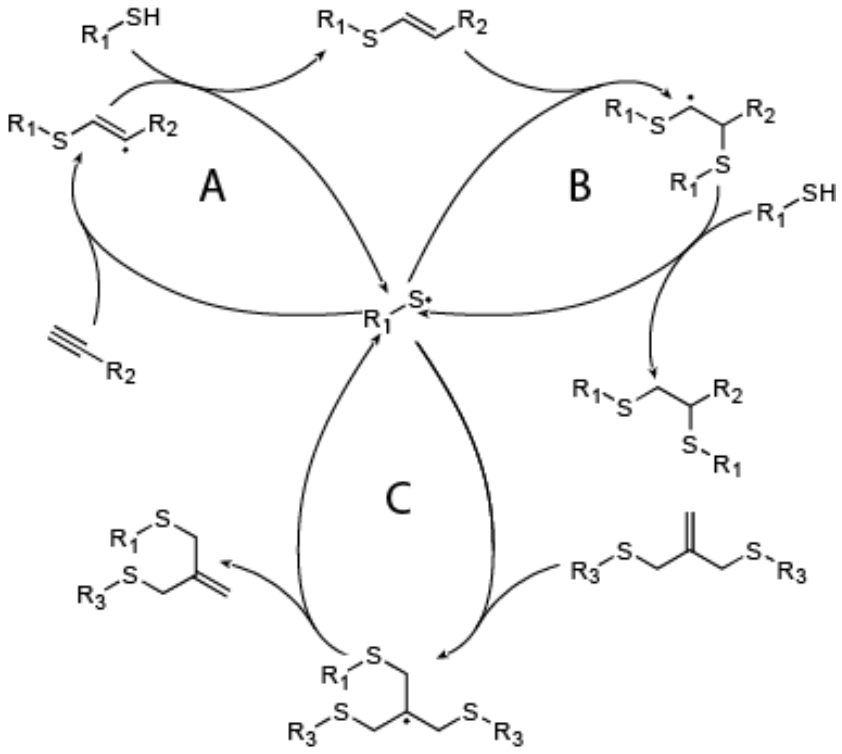

Figure 4.2. Schematic of concurrent thiol-yne (cycles A and B) and allyl sulfide AFCT (cycle C) mechanisms.

The thiol-yne mechanism is comprised of two sequential addition events, whereby addition of a thiyl radical to an ethynyl functional group yields a vinyl sulfide functional group (cycle A); subsequent thiyl radical addition across this vinyl completes the thiol-yne polymerization mechanism (cycle B)[8]. Thiyl radical addition to and subsequent fragmentation of the allyl sulfide functional group conserves the concentrations of both the thiyl radical and allyl sulfide functional group (cycle C).[3, 14]

The stress that accumulates during a polymerization is typically attributed to the extent of post-gelation shrinkage and the modulus of the polymerized material. A comparison of the

thermomechanical properties of the fully cured allyl and propyl sulfide-based materials demonstrates excellent similarity between the two network structures in regard to their crosslink density and glass transition behavior, as expected given the molecular structures (Figure 4.3). Both systems demonstrate 1.4 GPa elastic modulus at 25 ^{o}C (before heating) which is the stress measurement condition. More specifically, the onset of the thermal transition from a glassy to elastomeric material occurs at approximately the same temperature and the rubbery moduli, which are proportional to the crosslink density, are similar. The temperature at the tan δ maximum (assigned here as the T_g) [12-13] demonstrates that both allyl and propyl sulfide-based materials exhibit super-ambient T_gs (allyl sulfide-based system: 41 ± 1ºC, propyl sulfide-based system: 39 ± 1ºC). Overall, the similarity of these networks indicates that the propyl sulfide addition to the MeDTBY enables this system to serve as an excellent control for which the only significant differences in material behavior should all be related to the simultaneous AFCT-polymerization mechanism rather than differences in the network structure.

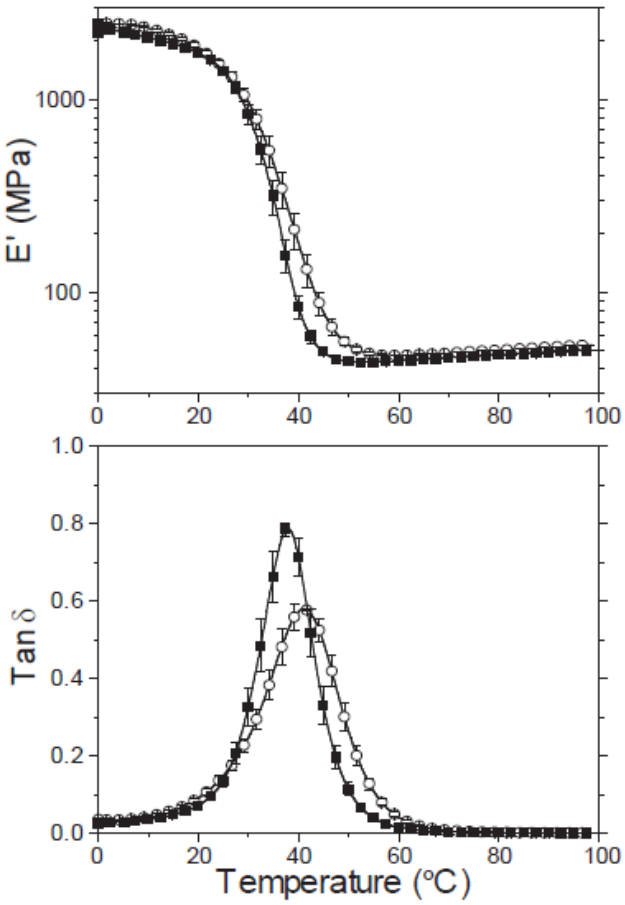

Figure 4.3. (A) Elastic modulus and (B) tan δ versus temperature for stoichiometrically balanced mixtures of PETMP-MDTBY (○) and PETMP-MeDTBY (■). Samples were formulated with 3 wt % HCPK and irradiated at 365 nm, 10 mW/cm^2, for 30 min.

The IR spectroscopy of PETMP-MeDTBY indicates rapid consumption of the ethynyl functional group; however, the ethynyl consumption does not proceed to complete conversion, presumably owing to severely reduced molecular mobility resulting from vitrification (Figure 4.4A)[15]. Conversely, the ethynyl consumption during the PETMP-MDTBY photopolymerization (i.e., the allyl sulfide-containing system) proceeds at a slower rate, attributable to the sequestration of radicals participating in the AFCT mechanism.[3] Moreover, consumption of the allyl sulfide is

observed during the PETMP-MDTBY photopolymerization (Figure 4.4A), in contrast to the idealized reaction mechanism detailed in Figure 4.2 (i.e., cycle C). Previous work in thiol-ene systems demonstrated a minor side reaction whereby the AFCT carbon-centered radical intermediate abstracts a thiol hydrogen, thus consuming a small fraction of both allyl sulfide and thiol[3]. In the current thiol-yne system (i.e., PETMP-MDTBY), a large fraction of the allyl sulfide is consumed during the polymerization (Figure 4.4A), presumably reacting with an equivalent amount of thiol and thus producing an ethynyl/thiol stoichiometric imbalance. This ethynyl/thiol imbalance results in a limited amount of ethynyl homopolymerization, effecting a mixed-mode step- and chain-growth polymerization mechanism[8] that would be expected, in the absence of any other differences, to increase both the crosslinking density and the corresponding stress. Furthermore, homopolymerization results in a lower gel-point conversion, which would reduce the stress dissipated by pre-gelation viscous flow, further heightening the stress level expected in such a system. Thus, in the absence of any network relaxation associated with the AFCT-mediated relaxation mechanism, the photopolymerization of PETMP-MDTBY is expected to exhibit a much higher polymerization stress level as compared to PETMP-MeDTBY. In contrast, Figure 4.4B demonstrates the dramatic effect of the AFCT-mediated relaxation mechanism as the PETMP-MDTBY resin exhibits significantly reduced polymerization stress (43%) as compared to the PETMP-MeDTBY control, attributable to the allyl sulfide AFCT mechanism facilitating network connectivity rearrangement during the polymerization. This relaxation behavior is observed despite the glassy nature of the polymer networks that are formed.

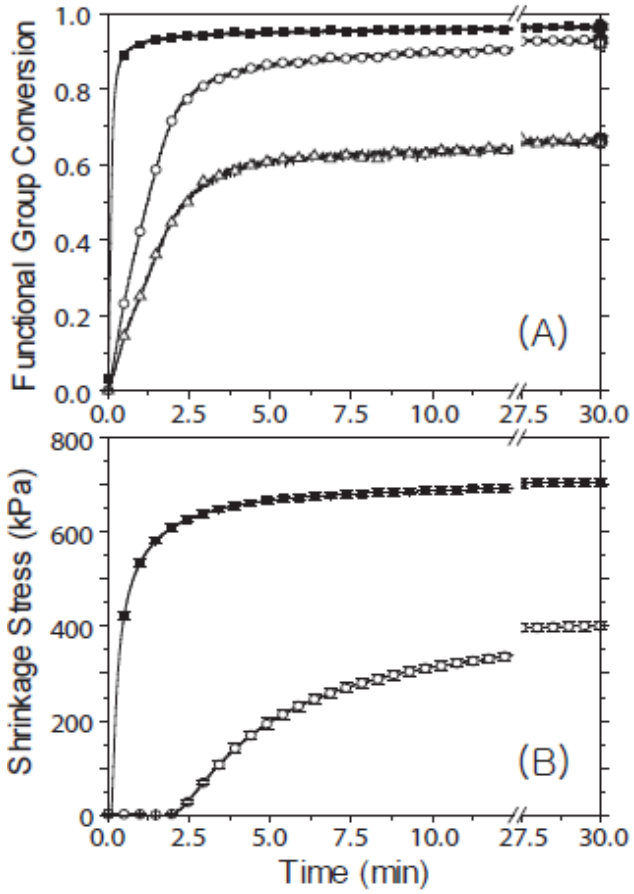

Figure 4.4. (A) Functional group conversion (ethynyl conversion of PETMP-MDTBY (○), ethynyl conversion of PETMP-MeDTBY (■), and allyl sulfide of PETMP-MDTBY (△)) and (B) polymerization shrinkage stress evolution (PETMP-MDTBY (○) and PETMP-MeDTBY (■)) versus time for a 2:1 stoichiometric mixture of thiol:yne. Samples contain 3 wt% HCPK and were irradiated at 10 mW/cm^2 using 365 nm light.

4.4 Conclusions

In this study, we found that the incorporation of allyl sulfide functional groups in the polymer backbone of a material possessing a super-ambient T_g reduces polymerization-induced shrinkage stress, owing to network connectivity rearrangement via a AFCT mechanism. To our knowledge,

this observation is the first successful demonstration of AFCT-mediated relaxation during the polymerization of a glassy polymer network to induce stress relaxation. As this approach is well-suited for incorporation in free radical polymerizations, or indeed any other thermosetting polymerization where radicals can be generated, the mitigation of polymerization stress can be achieved even in high performance materials.

4.5 Acknowledgments

This investigation was supported by NIDCR 2 R01 DE-010959-11 from the National Institutes of Health and NSF 0933828.

4.6 References

(1) Moad, G.; Rizzardo, E.; Thang, S. H. *Australian Journal of Chemistry* **2005,** *58,* 379-410.

(2) Meijs, G. F.; Rizzardo, E.; Thang, S. H. *Macromolecules* **1988,** *21,* 3122-3124.

(3) Kloxin, C. J.; Scott, T. F.; Bowman, C. N. *Macromolecules* **2009,** *42,* 2551-2556.

(4) Szmant, H. H.; Mata, A. J.; Namis, A. J.; Panthananickal, A. M. *Tetrahedron* **1976,** *32,* 2665-2680.

(5) Jacobine, A. F. *Radiation Curing in Polymer Science and Technology*; Elesvier Applied Science, London, 1993; Vol. 3, p 219-268.

(6) Chan, J. W.; Shin, J.; Hoyle, C. E.; Bowman, C. N.; Lowe, A. B. *Macromolecules* **2010,** *43,* 4937-4942.

(7) Chan, J. W.; Zhou, H.; Hoyle, C. E.; Lowe, A. B. *Chem Mater* **2009,** *21,* 1579-1585.

(8) Fairbanks, B. D.; Scott, T. F.; Kloxin, C. J.; Anseth, K. S.; Bowman, C. N. *Macromolecules* **2009,** *42,* 211-217.

(9) Lowe, A. B.; Hoyle, C. E.; Bowman, C. N. *J Mater Chem* **2010,** *20,* 4745-4750.

(10) Lu, H.; Carioscia, J. A.; Stansbury, J. W.; Bowman, C. N. *Dent Mater* **2005,** *21,* 1129-1136.

(11) Lu, H.; Stansbury, J. W.; Dickens, S. H.; Eichmiller, F. C.; Bowman, C. N. *J Mater Sci-Mater M* **2004,** *15,* 1097-1103.

(12) Ferrillo, R. G.; Achorn, P. J. *J Appl Polym Sci* **1997,** *64,* 191-195.

(13) Li, G.; Lee-Sullivan, P.; Thring, R. W. *J Therm Anal Calorim* **2000,** *60,* 377-390.

(14) Scott, T. F.; Schneider, A. D.; Cook, W. D.; Bowman, C. N. *Science* **2005,** *308,* 1615-1617.

(15) Cook, W. D. *Polymer* **1992,** *33,* 2152-2161.

Chapter 5

Stress Reduction and T_g Enhancement in Ternary Thiol-Yne-Methacrylate Systems via Addition-fragmentation Chain Transfer

Previously, the AFCT-capable allyl sulfide functional group was incorporated into multifunctional monomer structures as a part of the thiol-yne system and excellent stress relaxation was demonstrated as compared with non-allyl sulfide containing thiol-yne resins. Despite these benefits, the thiol-yne system remains limited in the crosslink density and glass transition temperatures that are achievable in these binary formulations. Here, multifunctional methacrylate monomer was incorporated into the allyl sulfide-based thiol-yne resin to increase the glass transition temperature and reduce the final stress. As a negative control, to as great an extent as possible isolate the effect of AFCT of the allyl sulfide moiety, a propyl sulfide-based diyne, which has an identical chemical structure with the allyl sulfide moiety replaced by a propyl sulfide, was formulated for the resins in the place of allyl sulfide-based diyne. The glass transition temperature of the ternary systems was increased as the methacrylate content increased. Excitingly, the shrinkage stress of the optimal ternary resin was lower than either the binary thiol-yne resin or the pure methacrylate resin. The stress relaxation benefit associated with AFCT was improved as the allyl sulfide concentration increased in the ternary resin. The allyl sulfide-based thiol-yne-methacrylate system exhibits stress relaxation up to 55% and increased T_g up to 40^{o}C compared with the control AFCT-incapable thiol-yne. This ternary system

demonstrates approximately 3 times lower stress compared with conventional dimethacrylate monomers[1] while possessing similarly outstanding mechanical behavior.

5.1 Introduction

Shrinkage stress represents one of the most detrimental characteristics of photopolymerization and other thermosetting polymerization reactions where it ultimately leads to device failure by initiating microcracks, causing shape distortion, and leading to various mechanisms of delamination[2]. As a methodology for reducing polymerization-induced volume shrinkage and the corresponding shrinkage stress, many approaches have been proposed such as the implementation of thiol-ene polymerization reactions with delayed gelation[1-3], ring-opening polymerizations that lead to volume expansion or minimally shrinkage reduction[4-5], and polymerization-induced phase separation [6]. Recently, inclusion of reversible covalent bond structures into monomers and the resulting crosslinked polymer networks. These structures incorporate moieties that undergo addition-fragmentation chain transfer (AFCT) in the presence of radicals. Thus, this AFCT reaction occurs simultaneously with polymerization (or in the already formed polymer networks), promoting molecular rearrangement throughout the polymer network [7-8,9]. Hence, AFCT relaxes the shrinkage stress while preserving the crosslink density, mechanical properties and molecular structure of networks that do not contain the AFCT-capable moiety (Figure 5.1(A)) Therefore, the network architecture remains unchanged. The allyl sulfide functional group maximized the stress reduction in thiol-ene [10] and thiol-yne [11] binary polymerizations. The allyl sulfide group was ideal in these polymerizations because it undergoes reversible AFCT in the presence of the thiyl radical, enabling each allyl sulfide to react repeatedly to promote network rearrangement.

Thiol-ene [1] and thiol-yne reactions [12-13] have a number of advantages compared with conventional radically polymerized monomers undergoing chain-growth polymerization with the advantages including delayed gelation, low stress evolution, and oxygen inhibition as well as the click reaction nature. However, the crosslink density and resulting mechanical properties of the polymer networks are not sufficient for many applications since they have relatively low elastic modulus and sub-ambient or limited super-ambient glass transition temperatures. [1, 10-12]

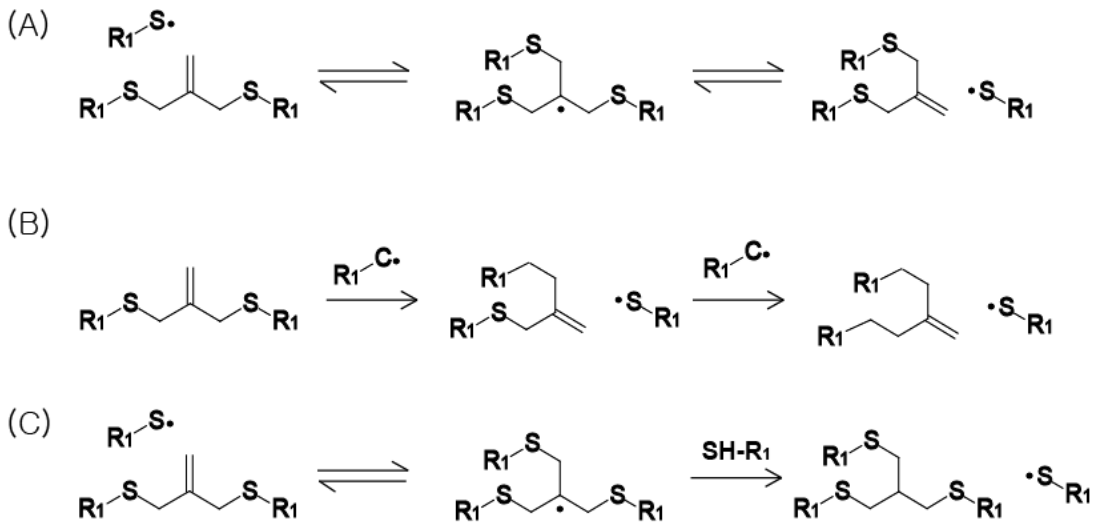

Figure 5.1. (A) Reversible AFCT mediated by reactions with the thiyl radical, (B) irreversible allyl sulfide AFCT mediated by reactions with a carbon-centered radical, and (C) consumption of the allyl sulfide moiety by abstraction of hydrogen from thiol.

Incorporation of methacrylate monomers into the allyl sulfide-containing thiol-ene polymerization improved the glass transition temperature as well as the stress relaxation effect [14]. However, since the T_g of the thiol-ene binary system was relatively low (~ -20^{o}C), a large

amount of methacrylate was required to form a polymer with a super-ambient T_g. Here, an allyl sulfide-containing diyne is synthesized and utilized to promote stress relaxation in ternary thiol-yne-methacrylate formulations. We hypothesized that this thiol-yne-methacrylate combination, which undergoes AFCT, will exhibit the desired high glass transition temperature and modulus as well as exhibit the stress relaxation effect. The shrinkage stress and functional group conversion are investigated by increasing the methacrylate content in these ternary resins. Elastic moduli and glass transition temperatures are also examined to determine the relationship between the stress and mechanical properties.

5.2 Experimental

5.2.1 Materials

Synthesis and Preparation of the Monomers

Materials used in this study are shown in Figure 5.2. 2-methylene-propane-1,3-di(thiobut-1-yne) (DYAS, diyne allyl sulfide) was synthesized from 4-bromo-1-butyne with 3-mercapto-2-(mercaptomethyl)-1-propene according to a previous method [14-16]. To remove possible residual di-sulfides which may reduce the polymerization rate, the monomers were further purified by being treated with a strong reducing agent. The distilled 14 grams of yne was dissolved in a mixture of methanol, water, and tetrahydrofuran (1 to 1 to 1.3 in volumetric ratio, respectively). 1.5 grams of sodium borohydride were added to the solution and stirred for 2 hours at ambient

temperature. The solvents were evaporated, residual dissolved in ethyl ether, and the ether phase was washed with strong aqueous sodium hydroxide. The ether extracts were dried with calcium chloride, evaporated, and redistilled to yield a clear, colorless liquid. Additionally, to isolate the stress relaxation effect of AFCT, 2-methyl-propane-1,3-di(thiobut-1-yne) (DYPS, diyne propyl sulfide), which has an otherwise identical molecular structure with DYAS but the allyl sulfide group is replaced with an AFCT-incapable propyl sulfide. DYPS was synthesized from 1,3-dimercapto-2-methylpropane in the same manner as with the synthesis of DYAS. Pentaerythritol tetrakis(3-mercaptopropionate (PETMP, Esstech) and ethoxylated bisphenol A dimethacrylate (EBPADMA, Esstech) were used as received.

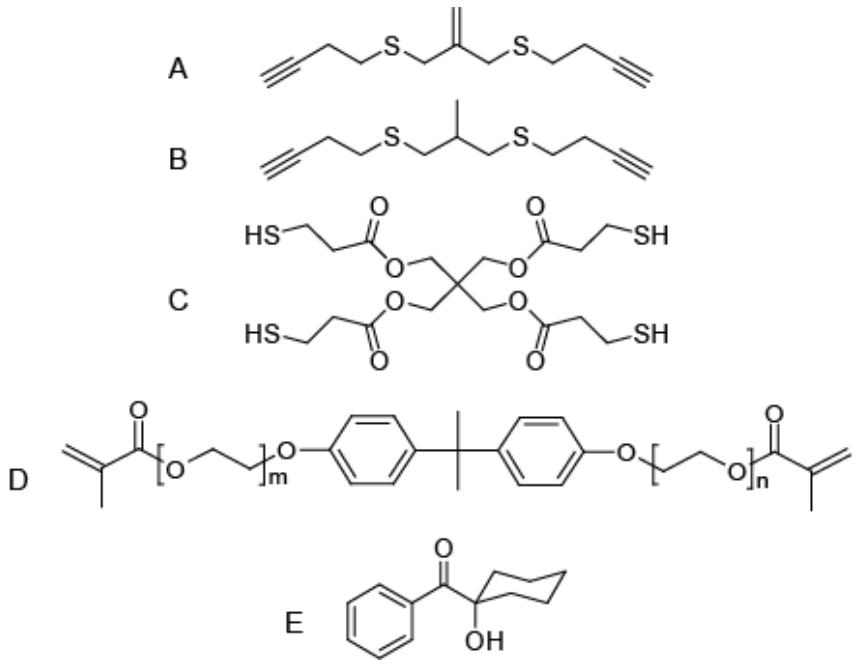

Figure 5.2. Materials used: (A) DYAS, (B) DYPS, (C) PETMP, (D) EBPADMA, and (E) HCPK.

Preparation of the resin mixture

Unless otherwise noted, resins were comprised of a stoichiometric mixture of DYAS (allyl sulfide-based diethynyl monomer) and PETMP (tetrathiol) at a 1:2 ethynyl/thiol ratio since each ethynyl group is capable of reacting with two thiol groups, and this mixture was then formulated with EBPADMA in various relative amounts. As a negative control, to isolate the effect of AFCT, DYPS, a DYAS analog that replaces the allyl sulfide moiety with a propyl sulfide, was used in place of DYAS. Additionally, an off-stoichiometric mixture of DYAS and PETMP at a 1:3 ethynyl/thiol ratio was formulated with various amount of EBPADMA to enhance the AFCT mechanism. Similar to the stoichiometric thiol-yne mixture, AFCT-incapable DYPS was used in place of DYAS to isolate the stress relaxation effect of the allyl sulfide functionality. Detailed formulations of each resin such as the ratio of functional groups and weight percent of EBPADMA are presented in Table 5.1. For all resins, 1-hydroxycyclohexylphenylketone (HCPK, Ciba Specialty Chemicals) was utilized at 3 wt% as a photoinitiator.

5.2.2 Methods and Equipment

Shrinkage stress and functional group conversion were monitored simultaneously using tensometry (Paffenbarger Research Center, American Dental Association Health Foundation) coupled with Fourier transform infrared (FTIR) spectroscopy (Nicolet 670) during the photopolymerization of each resin. A tensometer utilizes the cantilever beam deflection theory to evaluate how much the beam deflects under the force generated. Since the compliance of the cantilever beam affects the obtained stress value, it is optimal if the same experimental settings are used to compare the stress of each sample [1, 17]. Here, all resin formulations were evaluated

with a single set of compliance conditions (stainless steel beam with 9cm length) except the DYPS-PETMP resin for which the stress level is higher than can be accurately measured at this compliance. Ultimately, the stress of the thiol-yne resins (DYPS-PETMP and DYAS-PETMP) was measured in another experimental setting (Aluminum beam with 5cm length). The relative stress (see the notation in Figure 5.6) was utilized to estimate the stress of the DYPS-PETMP resin at the previous conditions to compare the stress of all samples on a relative basis.

The tensometer experiment was performed by loading resins (sample size: 6 mm in diameter and 1 mm thick) between two glass rods which grip the cantilever beam and are subsequently irradiated for 10 minutes at 10 mW/cm^2 intensity by a UV lamp (Acticure, EXFO) equipped with a 365 nm bandpass filter. The evolution of the yne, methacrylate, and allyl sulfide double bond concentrations were determined by monitoring the infrared absorption peaks centered at 6483 cm^{-1} (C≡**C-H** stretching, overtone), 6166 cm^{-1} (C=**C-H** stretching, overtone), and 6121 cm^{-1} (C=**C-H** stretching, overtone), respectively. Gaussian fitting was used to deconvolute the peak areas as the methacrylate peak is overlapped with the allyl sulfide peak. [10, 14]

To estimate mechanical properties of the materials, the elastic moduli (E′) and glass transition temperatures of polymerized samples were determined by dynamic mechanical analysis (DMA) (TA Instruments Q800). Samples were prepared by sandwiching the material between 2 glass slides with 1mm thickness spacer with the final sample size being 8mm*5mm*1mm (length*width*thickness, sample size was varied slightly for each experiment) and irradiated at the same conditions as the tensometer experiment. DMA experiments were performed at a strain

and frequency of 0.1% and 1 Hz, respectively, scanning the temperature twice at 1 ºC/minute. The T_g was assigned as the temperature of the tan delta maximum [18-19] of the second thermal scan.

5.3 Results and Discussion

Two primary foci of this work are improvements of the mechanical properties by incorporating methacrylate in the thiol-yne system and evaluation of the stress relaxation effect by AFCT of allyl sulfide functionality in these ternary resins. First, the elastic moduli of the thiol-yne and thiol-yne-methacrylate ternary resins as a function of temperature are shown in Figure 5.3 and summarized in Table 5.1. As the content of the methacrylate increases from 0 wt% to 78 wt%, the elastic modulus values are shifted to the higher temperature region which means that the polymer becomes more glassy owing to the stiff bisphenol A structure in EBPADMA. The rubbery elastic modulus, which is proportional to the crosslinking density of the DYPS-PETMP-EBPADMA network [20], is also increased with increasing EBPADMA content. However, the ternary systems have a lower rubbery elastic modulus as compared with the DYPS-PETMP system since the functional group conversions are lower than the binary system (Table 5.1).

To determine whether DYPS-PETMP-EBPADMA is an appropriate control system which isolates the effect of allyl sulfide AFCT, the elastic modulus of DYAS-PETMP-EBPADMA is presented in Figure 5.3 and Table 5.1. Since the stress evolution is a function of the modulus evolution at the curing temperature and the final network crosslinking density, the allyl sulfide-

containing ternary system which undergoes AFCT should have a similar modulus when compared with the AFCT-incapable propyl sulfide-containing ternary system. The DYAS-PETMP-EBPADMA resin has an almost identical elastic modulus throughout the entire temperature range whencompared with the control DYPS-PETMP-EBPADMA which implies that the allyl sulfide moiety and the AFCT reaction do not alter the polymer network.

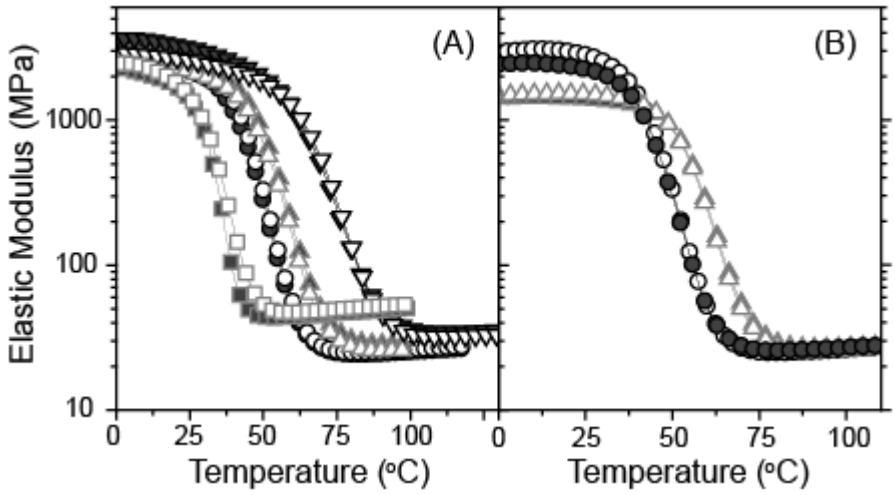

Figure 5.3. (A) Elastic moduli of the thiol-yne-methacrylate ternary resins. Stoichiometrically balanced thiol-yne (functional group ratio thiol : yne = 2 : 1) mixtures were used for the ternary resins. Allyl sulfide-containing resins are represented by an open symbol and propyl sulfide-based resins by a closed symbol. Thiol:yne:methacrylate ratio is 2:1:0 (■, 0 wt% methacrylate), 2:1:2 (●, 58 wt% methacrylate), 2:1:3 (▲, 68 wt% methacrylate), 2:1:5 (▼, 78 wt% methacrylate). (B) Elastic modulus of the off-stoichiometric thiol-yne-methacrylate ternary resins. Off-stoichiometric thiol-yne (functional group ratio thiol : yne = 3 : 1) was used for the ternary resins. Allyl sulfide-based resins are represented by an open symbol and propyl sulfide-based resins by a closed symbol. Thiol:yne:methacrylate ratio is 3:1:2.7 (●, 58 wt% methacrylate), 3:1:4 (▲, 68 wt% methacrylate).

The shrinkage stress that arises in DYPS-PETMP-EBPADMA (AFCT-incapable) polymerizations when varying the EBPADMA amount is presented in Figure 5.4. By incorporating methacrylate into a stoichiometrically balanced thiol-yne resin (thiol to yne = 2 to

1), the stress of the resins is reduced compared with the binary thiol-yne resin (Figure 5.4(A)) whether AFCT occurs or not. The reduced stress is caused by decreased crosslinking density due to the lower yne and methacrylate conversions (Table 5.1) as well as the potential increase in the gel point conversion that arises with the addition of a small amount of methacrylate. As the methacrylate content increases from 58 wt% to 78 wt%, the stress increases since the polymerization-induced stress mainly develops in the post-gelation region especially after vitrification. Here, the chain-growth polymerization of the methacrylate results in early gelation as compared with the step-growth polymerization of the thiol-yne. Excitingly, the shrinkage stress of the ternary resin was even lower than the binary thiol-yne resin even though the ternary resins all form polymers that have higher glass transition temperatures. As discussed before, the glass transition temperature of the thiol-yne and thiol-yne-methacrylate is directly related to the methacrylate monomer content in the resin (Figure 5.4(B)).

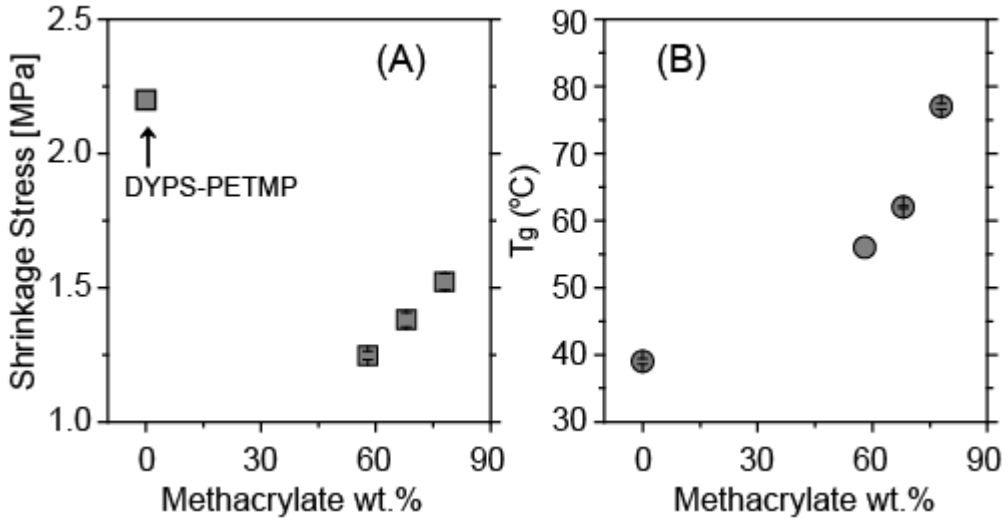

Figure 5.4. (A) Polymerization shrinkage stress and (B) glass transition temperature versus EBPADMA (methacrylate) weight fraction in DYPS-PETMP-EBPADMA ternary resins. The ratio between thiol:yne:methacrylate varies from 2:1:0 (0 wt% methacrylate) to 2:1:5 (78 wt% methacrylate). The thiol-yne mixture was stoichiometrically balanced for all formulations (thiol:yne = 2:1). Samples contain 3 wt% HCPK and are irradiated at 10 mW/cm^2 using 365 nm light. The stress of DYPS-PETMP was estimated according to the relative stress (see the methods and equipment section and Table 5.1).

In addition to the lower stress that occurs in ternary systems relative to binary thiol-yne reactions, stress relaxation was also found to depend strongly on the presence of AFCT-capable allyl sulfides in the yne monomer structure. In Figure 5.3, it was demonstrated that the allyl sulfide-containing DYAS-PETMP-EBPADMA has a nearly identical polymer network as compared with the AFCT-incapable control DYPS-PETMP-EBPADMA. In Figure 5.5, the shrinkage stress of the DYAS-PETMP-EBPADMA resins are compared with the stress of the DYPS-PETMP-EBPADMA. As the allyl sulfide concentration is increased, the stress of the thiol-yne-methacrylate decreased (Figure 5.5(A)). (Note that propyl sulfide-based resin (DYPS-PETMP-EBPADMA) does not include an allyl sulfide functionality but comparative formulations which have the same amount of the thiol/yne/methacrylate are plotted using the corresponding allyl

sulfide concentration. Resin formulations are given in Table 5.1). While the stress of both the propyl and allyl sulfide-containing resins decrease as the allyl sulfide content increases, owing to the decreasing methacrylate content, the difference between the stress of DYAS-PETMP-EBPADMA and DYPS-PETMP-EBPADMA becomes larger. Here, the stress differences between these systems arise almost exclusively because of the AFCT mechanism.

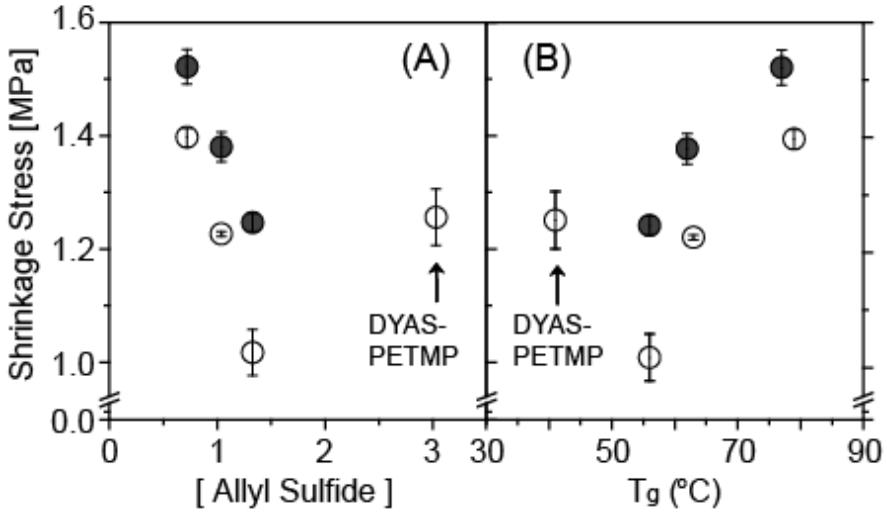

Figure 5.5. (A) Polymerization shrinkage stress versus allyl sulfide concentration and (B) versus glass transition temperature for DYAS-PETMP-EBPADMA (○) and DYPS-PETMP-EBPADMA (●) resins. The ratio of the thiol:yne:methacrylate resin varies from 2:1:0 to 2:1:5. The thiol-yne mixture was stoichiometrically balanced at all conditions (thiol:yne = 2:1). Samples contain 3 wt% HCPK and are irradiated at 10 mW/cm^2 using 365 nm light.

To quantify the stress relaxation associated with AFCT and eliminate the effect of slightly different crosslinking densities between the model and control resin, the final stresses for the allyl and propyl sulfide-containing resins were divided by the rubbery elastic modulus, which is directly related to the crosslink density through rubbery elasticity theory [20]. The ratio of dimensionless stresses in allyl to propyl sulfide-containing resins is denoted as the relative

shrinkage stress (Figure 5.6). The relative stress decreases with increasing allyl sulfide concentration (Figure 5.6A) and decreasing T_g of the material (Figure 5.6B). This result indicates that AFCT reduced the stress effectively even in the glassy ternary system through the mechanism shown in Figure 5.1. Also, the glass transition temperature was improved compared with the binary system while preserving the stress relaxation behavior. A ternary resin consisting of an off-stoichiometric thiol-yne mixture with an excess of thiol functional groups relative to the yne (3 to 1 thiol to yne) exhibited slightly lower relative stress compared with those of the stoichiometric thiol-yne-methacrylate mixture since the increased thiol content promoted the AFCT reaction and the resulting stress relaxation (Figure 5.6).

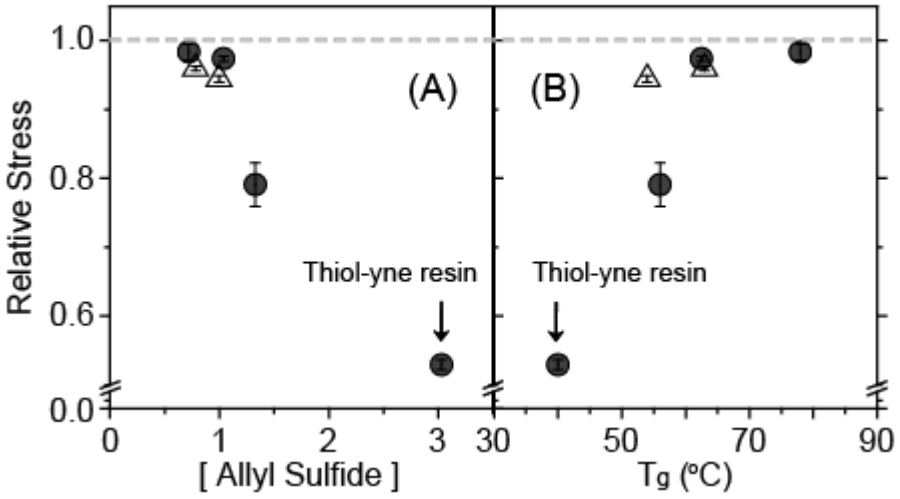

Figure 5.6. (A) Relative polymerization shrinkage stress versus allyl sulfide concentration and (B) versus glass transition temperature for stoichiometric thiol-yne-methacrylate (●, thiol to yne ratio was maintained as 2:1 and methacrylate ratio varies from 0 to 5, thiol:yne:methacrylate = 2:1:0 ~ 2:1:5) and off-stoichiometric thiol-yne-methacrylate (△, thiol to yne ratio was maintained as 3:1 and methacrylate ratio varies from 2.7 to 4, thiol:yne:methacrylate = 3:1:2.7 ~ 3:1:4). Relative stress = (The stress of allyl sulfide-based resin/the rubbery elastic modulus)/ (The stress of propyl sulfide-based resin/the rubbery elastic modulus). The rubbery elastic moduli are taken from the same temperature for allyl and propyl sulfide-based resins. Samples contain 3 wt% HCPK and are irradiated at 10 mW/cm^2 using 365 nm light.

Table 5.1. Summary of the final conversion, T_g, elastic moduli, and shrinkage stress for various resin formulations. Rubbery moduli are measured at the same temperature for both the allyl sulfide-based resin and its analogous non-allyl sulfide containing resin. When the T_gs are different for these formulations, the modulus is taken at the higher T_g + 40°C. *Shrinkage stress of the thiol-yne binary systems are measured at two different tensometer settings (see the experimental method and equipment section). The stress in parenthesis represents the stress value at a different compliance. † The stress of DYPS-PETMP was estimated according to the relative stress.

Yne monomer used in the ternary system (thiol:yne:methacrylate ratio)	Methacrylate weight percent (%)	Allyl sulfide concentration (mol/L)	Final functional group conversion [%]			T_g (°C)	Rubbery E′ at T = 25°C (Before heating) (GPa)	Rubbery E′ at T = T_g + 40°C (MPa)	Shrinkage stress (MPa)
			Methacrylate	Yne	Allyl sulfide				
DYAS (2:1:0)	0	3.03	-	97 ± 0.5	42 ± 2	41 ± 0.4	1.4 ± 0.7	50.3 ± 0.02	1.25 ± 0.005 (0.4 ± 0.0005)*
DYPS (2:1:0)	0	-	-	99 ± 0.2	-	39 ± 0.2	1.4 ± 0.5	47.5 ± 0.02	*2.2*† (0.7 ± 0.0006)*
DYAS (2:1:2)	58	1.33	100 ± 0.4	85 ± 4	67 ± 5	56 ± 0.01	3.0 ± 0.8	25.8 ± 0.03	1.02 ± 0.004
DYPS (2:1:2)	58	-	98 ± 0.2	89 ± 1	-	56 ± 0.1	3.0 ± 0.7	25 ± 0.04	1.25 ± 0.002
DYAS (2:1:3)	68	1.04	98 ± 0.2	76 ± 3	66 ± 4	63 ± 0.2	3.6 ± 0.8	26.1 ± 0.06	1.23 ± 0.0004
DYPS (2:1:3)	68	-	97 ± 0.4	81 ± 2	-	62 ± 0.3	3.2 ± 0.8	28.6 ± 0.6	1.38 ± 0.003
DYAS (2:1:5)	78	0.72	95 ± 0.3	68 ± 3	74 ± 0.2	79 ± 0.4	3.0 ± 0.9	32.5 ± 0.09	1.40 ± 0.002
DYPS (2:1:5)	78	-	94 ± 0.3	73 ± 1	-	77 ± 1	3.0 ± 1.0	34.8 ± 0.07	1.52 ± 0.003
DYAS (3:1:2.7)	58	1.00	99 ± 0.2	90 ± 1	73 ± 4	54 ± 0.1	3.4 ± 0.7	26.5 ± 0.2	1.15 ± 0.0006
DYPS (3:1:2.7)	58	-	99 ± 0.4	94 ± 0.7	-	54 ± 0.5	3.2 ± 0.7	27.1 ± 0.2	1.24 ± 0.003
DYAS (3:1:4)	67	0.78	98 ± 0.1	80 ± 0.2	76 ± 0.2	63 ± 2	1.7 ± 0.5	26 ± 0.1	1.2 ± 0.0004
DYPS (3:1:4)	67	-	98 ± 0.2	90 ± 2	-	63 ± 1	1.7 ± 0.2	27.1 ± 0.2	1.31 ± 0.004

5.4 Conclusions

Methacrylate monomer was incorporated into propyl and allyl sulfide-based thiol-yne resins to increase the polymer glass transition temperature and reduce the stress in addition to investigating stress relaxation associated with AFCT of the allyl sulfide functional group. The glass transition temperature of the ternary systems increased as the methacrylate content increased. One unique outcome was that the shrinkage stress of the ternary resin was even lower than the binary thiol-yne resin until the methacrylate content was 68 wt.% owing to the reduced crosslinking density. The stress relaxation effect associated with AFCT, which is interpreted as the non-dimensionalized relative stress, was improved with increasing allyl sulfide concentration in the ternary resin. In this study, the allyl sulfide-based thiol-yne-methacrylate system demonstrates stress relaxation up to 55% and T_g increase by up to 40^oC compared with the control AFCT-incapable thiol-yne. This ternary system demonstrates approximately 3 times lower stress compared with dimethacrylate monomers [1] while possessing excellent mechanical properties that will be utilized for a variety of structural applications replacing the conventional dimethacrylate monomers.

5.5 Acknowledgements

This investigation was supported by NIDCR 2 R01 DE-010959-11 from the National Institutes of Health and NSF 0933828.

5.6 References

(1) Lu, H.; Carioscia, J. A.; Stansbury, J. W.; Bowman, C. N. *Dent Mater* **2005,** *21,* 1129-1136.

(2) Burke, F. J. T.; Cheung, S. W.; Mjor, I. A.; Wilson, N. H. F. *Quintessence International* **1999,** *30,* 234-242.

(3) Carioscia, J. A.; Lu, H.; Stanbury, J. W.; Bowman, C. N. *Dent Mater* **2005,** *21,* 1137-1143.

(4) Ge, J. H.; Trujillo-Lemon, M.; Stansbury, J. W. *Macromolecules* **2006,** *39,* 8968-8976.

(5) Stansbury, J. W. *Polymers of Biological and Biomedical Significance* **1994,** *540,* 171-183.

(6) Lee, T. Y.; Cramer, N. B.; Hoyle, C. E.; Stansbury, J. W.; Bowman, C. N. *J Polym Sci Pol Chem* **2009,** *47,* 2509-2517.

(7) Scott, T. F.; Draughon, R. B.; Bowman, C. N. *Advanced Materials* **2006,** *18,* 2128-+.

(8) Scott, T. F.; Schneider, A. D.; Cook, W. D.; Bowman, C. N. *Science* **2005,** *308,* 1615-1617.

(9) Kloxin, C. J.; Scott, T. F.; Adzima, B. J.; Bowman, C. N. *Macromolecules* **2010,** *43,* 2643-2653.

(10) Kloxin, C. J.; Scott, T. F.; Bowman, C. N. *Macromolecules* **2009,** *42,* 2551-2556.

(11) Park, H. Y.; Kloxin, C. J.; Scott, T. F.; Bowman, C. N. *Macromelecules* **2010,** *43,* 10188-10190.

(12) Fairbanks, B. D.; Scott, T. F.; Kloxin, C. J.; Anseth, K. S.; Bowman, C. N. *Macromolecules* **2009,** *42,* 211-217.

(13) Chan, J. W.; Shin, J.; Hoyle, C. E.; Bowman, C. N.; Lowe, A. B. *Macromolecules* **2010,** *43,* 4937-4942.

(14) Park, H. Y.; Kloxin, C. J.; Scott, T. F.; Bowman, C. N. *Dent Mater* **2010,** *26,* 1010-1016.

(15) Evans, R. A.; Rizzardo, E. *Macromolecules* **2000,** *33,* 6722-6731.

(16) Evans, R. A.; Rizzardo, E. *J Polym Sci Pol Chem* **2001,** *39,* 202-215.

(17) Lu, H.; Stansbury, J. W.; Dickens, S. H.; Eichmiller, F. C.; Bowman, C. N. *Journal of Materials Science-Materials in Medicine* **2004,** *15,* 1097-1103.

(18) Ferrillo, R. G.; Achorn, P. J. *Journal of Applied Polymer Science* **1997,** *64,* 191-195.

(19) Li, G.; Lee-Sullivan, P.; Thring, R. W. *Journal of Thermal Analysis and Calorimetry* **2000,** *60,* 377-390.

(20) Flory, P. J. *Principles of Polymer Chemistry*; Cornell University Press, Ithaca, NY, 1953.

Chapter 6

Stress relaxation via addition-fragmentation chain transfer in high T_g, high conversion methacrylate-based systems

To reduce shrinkage stress which arises during polymerization of crosslinked polymers, allyl sulfide functional groups were incorporated into methacrylate polymerizations to determine their effect on stress relaxation via addition-fragmentation chain transfer (AFCT). Additionally, stoichiometrically balanced thiol and allyl sulfide-containing norbornene monomers were incorporated into the methacrylate resin to maximize the overall functional group conversion and promote AFCT while also enhancing the polymer's mechanical properties. Shrinkage stress and reaction kinetics for each of the various functional groups were measured by tensometry and Fourier-transform infrared (FTIR) spectroscopy, respectively. AFCT resulted in a 63% reduction of polymerization stress in the allyl sulfide-containing thiol-norbornene-methacrylate system when compared with dimethacrylates. Inclusion of a monomer that contained both a methacrylate functional group and a cyclic structure that ring opens during polymerization to incorporate an allyl sulfide moiety into the polymer structure was evaluated. This approach improved the T_g and crosslinking density without any concomitant increase in stress as compared to an analogous AFCT incapable ethyl sulfide-based methacrylate.

6.1 Introduction

Polymerization shrinkage stress is a deleterious phenomenon that plagues numerous polymer material applications[1-3] and results in warping, microcracks, and material failure. Polymerization shrinkage itself results from the decrease in molecular spacing between monomers as the van der Waals interactions present in the monomer are replaced with covalent bonds that bring the monomer units together more closely. Previous approaches used to combat polymerization stress have focused on minimizing the volume change, using materials that exhibit low polymerization shrinkage, such as ring-opening polymerizations[4] or polymerization induced phase separation[5]. Additionally, strategies that delayed the gel-point conversion, such as thiol-ene[6] and thiol-yne[7-9] polymerizations, have been used to enable the material to shrink in the early stages of the reaction without leading to any significant stress accumulation. Here, prior to the gel-point, a material is capable of dissipating shrinkage via the viscous flow of the monomer/oligomer species; however, after gelation molecular rearrangement is reduced and stress accumulates. To address this issue, we have explored a methodology of utilizing radical-mediated reversible covalent bond structures to induce the rearrangement of network strands, thus providing a route for post-gel-point network stress relaxation through accommodation of the shrinkage. Specifically, we have utilized addition-fragmentation chain transfer (AFCT) which enables the radical-mediated repetitive breaking and reforming of polymer network strands throughout the polymerization[10-12]. The initial demonstrations of reduced polymerization shrinkage stress using ACFT employed the allyl sulfide functional group in both thiol-ene[11] and thiol-yne[13] materials. These systems have the additional advantages of possessing delayed

gelation as well as negligible oxygen inhibition[6, 14]. While these systems demonstrated decreased polymerization stress, the crosslinking density of these step-growth polymers was necessarily lower than their chain growth counterparts, leading to a lower glass transition temperature and modulus which precluded their use in many applications, even though thiol-yne materials do possess significantly improved mechanical properties.

Methacrylate-based materials are widely used in a variety of applications, such as electrical materials[15], optical materials, and dental restorative materials[16], as they are typically strong, lightweight, possess good impact-strength, and transparency. Unfortunately, the rapid polymerization of multifunctional methacrylate monomers generates a large amount of stress, on the order of megapascals[17], owing to the typical chain-growth polymerization characteristics, particularly early gelation[18-19]. To achieve enhanced mechanical properties with the stress relaxing capabilities of the AFCT mechanism, thiol-ene resins containing allyl sulfide moieties were incorporated into dimethacrylate resins[20] to induce both a mixed step-chain growth mechanism while simultaneously enabling AFCT-induced relaxation. As expected, the increased methacrylate content enhances the mechanical properties such as glass transition temperature and elastic modulus.[21-22] While stress relaxation was observed, the effect was significantly reduced for materials possessing a super-ambient glass transition temperature due to a limited concentration of allyl sulfides from the thiol-ene component of the resin.

Here, we incorporate the allyl sulfide functional group directly into the methacrylate monomer to investigate its effect on stress relaxation. In addition, tetrafunctional thiol and allyl sulfide-

containing difunctional norbornene monomers were formulated into the methacrylate resin to further enhance the mechanical properties and increase the capability for undergoing AFCT, as the bulky norbornene structure is expected to increase the glass transition temperature.

6.2 Experimental section

6.2.1 Materials

To investigate stress relaxation via the AFCT capability of the allyl sulfide functional group in the methacrylate system, 1,9-bis[2-(methacryloyloxyethyl) succinyloxy]-3,7-dithia-5-methylene-nonane (SAS, Succinate Allyl Sulfide, ***(1)*** in Figure 6.1) and 2-(methacryloyloxyethyl) 7-methylene-1,5-dithiocan-3-yl phthalate (PAS, Phthalate Allyl Sulfide, ***(3)*** in Figure 6.1) were designed and synthesized. To isolate the effect of the allyl sulfide functional group, 1,9-bis[2-(methacryloyloxyethyl) succinyloxy]-3,7-dithia-5-methyl-nonane (SPS, Succinate Propyl Sulfide, ***(2)*** in Figure 6.1) and 2-(methacryloyloxyethyl) 7-methyl-1,5-dithiocan-3-yl phthalate (PES, Phthalate Ethyl Sulfide, ***(4)*** in Figure 6.1) were additionally designed and synthesized to be used as molecular analogs, since these monomers are nearly identical in structure but are incapable of undergoing AFCT. PAS and PES were synthesized by the procedure in the literature [23]. 2-Methylene-propane-1,3-di(norbornene sulfide) (NAS, ***(5)*** in Figure 6.1) and 2-Methyl-propane-1,3-di(norbornene sulfide) (NPS, ***(6)*** in Figure 6.1) which is an AFCT-incapable analog of NAS were synthesized from 5-bromomethyl norbornene with 3-mercapto-2-(mercaptomethyl)-1-propene and 1,3-dimercapto-2-methylpropane, respectively, according to the method described

in the literature [11, 24-25]. The waxy/hazy solid (NAS) and viscous/colorless liquid (NPS) were received after vacuum distillation at 230°C at 0.3 mmHg and 200°C at 0.3 mmHg, respectively. Throughout this study, all resins includes 1 wt% of 1-hydroxycyclohexylphenylketone (HCPK, ***(8)*** in Figure 6.1) as a UV-photoinitiator.

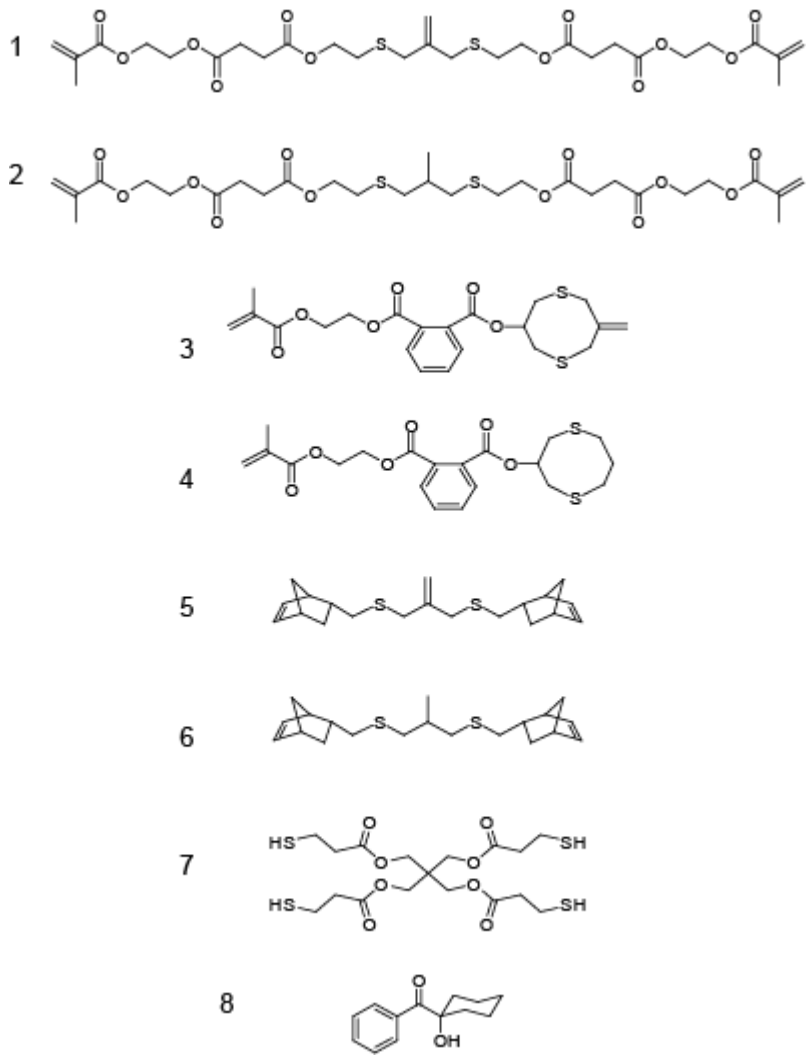

Figure 6.1. Materials used: (1) SAS, (2) SPS, (3) PAS, (4) PES, (5) NAS, (6) NPS, (7) PETMP, and (8) HCPK.

Synthesis of 2-Methylenepropane-1,3-bis(2-hydroxyethyl sulfide)

2-Mercaptoethanol (25.60 g, 0.328 mol, Alfa Aesar) was dissolved in 100 ml ethanol in a 500 ml 2-neck round-bottom flask equipped with a magnetic stirring bar, condenser and a dropping funnel. With vigorous stirring, sodium metal (8.20 g, 0.356 mol, Alfa Aesar) was added in small pieces in a slow manner to control the exotherm during addition. After complete addition of the sodium metal, the mixture was stirred under nitrogen blanket until the flask contents cooled down to room temperature. A solution of 3-chloro-2-chloromethyl-1-propene (20 g, 0.16 mol, Secant Chemicals Inc.) in 50 mL ethanol was added drop-wise using the dropping funnel to give a white cloudy mixture then a heterogeneous mixture with a white solid by the time all the dichloro propene component was added. The flask contents were then refluxed for 45 minutes then cooled to room temperature. The white solid was removed by vacuum filtration and filter cake was washed with excess ethanol on top of the original filtrate. The solvent was removed in a rotary evaporator followed by drying in a vacuum pump to give a colorless liquid. The structure of the obtained product was confirmed by Nuclear Magnetic Resonance (NMR). If required, vacuum distillation (6-7 torr) at 135-150 ^{o}C can be used for purification of the crude product.

Synthesis of 2-Methylpropane-1,3-bis(2-hydroxyethyl sulfide)

Crude 2-methylpropane-1,3-bis(2-hydroxyethyl sulfide) was prepared from 2-methyl-1-bromo-3-chloropropane (9.57g, 0.169 mol, Sigma Aldrich), mercaptoethanol (26.44 g, 0.339 mol, TCI America) and sodium metal (8.6 g, 0.374 mol, Lancaster Synthesis Inc.) in a method similar to the one used for methylenepropane-1,3-bis(2-hydroxyethyl sulfide) above. Vacuum distillation of 2-methypropane-1,3-bis(2-hydroxyethyl sulfide) at 6-8 torr and 140-160 ^{o}C gave a colorless

liquid with 77.5% recovery. NMR was used to confirm the identity.

Synthesis of 2-Methylenepropane-1,3-bis(2-[2-methacryloyloxyethyl succinyl]ethyl sulfide) ***(SAS, Figure 6.1(1))***

2-Methylenepropane-1,3-bis(2-hydroxyethyl sulfide) (10.6 g, 0.051 mol) was dissolved in 100 ml ethylacetate in a 500 ml 3-neck round bottom flask equipped with a dropping funnel on one arm, a magnetic stirring bar and dry air blanket. To the solution was added *mono*-methacryloyloxyethylsuccinic acid (25 g, 0.108 mol, Sigma Aldrich), followed by N,N-dimethylamino pyridine (DMAP, 1.35 g, 0.011 mol, Alfa Aesar). The mixture was cooled in an ice batch with continuous stirring. In a separate flask, dicyclohexyl carbodiimide (DCC, Alfa Aesar) was dissolved in 150 ml ethylacetate. The DCC solution was placed in the dropping funnel then added drop-wise to the flask as the flask contents were kept cold (0 – 10 ^{o}C). After complete addition of the DCC solution, the flask contents were continuously stirred in the ice bath for 30 minute then at room temperature overnight. Next day, 50 ml of hexanes were added and all solid formed in the reaction flask was removed and washed by vacuum filtration. The filtrate was then extracted with a mixture of 100 ml 1 N HCl, 150 mL 10% aqueous sodium bicarbonate, and 100 ml water. The organic layer was dried (Na_2SO_4) then concentrated in a rotary evaporator followed by drying to give a light yellow liquid in 90% yield. The structure was confirmed by NMR.

Synthesis of 2-Methylpropane-1,3-bis(2-[2-methacryloyloxyethyl succinyl]ethyl sulfide) ***(SPS, Figure 6.1(2))***

Mono-HEMA succinic acid intermediate was made in-situ then used in the second step in a one-pot fashion. 2-Hydroxyethyl 2-methylprop-2-enoate (HEMA, 10 g, 0.084 mol, Sigma Aldrich) and succinic anhydride (9.35 g, 0.094 mol, Sigma Aldrich) were charged into a round bottom flask equipped with a magnetic stirring bar, a dry air blanket and dropping funnel. DMAP (1.15 g, 0.009 mol) and BHT (0.035 g) were added to the flask. The mixture was heated with stirring at 90 ^{o}C for 5 hours to give a colorless viscous liquid. The flask was left to cool to room temperature. Ethyl acetate (approximately 50 ml) was added and the mixture was cooled in an ice bath to 0-5^{o}C. Charged into the dropping funnel was a solution of DCC (17.3 g, 0.089 mol, Alfa Aesar) in 50 ml ethylacetate. The DCC solution was carefully and slowly added to the vigorously stirred cold solution over 30 minutes. The mixture was stirred at 0-5^{o}C for 30 minutes then at room temperature overnight. Next day, the reaction was worked up similarly to SAS above. The structure was confirmed by NMR.

Synthesis of 5-bromomethyl norbornene

1,3-dicyclopentadiene (16g, 0.12mol, ACROS), allyl bromide (35g, 0.29mol, Sigma Aldrich), and hydroquinone (81mg, 0.74mmol, Aldrich) were added in a 50 ml pressure vessel and heated at 170 °C for 12 hours. The crude oil was purified with normal distillation at 175 °C before use. The structure was confirmed by NMR.

6.2.2 Methods and Equipment

The shrinkage stress and functional group conversion were simultaneously observed during polymerization using a tensometer coupled with a FTIR spectrometer (Nicolet 670), which was equipped with near-infrared transmitting optical fiber patch cables and an indium gallium arsenide (InGaAs) detector [6, 26]. The tensometer was developed by the Paffenbarger Research Center (American Dental Association Health Foundation) to measure the stress during photopolymerization. Stress evolution is measured by the cantilever beam deflection that is detected by the LVDT (linear variable displacement transducer) displacement. In the tensometer, one glass rod is fixed to the bottom plate and another rod is connected to the cantilever beam. The formulated resin was injected between the two glass rods, which results in a specimen geometry of 6mm diameter and 1mm thickness. Samples were irradiated with 365nm-isolated UV light at 10 or 50mW/cm^2 (Acticure 4000, EXPO) for 5 or 16 minutes. Evolution of the methacrylate, norbornene and allyl sulfide double bond concentrations were determined by monitoring the infrared absorption peaks centered at 6166 cm^{-1} (C=**C-H** stretching, overtone), 6111 cm^{-1} (C=**C-H** stretching, overtone), and 6121 cm^{-1} (C=**C-H** stretching, overtone), respectively. As the methacrylate peak is overlapped with the norbornene and allyl sulfide peaks, Gaussian fitting was used to deconvolute these peak areas.

The elastic moduli (E′) and glass transition temperatures (T_gs) of polymerized samples were measured by dynamic mechanical analysis (DMA, TA Instruments Q800). Specimens were prepared and irradiated under the identical conditions as performed in the tensometer experiment.

DMA experiments were performed at a constant strain and frequency of 0.1% and 1 Hz, respectively, scanning the temperature from -50°C to 140°C twice at 1°C/minute; the temperature scan was repeated to ensure the absence of dark polymerization at temperatures greater than the T_g [27-28].

6.3 Results and Discussion

The allyl sulfide functional group was incorporated into two different monomers containing methacrylate functionalities: a symmetrical dimethacrylate with a central allyl sufide functional group (succinate-based allyl sulfide, SAS - Figure 6.1, structures 1) and asymmetrical monomethacrylate with an allyl sulfide containing ring that participates in the polymerization through ring opening (phathalate-based allyl sulfide, PAS - Figure 6.1, structures 3). Both monomers were designed to form polymer networks while PAS has the ring opening functional group and the less flexible structure for further stress reduction and higher glass transition temperature, respectively. To isolate the stress relaxation effect of the allyl sulfide group, analogous monomers were synthesized that possess a nearly identical molecular structure, however, each "control" monomer does not contain an allyl sulfide and is thus incapable of undergoing AFCT. These monomers were created such that, to the greatest extent possible, differences in the polymerization stress development could be attributed to the presence of the AFCT mechanism for stress relaxation. Specifically, the allyl sulfide in SAS and PAS was replaced by ethyl sulfide (SPS - Figure 6.1, structure 2) or propyl sulfide (PES - Figure 6.1, structure 4), respectively.

The comparison between the conversion and stress evolution in the methacrylate monomers is shown in Figure 6.3. When the allyl sulfide was incorporated into the dimethacrylate-based monomer (SAS), the stress evolution was nearly identical whether the methacrylate monomer capable of stress relaxation or not, indicating that the allyl sulfide functional group participates only minimally in AFCT during this polymerization. One possible explanation for this behavior is that the allyl sulfide exhibits reduced reactivity towards carbon-centered radicals such as those involved in the methacrylate polymerization. (Figure 6.2 (B)). This explanation would also result in low conversion of the allyl sulfide in SAS (Table 6.1) and lead to SAS and SPS exhibiting similar mechanical properties (Figure 6.4), as observed. To explore this possibility further, a tetra-functional thiol (PETMP) was formulated into these resins to introduce thiyl radicals, which have been shown to have excellent reactivity towards allyl sulfides and thus promote AFCT, as shown in Figure 6.2 (A).[11] Unfortunately, the addition of PETMP resulted in an enhanced shrinkage stress for the allyl sulfide-containing resins compared with the propyl sulfide-containing resins (Figure 6.3(B)). This outcome is attributed to the enhanced crosslinking density of SAS-PETMP resin owing to high conversion of the allyl sulfide functional group (30%).

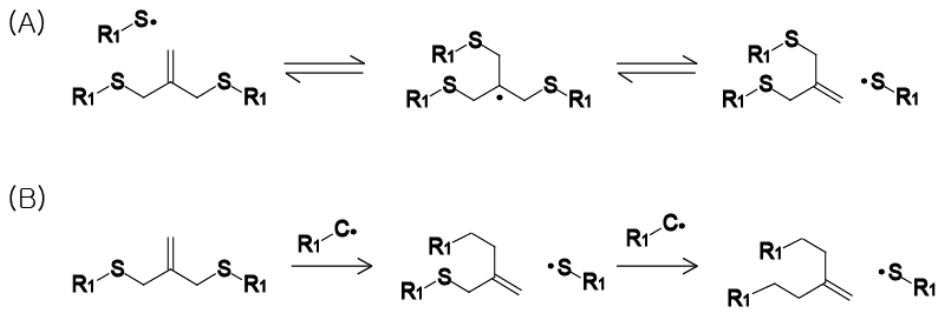

Figure 6.2. (A) Reversible AFCT mediated by reactions with the thiyl radical and (B) irreversible allyl sulfide AFCT mediated by reactions with a carbon-centered radical.

The shrinkage stress of the phthalate allyl sulfide-based methacrylate (PAS) resin is lower than in the succinate allyl sulfide-based methacrylate resin. However, as shown in Figure 6.3(B), the phthalate ethyl sulfide methacrylate (PES) demonstrated similar stress evolution behavior as the allyl sulfide-containing material (PAS). While the molecular structures of the two monomers (PAS and PES) are nearly identical, the allyl sulfide acts as an additional polymerizable functional group upon ring opening, which is essential for crosslinking in this material. This effect is clearly seen in the material properties for these two resins (see Figure 6.4) as well, where PES does not exhibit a clearly defined rubbery modulus but instead the behavior more closely resembles that of a loosely crosslinked polymer melt. This outcome suggests that, as expected, the ethyl sulfide ring in the PES structure does not significantly react to form crosslinks. Nevertheless, it should be noted that the two materials have nearly identical polymerization stresses, indicating that the additional crosslinking and higher modulus resulting from the allyl sulfide monomer enhance the mechanical properties while not effecting the polymerization stress.

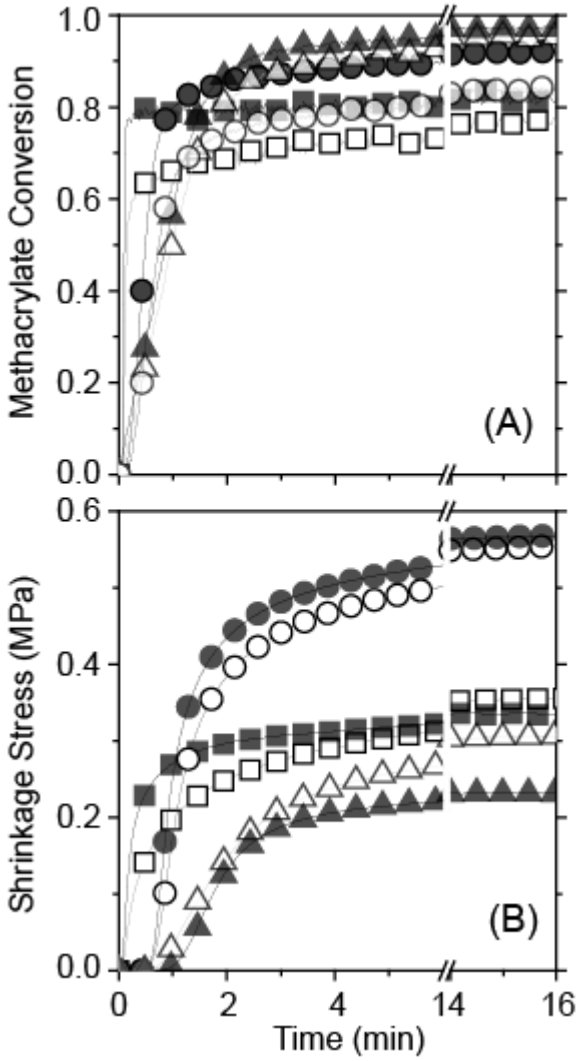

Figure 6.3. (A) Methacrylate conversion, (B) shrinkage stress versus time for PAS(□) (allyl sulfide-based monomethacrylate, structure ***3*** in Figure 6.1), PES(■) (ethyl sulfide-based monomethacrylate, structure ***4*** in Figure 6.1), SAS(○) (allyl sulfide-based dimethacrylate, structure ***1*** in Figure 6.1), SPS(●) (propyl sulfide-based dimethacrylate, structure ***2*** in Figure 6.1), SAS-PETMP(△), and SPS-PETMP(▲). Samples were formulated with 1 wt % HCPK. All resins except PAS and PES (50mW/cm^2) were irradiated at 365 nm, 1 mW/cm^2 for 16 min.

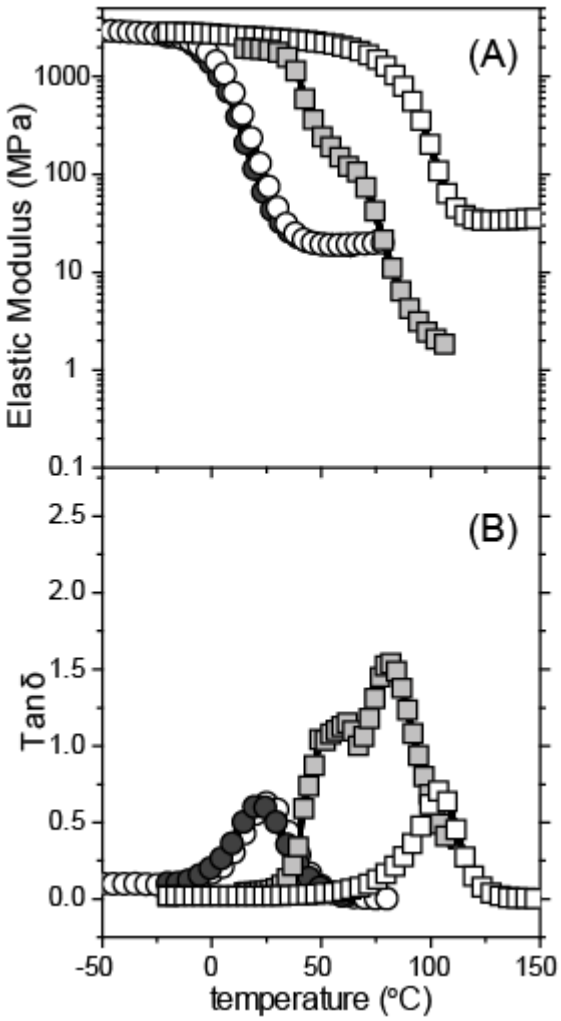

Figure 6.4. (A) Elastic modulus, (B) tanδ versus temperature of PAS(□) (allyl sulfide-based monomethacrylate, structure ***3*** in Figure 6.1), PES(■) (ethyl sulfide-based monomethacrylate, structure ***4*** in Figure 6.1), SAS(○) (allyl sulfide-based dimethacrylate, structure ***1*** in Figure 6.1), and SPS(●) (propyl sulfide-based dimethacrylate, structure ***2*** in Figure 6.1). Samples were formulated with 1 wt % HCPK. SAS and SPS were irradiated at 365 nm, 1 mW/cm^2 for 16 min. PAS and PES were irradiated at 365 nm, 50 mW/cm^2 for 16 min.

As discussed above, the addition of thiol-ene monomers into a methacrylate resin can have the effect of enhancing stress reduction by promoting allyl sulfide AFCT in the methacrylate system [20]. As our goal is to have a low-stress material possessing a super-ambient T_g, a stoichiometrically balanced mixture of thiol-ene monomers was incorporated into phthalate-based methacrylates (PAS and PES), since their T_gs are higher than those of the SAS and SPS resins. Further, to maximize the amount of allyl sulfide in the crosslinked network, a dinorbornene (i.e., 'diene') monomer was synthesized. The dinorbornene allyl sulfide (NAS) monomer was compared with a propyl sulfide-containing norbornene (NPS) to isolate the stress relaxation effect of the allyl sulfide functional group. Thus, by utilizing PAS and PES with thiol-NAS and thiol-NPS, the effect of the allyl sulfide being in either the thiol-norbornene or the methacrylate component of this ternary resin is elucidated. In each of the four combinations presented here, the norbornene, thiol, and methacrylate group were stoichiometrically balanced.

The reaction kinetics in all four resins exhibited similar behavior, where the methacrylate functional group proceeded to nearly complete conversion at a more rapid rate than the thiol-ene component (Figure 6.5(A)). The slightly slower step-growth polymerization of norbornene and thiol demonstrated a similar reaction rate for all samples as well as a lower final conversion which presumably owes to the reduced molecular mobility associated with vitrification (Figure 6.5(B)). The allyl sulfide conversion was slow and limited to at most 20% conversion (Figure 6.5(C)). Surprisingly, the allyl sulfide functional group exhibited negligible loss when present only in the methacrylate monomer (i.e., NPS-PETMP-PAS). As the rubbery modulus of the NPS-PETMP-PAS is much greater than NPS-PETMP-PES (i.e., without the ring opening

component), the allyl sulfide is being incorporated into the network via ring-opening, but it is not being consumed. Since the AFCT mechanism results in ring-opening while also preserving the allyl sulfide functional group (see Figure 6.2A), we conclude that stress relieving AFCT must be occurring subsequent to the ring opening reaction. This outcome is further evidence by NAS-PETMP-PAS having lower polymerization stress than NPS-PETMP-PAS, which has a reduced allyl sulfide content in the formulation (i.e., NPS versus NAS). Moreover, NAS-PETMP-PAS has a higher crosslink density, which in the absence of AFCT would lead to larger polymerization stress – that is not observed because of the AFCT-induced rearrangement of the network.

While the shrinkage stress of NAS-PETMP-PES is lower than that of NPS-PETMP-PAS (Figure 6.5(D)), the rubbery modulus is also found to be lower, indicating a lower crosslinking density. This behavior is similar to what was found in the comparison of PAS and PES when they were polymerized as a single component, where the low crosslinking density most likely accounted for the lower stress (Figure 6.6(A)). Unlike the PES single component resin, the modulus as a function of temperature for the tertiary resin reveals a rubbery modulus that owes to the additional crosslinking of the thiol-ene component. Despite the increased crosslinking, the polymerization stress is over an order of magnitude less in these systems while still possessing a super-ambient glass transition temperature.

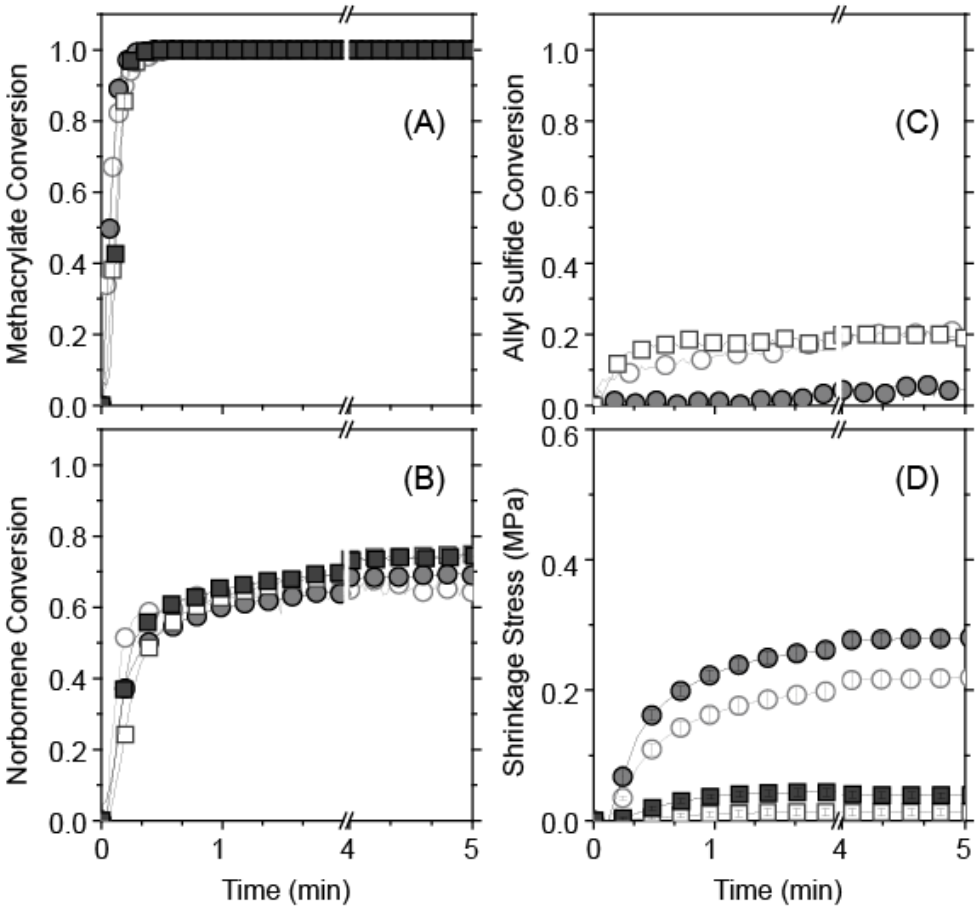

Figure 6.5. (A) Methacrylate conversion, (B) norbornene conversion, (C) allyl sulfide conversion, and (D) shrinkage stress versus time for stoichiometric mixtures of NAS-PETMP-PAS(○), NPS-PETMP-PAS(●), NAS-PETMP-PES(□), and NPS-PETMP-PES(■). Samples were formulated with 1 wt % HCPK, and irradiated at 365 nm and 50 mW/cm^2 for 5 min.

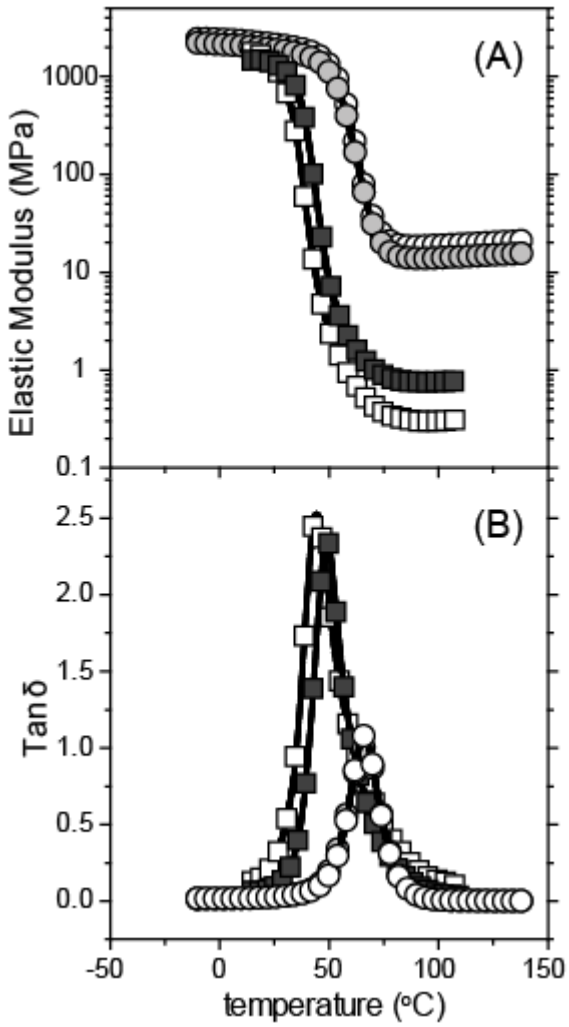

Figure 6.6. (A) Elastic modulus and (B) tan δ versus temperature for stoichiometrically balanced mixtures of NAS-PETMP-PAS(○), NPS-PETMP-PAS(●), NAS-PETMP-PES(□), and NPS-PETMP-PES(■). Norbornene:thiol:methacrylate ratio is 1:1:1 for all resins. Samples were formulated with 1 wt % HCPK, and irradiated at 365 nm and 50 mW/cm^2 for 5 min.

Table 6.1. Summary of final conversion, T_g, and elastic moduli. Rubbery moduli are measured at the same temperature for both the allyl sulfide-based resin and its analogous non-allyl sulfide containing resin. When the T_gs are different for these formulations, the modulus is taken at the higher T_g + 40°C.

Vinyl ether monomer used in the ternary system (thiol:vinyl ether:methacrylate ratio)	Final functional group conversion [%]			Stress (MPa)	T_g (°C)	Rubbery elastic modulus at $T = T_g + 40°C$ (MPa)	Elastic modulus at T = 25°C (before heating) (GPa)
	Methacrylate	Norbornene	Allyl sulfide				
SAS	84 ± 0.8	-	10 ± 1.5	0.55 ± 0.004	24 ± 1	19 ± 0.2	0.7 ± 0.08
SPS	92 ± 0.5	-	-	0.57 ± 0.004	20 ± 1	18 ± 0.1	0.6 ± 0.02
PAS	77 ± 0.2	-	16 ± 0.2	0.36 ± 0.01	102 ± 0.7	35 ± 0.3	3.1 ± 0.6
PES	82 ± 0.7	-	-	0.33 ± 0.01	80 ± 4	2 ± 0.8	1.3 ± 0.4
NAS-PETMP-PAS	100 ± 0.1	64 ± 0.5	21 ± 0.9	0.21 ± 0.01	65 ± 1	19 ± 0.5	2.3 ± 0.3
NPS-PETMP-PAS	100 ± 0.1	70 ± 0.8	5 ± 0.2	0.28 ± 0.01	65 ± 2	14 ± 0.4	2.0 ± 0.4
NAS-PETMP-PES	100 ± 0.1	75 ± 0.4	19 ± 0.6	0.01 ± 0.005	43 ± 1	0.3 ± 0.01	1.0 ± 0.08
NPS-PETMP-PES	100 ± 0.1	74 ± 0.2	-	0.04 ± 0.005	48 ± 0.8	0.8 ± 0.01	1.1 ± 0.06

6.4 Conclusions

Stress relaxation during the photopolymerization of monomers containing allyl sulfide functional groups was evaluated in methacrylate and thiol-norbornene-methacrylate systems. The allyl sulfide's capability to undergo AFCT resulted in a decrease in polymerization stress when compared with analogous materials incapable of undergoing AFCT while also having similar crosslink densities. The ring opening allyl sulfide-based methacrylate (PAS) enhanced the T_g and crosslinking density without a concomitant increase in stress compared with ethyl sulfide-based methacrylate (PES). Thiol-norbornene resins were copolymerized in ring opening allyl sulfide-based methacrylate (PAS) to facilitate AFCT as well as to incorporate the benefits associated with the thiol-ene reaction. The allyl sulfide functional group in the NAS-PETMP-PAS system demonstrated 3 times lower stress compared to dimethacrylate resin (SPS) as well as high T_g and high conversion.

6.5 Acknowledgements

This investigation was supported by NIDCR 2 R01 DE-010959-11 from the National Institutes of Health and NSF 0933828.

6.6 References

(1) Drury, C. J.; Mutsaers, C. M. J.; Hart, C. M.; Matters, M.; de Leeuw, D. M. *Applied Physics Letters* **1998,** *73,* 108-110.

(2) Stansbury, J. W.; Bowman, C. N.; Newman, S. M. *Physics Today* **2008,** *61,* 82-83.

(3) Yoffe, A. D. *Advances in Physics* **2001,** *50,* 1-208.

(4) Alcoutlabi, M.; McKenna, G. B.; Simon, S. L. *Journal of Applied Polymer Science* **2003,** *88,* 227-244.

(5) Lu, H.; Trujillo-Lemon, M.; Ge, J.; Stansbury, J. W. *Compend Contin Educ Dent* **2010,** *31 Spec No 2,* 1-4.

(6) Lu, H.; Carioscia, J. A.; Stansbury, J. W.; Bowman, C. N. *Dent Mater* **2005,** *21,* 1129-1136.

(7) Chan, J. W.; Shin, J.; Hoyle, C. E.; Bowman, C. N.; Lowe, A. B. *Macromolecules* **2010,** *43,* 4937-4942.

(8) Fairbanks, B. D.; Scott, T. F.; Kloxin, C. J.; Anseth, K. S.; Bowman, C. N. *Macromolecules* **2009,** *42,* 211-217.

(9) Lowe, A. B.; Hoyle, C. E.; Bowman, C. N. *Journal of Materials Chemistry* **2010,** *20,* 4745-4750.

(10) Kloxin, C. J.; Scott, T. F.; Adzima, B. J.; Bowman, C. N. *Macromolecules* **2010,** *43,* 2643-2653.

(11) Kloxin, C. J.; Scott, T. F.; Bowman, C. N. *Macromolecules* **2009,** *42,* 2551-2556.

(12) Scott, T. F.; Schneider, A. D.; Cook, W. D.; Bowman, C. N. *Science* **2005,** *308,* 1615-1617.

(13) Park, H. Y.; Kloxin, C. J.; Scott, T. F.; Bowman, C. N. *Macromelecules* **2010,** *43,* 10188-10190.

(14) Carioscia, J. A.; Lu, H.; Stanbury, J. W.; Bowman, C. N. *Dent Mater* **2005,** *21,* 1137-1143.

(15) Kloosterboer, J. G. *Advances in Polymer Science* **1988,** *84,* 1-61.

(16) Peutzfeldt, A. *European Journal of Oral Sciences* **1997,** *105,* 97-116.

(17) Kleverlaan, C. J.; Feilzer, A. J. *Dent Mater* **2005,** *21,* 1150-1157.

(18) Labella, R.; Lambrechts, P.; Van Meerbeek, B.; Vanherle, G. *Dent Mater* **1999,** *15,* 128-137.

(19) Walls, A. W. G.; Mccabe, J. F.; Murray, J. J. *Journal of Dentistry* **1988,** *16,* 177-181.

(20) Park, H. Y.; Kloxin, C. J.; Scott, T. F.; Bowman, C. N. *Dent Mater* **2010,** *26,* 1010-1016.

(21) Lee, T. Y.; Carioscia, J.; Smith, Z.; Bowman, C. N. *Macromolecules* **2007,** *40,* 1473-1479.

(22) Lee, T. Y.; Smith, Z.; Reddy, S. K.; Cramer, N. B.; Bowman, C. N. *Macromolecules* **2007,** *40,* 1466-1472.

(23) Ahmed S. Abuelyaman, S. B. M., Kevin M. Lewandowski, David J. Plaut Dental compositions containing hybrid monomers. 2011.

(24) Evans, R. A.; Rizzardo, E. *Macromolecules* **2000,** *33,* 6722-6731.

(25) Evans, R. A.; Rizzardo, E. *J Polym Sci Pol Chem* **2001,** *39,* 202-215.

(26) Lu, H.; Stansbury, J. W.; Dickens, S. H.; Eichmiller, F. C.; Bowman, C. N. *Journal of Materials Science-Materials in Medicine* **2004,** *15,* 1097-1103.

(27) Ferrillo, R. G.; Achorn, P. J. *Journal of Applied Polymer Science* **1997,** *64,* 191-195.

(28) Li, G.; Lee-Sullivan, P.; Thring, R. W. *Journal of Thermal Analysis and Calorimetry* **2000,** *60,* 377-390.

Chapter 7

Novel Dental Restorative Materials having Low Polymerization Shrinkage Stress via Stress Relaxation by Addition-Fragmentation Chain Transfer

To produce a reduced stress dental restorative material while simultaneously maintaining excellent mechanical properties, we have incorporated an allyl sulfide functional group into norbornene-methacrylate monomer resins. We hypothesize that the addition-fragmentation chain transfer (AFCT) enabled by the allyl sulfide will relieve stress in these methacrylate-based systems while retaining excellent mechanical properties owing to the high glass transition temperature of the norbornene. Allyl sulfide-containing dinorbornene was stoichiometrically formulated with a ring-structured allyl sulfide-possessing methacrylate. To evaluate the stress relaxation effect as a function of the allyl sulfide concentration, a propyl sulfide-based dinorbornene, not capable of addition-fragmentation, was also formulated with the methacrylate monomer. Shrinkage stress, the glass transition temperature and the elastic modulus were all measured. The composite flexural strength and modulus were also measured. Increasing the allyl sulfide content in the resin dramatically reduces the final stress in the norbornene-methacrylate systems. Both norbornene-methacrylate resins demonstrated almost zero stress (more than 96% stress reduction) compared with the conventional BisGMA/TEGDMA 70/30 wt% control. Mechanical properties of the allyl sulfide-based dental composites were improved to the

point of being statistically indistinguishable from the control BisGMA-TEGDMA by changing the molar ratio between methacrylate and norbornene.

7.1 Introduction

Modern dental restorative materials have favored photoactivated polymer-based composites over the previous mercury-based amalgams due to several advantages including on-demand and rapid curing as well as the formation of a material that possesses an aesthetically pleasing natural tooth color. Unfortunately, the volume shrinkage which occurs during photopolymerization results in a stress that has the potential to cause adhesive failure, initiate microleakage and recurrent caries[1]. Polymerization stress in commercial dimethacrylate-based composites is especially problematic due to the early gelation exhibited in chain-growth polymerizations[2-3]. Many researchers have attempted to mitigate this stress by minimizing volume shrinkage via novel polymerization schemes, such as thiol-ene polymerization[4-5] [6-7], ring-opening polymerization[8-9], and polymerization-induced phase separation[10]. In the present work, we utilize addition-fragmentation chain transfer (AFCT) to create adaptable polymer networks with radical-mediated bond rearrangement that occurs throughout the polymerization, leading to stress relaxation and the formation of a low stress material.

Addition-fragmentation chain transfer (AFCT) enables the relaxation of polymerization shrinkage-induced stress within a forming polymer network by promoting the rearrangement of the network connectivity without any associated reduction in the crosslink density or the mechanical properties of the ultimate materials[11-13,14]. In previous studies, the presence of the allyl sulfide functional group was shown to reduce the final stress in thiol-ene[12] and thiol-yne[14] resins via AFCT. The AFCT mechanism is a non-degradative process of recurring chain scission

and recombination which enables the network to maintain its chemical and mechanical properties before and after AFCT is activated. In the previous thiol-ene and thiol-yne studies, the thiyl radical would react with the allyl sulfide bond to induce AFCT, while simultaneously regenerating a thiyl radical and thereby inducing a cascade of reactions (Figure 7.1(A)).

The incorporation of the AFCT mechanism into a methacrylate-based resin was recently performed by formulating a bisphenyl-a-dimethacrylate monomer with thiol-ene monomers that contained allyl sulfide moieties[13]. A dramatic reduction in stress was observed upon increasing the allyl sulfide-containing thiol-ene fraction of the resin; however, this reduction was accompanied by reduced mechanical properties (i.e., glass transition temperature and modulus). Nevertheless, this work demonstrated that allyl sulfide AFCT was capable of reducing the stress in glassy, methacrylate-based materials.

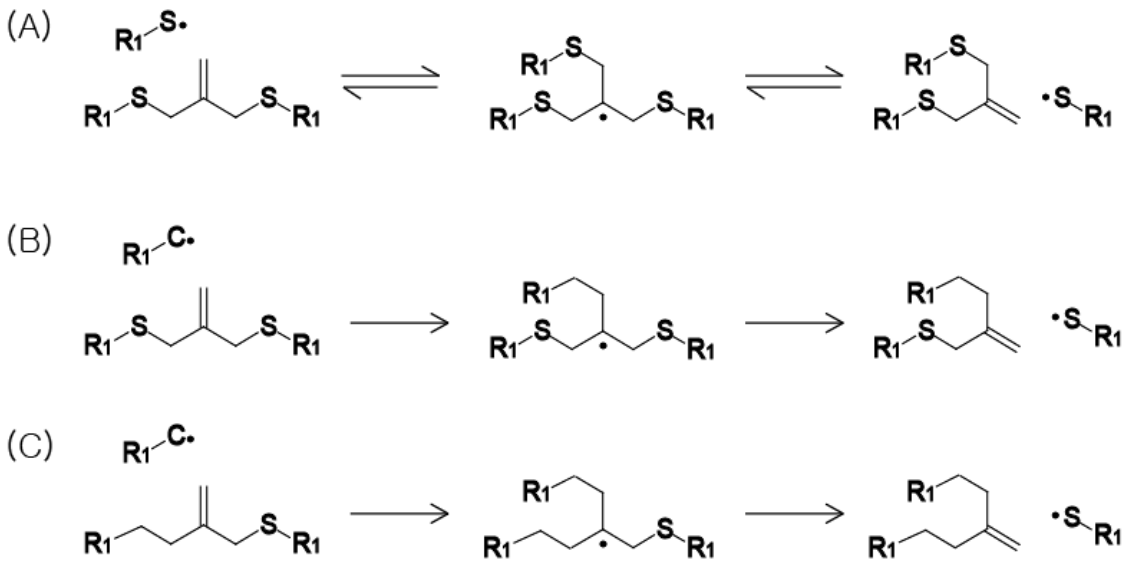

Figure 7.1. (A) Schematic of allyl sulfide AFCT mechanism in the presence of a thiyl radical which results in bond rearrangement but regeneration of the identical chemical structure. (B) Schematic of allyl sulfide AFCT mechanism in the presence of a carbon-centered radical which results in an asymmetric chemical structure. (C) Schematic of AFCT mechanism in the presence of a carbon-centered radical which results in a symmetric but AFCT-incapable structure.

In an effort to produce a low stress material while also achieving mechanical properties appropriate for a dental restorative material, we have incorporated an allyl sulfide functional group into a norbornene-methacrylate monomer system. We hypothesize that AFCT of the allyl sulfide would relieve stress in this methacrylate-based system while retaining the desirable mechanical properties associated with the bulky molecular structure of the norbornene which increases the glass transition temperature of the ultimate resin and composite. The desired curing behavior of the resin was achieved by using 470nm wavelength light in combination with Ge-based photoinitiators. The mechanical properties and shrinkage stress of the systems were evaluated and compared with a control formulation comprised of 70/30 wt%

BisGMA/TEGDMA. The flexural strength and modulus as well as the glass transition temperature of the composite were examined, with the composites containing 75 wt% glass filler.

7.2 Materials & Methods

7.2.1 Materials

The materials used in this study are shown in Figure 7.2. 2-Methylene-propane-1,3-di(norbornene sulfide) (MDNS) was designed and synthesized to form a polymer network that simultaneously achieves a high glass transition temperature associated with the norbornene groups and lower stress through AFCT of the allyl sulfide. As a negative control, 2-methyl-propane-1,3-di(norbornene sulfide) (MeDNS), which is analogous to MDNS though not capable of undergoing AFCT, was also synthesized. MDNS and MeDNS were synthesized from 5-bromomethyl norbornene with 3-mercapto-2-(mercaptomethyl)-1-propene and 1,3-dimercapto-2-methylpropane, respectively, according to the method described in the literature [12]. The waxy/hazy solid (MDNS) and viscous/colorless liquid (MeDNS) were received after purification. To synthesize 5-bromomethyl norbornene, a reaction of 1,3-dicyclopentadiene with allyl bromide was performed in a pressure vessel heated at 170 °C for 12 hours. It was distilled at 175 °C at 1 atmosphere pressure before use. Additionally, 2-(methacryloyloxyethyl) 7-methylene-1,5-dithiocan-3-yl phthalate (PAS, phthalate allyl sulfide, synthesized by 3M) was also evaluated. This monomer has the stress-relieving benefits of an allyl sulfide moiety (in the ring) as well as the enhanced crosslinking density associated with the methacrylate chain-growth

mechanism. Bisphenylglycidyl dimethacrylate (BisGMA, provided by Esstech) and triethylene glycol dimethacrylate (TEGDMA, provided by Esstech) were used as given. Ge-based photoinitiator (Dibenzoyl diethyl germane, synthesized) and phosphine oxide, phenyl bis(2,4,6-trimethyl benzoyl) (BAPO, Ciba Specialty Chemicals), visible light-active photoinitiators, were utilized at 3 wt%. Ge-based photoinitiator (Dibenzoyl diethyl germane, synthesized) was prepared by a synthesis from diethyldi(2-phenyl-1,3-dithian-2-yl)germane, $CaCO_3$, and iodine following a procedure in a literature [15]. A surface treated microparticle silica filler (size range: 0.01 to 3.6 μm, average size 0.6 μm) was obtained from 3M.

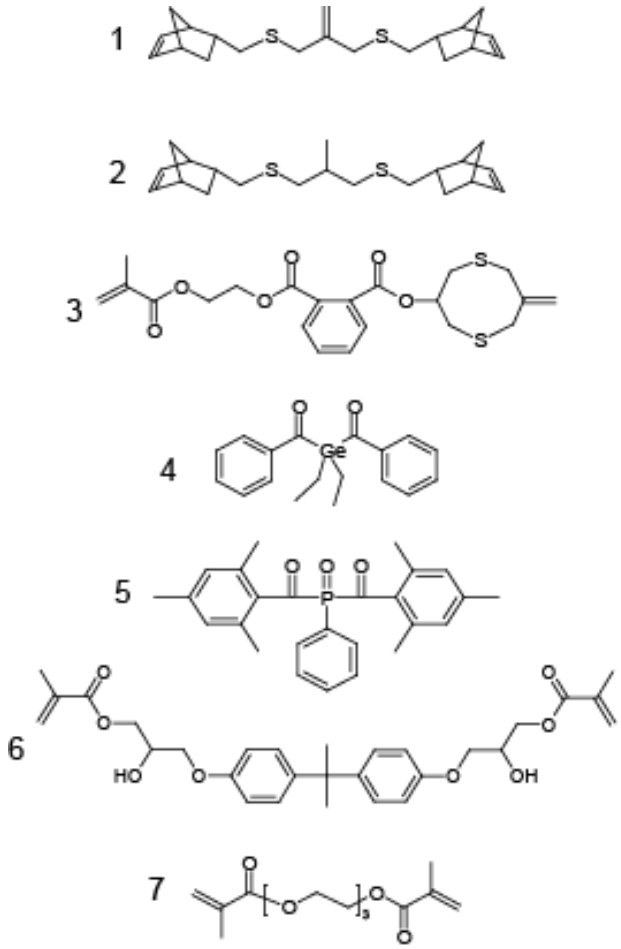

Figure 7.2. Materials used: (1) MDNS (2) MeDNS (3) PAS (4) Dibenzoyldiethylgermane (5) BAPO (6) Bis-GMA (7) TEGDMA

7.2.2 Methods

The vinyl functional group conversion in each resin was determined using Fourier transform infrared (FTIR) spectroscopy (Nicolet 750) during photopolymerization. Samples (50μm thickness) were irradiated for 5 minutes at 10 mW/cm^2 intensity by one of two visible-light dental lamps (G-light equipped with a 470 nm band-pass filter (GC America Inc.) and 430nm dental LED light (MODEL 5560 ALZ, 3M)). The conversions of the methacrylate, norbornene, and allyl sulfide were determined by monitoring infrared absorption peaks centered at 3105 cm^{-1} (C=**C-H** stretching), 3058 cm^{-1} (C=**C-H** stretching), and 3077 cm^{-1} (C=**C-H** stretching), respectively. Gaussian fitting was used to deconvolute the peak areas as the methacrylate peak is overlapped with the norbornene and allyl sulfide peaks.[12-13]

The shrinkage stress was monitored using tensometry (Paffenbarger Research Center, American Dental Association Health Foundation)[5, 16] during the photopolymerization of each resin or composite. A tensometer utilizes the cantilever beam deflection theory to evaluate how much the beam deflects for a given stress level. In this study, three different compliance beams were necessary to measure the model and control resins due to the limitation of each beam for the stress level. Since the obtained stress value decreases in longer beam configurations [16], the stress value of the control resin, which was obtained with the longer beam configuration, would be higher if it could be measured accurately at the same compliance as the sample. Therefore, the difference between the model and control system is even larger than what it is reported here, and what is reported here represents a conservative estimate of the difference between the sample and

control. The experiments were performed by irradiating samples (6 mm in diameter and 1 mm thick) for 5 minutes at 10 mW/cm^2 intensity using the G-light dental lamp (equipped with a 470 nm filter).

The elastic moduli (E′) and glass transition temperatures (T_g) of polymerized samples were determined by dynamic mechanical analysis (DMA) (TA Instruments Q800). Rectangular samples (length*width*thickness : ~8mm*5mm*1mm) were prepared by sandwiching the material between 2 glass slides with 1mm thickness spacers and cured under same irradiation conditions as used in the tensometer experiments. Experiments were performed at a strain and frequency of 0.1% and 1 Hz, respectively, and scanning the temperature twice at a ramp rate of 1 ºC/minute. The T_g was assigned as the temperature at tan delta peak maximum [17-18] of the second scan. Flexural strength and modulus were measured by using Mechanical Test System (MTS, The 858 Mini Bionix II Test System) using a 3-point bending test procedure with 20mm span and 1mm/minute rate. For these tests, 2mm samples were prepared by the same method as described for the DMA preparation.

7.3 Results

Methacrylate conversions for samples formulated with a 1:2 molar ratio of MDNS to PAS (i.e., a 1:1 norbornene to methacrylate functional group ratio due to the two norbornenes per MDNS molecule), which contains 3wt% of either a Ge-based photoinitiator (dibenzoyldiethylgermane) or BAPO (phosphine oxide, phenyl bis(2,4,6-trimethyl benzoyl)), are shown as a function of time in Figure 7.3(A). Additionally, we examined the effect of the irradiation wavelength, using either 470 or 430 nm light, on the curing kinetics. Formulating the resin with BAPO resulted in a slow reaction rate for both 470nm and 430nm light owing to the low quantum yield of BAPO at these wavelengths. In contrast, the Ge-based photoinitiator, which absorbs light in the 470nm region, yields an enhanced reaction rate due to the greater photon absorption rate.

A resin containing MeDNS, a propyl sulfide-containing analog monomer, is also evaluated as a negative control relative to the resin containing MDNS. The propyl sulfide has a nearly identical molecular volume as the allyl sulfide but is incapable of undergoing AFCT. The polymerization rate of the propyl sulfide-containing system is faster than for the allyl sulfide-containing system due to AFCT of the allyl sulfide, as noted previously [12-14]. The norbornene conversion of the resins examined here demonstrates similar reaction trends as the methacrylate conversion, but with a lower final conversion (~40%). The allyl sulfide conversion is less than 6% for all systems, indicating that radical addition across the allyl sulfide primarily proceeds through the desired AFCT mechanism rather than through a variety of other reactions that would lead to consumption of the allyl sulfide functional group.

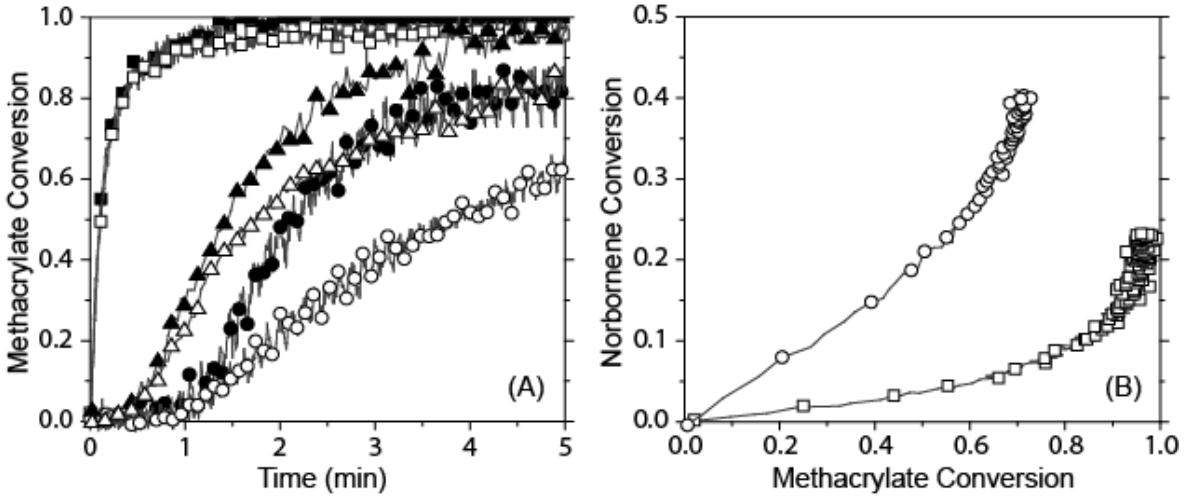

Figure 7.3. (A) Reaction behavior of the methacrylate functional group using 470nm light with Dibenzoyldiethylgermane (square), 470nm light with BAPO (circle), and 430nm light with BAPO (triangle) versus time for allyl sulfide-containing MDNS-PAS (open symbols) and propyl sulfide-containing MeDNS-PAS (closed symbols) resins. Resins are composed in a 1:1 norbornene:methacrylate mol ratio. (B) Norbornene conversion versus Methacrylate conversion of 1:1 (square) and 1:4 (circle) norbornene:methacrylate mol ratio in MDNS-PAS resins which contain 3 wt% Dibenzoyldiethylgermane, irradiated at 10 mW/cm^2 using 470nm light.

Shrinkage stress during polymerization was measured using 470nm light with the Ge-based initiator for BisGMA-TEGDMA 70/30 wt%, MDNS-PAS, and MeDNS-PAS resins (Figure 7.4(A)). Both MDNS-PAS and MeDNS-PAS systems demonstrated 96% and 92% reduced stress, respectively, compared with the conventional BisGMA-TEGDMA 70/30 wt% resin. Since both the allyl sulfide-containing norbornene-methacrylate resins possess too low a stress level, different compliance configurations were necessary to measure them. The MDNS-containing resin exhibits a 50% lower final stress when compared with the MeDNS-containing resin as the concentration of allyl sulfide moiety is increased in MDNS. Selected mechanical

properties of the polymerized resins and composites (i.e., resins filled with silica) are shown in Table 2. As the stress is reduced in the norbornene-methacrylate system, mechanical properties such as the elastic modulus and glass transition temperature are also reduced when compared with the BisGMA-TEGDMA control system. However, as the methacrylate ratio was increased (1:1 to 1:2 or 1:4 norbornene:methacrylate ratio), the flexural strength and modulus exhibited significant improvement (Figure 7.4(C)) while maintaining the stress level significantly lower than in the BisGMA/TEGDMA composite (Figure 7.4(B)).

In Table 1, the norbornene conversions in all the materials demonstrate similar reaction behavior with the methacrylate, but the final conversion is lower than the methacrylate functional group. Recognizing the inability of the norbornene group to homopolymerize, to improve the final conversion of the norbornene functional group, the methacrylate ratio was increased in the MDNS-PAS resin. The conversion of these resins, which includes a resin with a 1:8 molar ratio of MDNS to PAS (1:4 of norbornene to methacrylate functional group ratio) is shown in Figure 7.3(B). The ultimate norbornene conversion increases with increasing methacrylate content in the system.

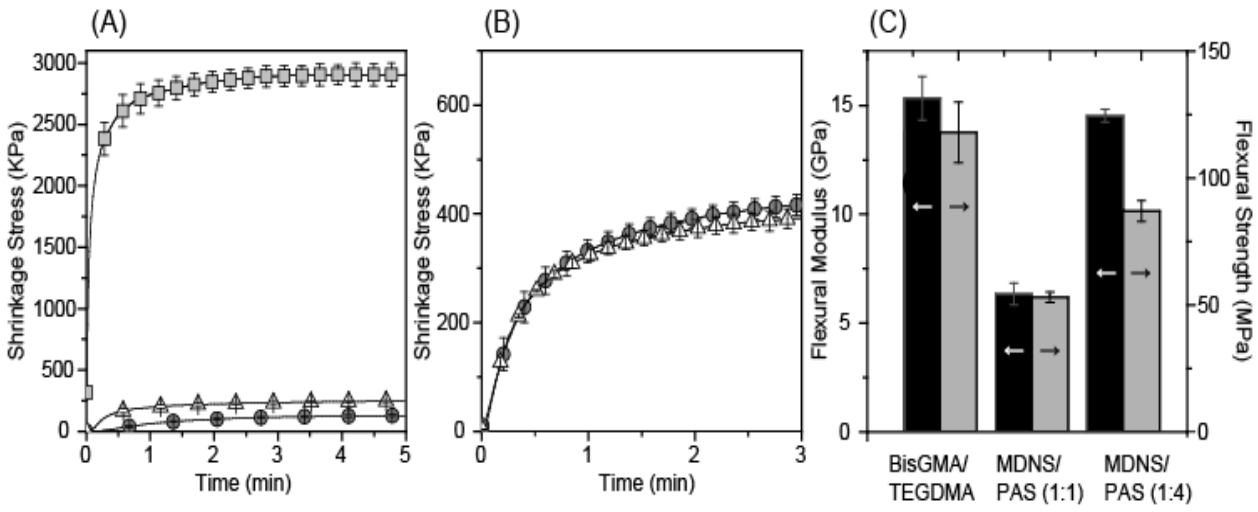

Figure 7.4. (A) Polymerization shrinkage stress versus time of BisGMA-TEGDMA 70/30 wt% resin (square), MeDNS-PAS resin (1:1 norbornene to methacrylate) (triangle), and MDNS-PAS resin (1:1 norbornene to methacrylate) (circle). Different compliance beams were necessary. (See the methods section) (B) Polymerization shrinkage stress versus time of MDNS-PAS composites as the ratio of norbornene to methacrylate changes from 1:1 (triangle) to 1:4 (circle). (C) Flexural modulus and flexural strength of BisGMA-TEGDMA 70/30 wt%, MDNS-PAS (1:1 norbornene to methacrylate), and MDNS-PAS (1:4 norbornene to methacrylate) composites. Composites include 75 wt% silica filler and 25 wt% resins. Resins include 3 wt% Dibenzoyldiethylgermane. Samples irradiated at 10 mW/cm^2 using 470 nm light.

Table 7.1. Final conversion of resin systems.

Resin System (Norbornene:Methacrylate)	Irradiation wavelength/ photoinitiator (wt%)	Functional group conversions [%]		
		Methacylate	Norbornene	Allyl sulfide
MeDNS_PAS (1:1)	470nm/ Ge-based PI (3wt%)	100 (1)	25 (2)	5 (1)
MDNS_PAS (1:1)		97 (1)	23 (2)	2 (1)
MDNS_PAS (1:4)		71 (1)	41 (1)	4 (1)
MeDNS_PAS (1:1)	470nm/ BAPO (3wt%)	83 (1)	9 (1)	4 (1)
MDNS_PAS (1:1)		60 (1)	5 (1)	3 (1)
MeDNS_PAS (1:1)	430nm/ BAPO (3wt%)	98 (1)	11 (1)	6 (1)
MDNS_PAS (1:1)		83 (1)	9 (1)	2 (1)

Table 7.2. Summary of T_g, Elastic modulus (E'), Flexural strength, and Flexural modulus of unfilled resins and filled dental composites. The composite is formulated with 75wt% of silica filler and 25wt% resin. Compliance of the tensometer : A > B> C (See methods section)

Systems (Norbornene : Methacrylate)	Stress [KPa]	Compliance of the tensometer	T_g [℃]	E' at 0℃ [GPa]	E' at 25℃ Before heating [GPa]	Flexural modulus [GPa]	Flexural strength [MPa]
Resin MeDNS_PAS (1:1)	250 (10)	A	70	1.7	1.4	-	-
Resin MDNS_PAS (1:1)	130 (10)	A	55	2.2	1.0	-	-
Resin BisGMA_TEGDMA 70/30 wt%*	2900 (100)	C	160	3.5	1.8	-	-
Composite MDNS_PAS (1:1)	370 (30)	B	65	13	9.8	6.3 (0.5)	53 (2)
Composite MDNS_PAS (1:2)	400 (10)	B	90	14	13.4	13.5 (1)	92 (10)
Composite MDNS_PAS (1:4)	420 (30)	B	110	13	12.9	14.5 (0.3)	87 (4)
Composite BisGMA_TEGMA 70/30 wt%	640 (20)	B	210	13	12.5	15.3 (1)	118 (10)

7.4 Discussion

The total curing time for the material must be sufficiently short to be considered practical for dental applications. Classically, the photopolymerization rate is proportional to the square root of the initiation rate, which depends on the photoinitiator concentration and its absorption of the incident irradiation [19]. The Ge-based initiator has a relatively high light absorption at 470nm in comparison with BAPO [15]. The effect of light absorption is clearly observed in the large differences in reaction rates between resins using the Ge-based initiator versus BAPO (figure 7.3(A)). The faster reaction rate observed in the propyl sulfide-containing system (MeDNS-PAS) compared with the allyl sulfide-based system (MDNS-PAS) owes to the higher concentration of the AFCT capable allyl sulfide functional group (Figure 7.3). While both resins contain allyl sulfide functional groups resulting from the PAS monomer, the MDNS-PAS system also has allyl sulfide in the MDNS monomer. The presence of the allyl sulfides reduces the reaction rate through sequestration of some of the radicals in the AFCT process as illustrated in Figure 7.1(B) and (C).

Polymerization shrinkage stress is the superposition of stress stored during network formation and dissipated by flow and, in the case of AFCT capable materials, network rearrangement. MeDNS has a similar molecular structure to MDNS, however the allyl sulfide is replaced with propyl sulfide. The final network structure, as represented primarily by the crosslink density, of both materials will be similar since chain propagation through the allyl sulfide group is limited. As demonstrated in Figure 7.4(A), incorporation of the allyl sulfide functionality provides an

excellent mechanism for stress relaxation via network rearrangement, as observed in the reduced polymerization shrinkage stress in the MDNS-PAS system containing a larger amount of the allyl sulfide functional group.

Both the MDNS-PAS and MeDNS-PAS resins demonstrated excellent stress reduction (more than 96%) as compared to the conventional BisGMA/TEGDMA 70/30 wt% resin (Figure 7.4(A)). The lower stress is due to at least two effects. AFCT through the allyl sulfide moieties relaxes stress during polymerization by network rearrangement. Additionally, the nature of the ring-opening reaction of the allyl sulfide-containing ring in PAS also reduces volume shrinkage and the corresponding stress. While there are other minor effects, the very low stress, which is so much different than the BisGMA/TEGDMA control as to necessitate the use of a higher compliance cantilever to measure the stress, indicates AFCT and ring opening are the likely reasons for the reduced shrinkage stress observed in the norbornene-PAS system.

The mechanical properties of the filled composite, varying the ratio of norbornene to methacrylate, are shown in Figure 7.4(C) and Table 2. The flexural strength and modulus of the MDNS-PAS composite in 1:1 norbornene to methacrylate functional group ratio were lower than those of the BisGMA/TEGDMA-based composite (Figure 7.4(C)). Further enhancement of the mechanical properties is achieved simply by, for example, the incorporation of other crosslinking agents or the adjustment of the norbornene to methacrylate ratio. The reduced mechanical properties most likely result from the low norbornene conversion, which is attributed to poor copolymerization with the methacrylate and the inability of the norbornene to homopolymerize.

As the ratio of norbornene to methacrylate functional groups is 1 to 1, homopolymerization of the methacrylate produces a stoichiometric imbalance, significantly effecting the copolymerization and final norbornene conversion. Increasing the methacrylate ratio improved the norbornene conversion by increasing the likelihood of reaction between the norbornene and a carbon-centered radical. Using excess methacrylate improved the flexural modulus and strength while maintaining a similar though slightly increased level of polymerization stress.

7.5 Conclusions

Incorporation of AFCT of allyl sulfide and ring-opening polymerization mechanism in the norbornene-methacrylate resin demonstrated almost zero shrinkage stress compared with a conventional BisGMA/TEGDMA 70/30 wt% resin. Increasing the amount of the allyl sulfide-containing species in the resin formulation further reduces the final stress as shown in the MDNS-PAS system which is reduced by as much as 50% compared with the MeDNS-PAS system. The mechanical properties of the allyl sulfide-based dental resins were improved by changing the molar ratio between the methacrylate and norbornene functional groups while maintaining a similar shrinkage stress level. Although more development remains, these low stress resins exhibit excellent mechanical properties that promise to be a positive component as dental restorative materials.

7.6 Acknowledgements

This investigation was supported by NIDCR 2 R01 DE-010959-11 from the National Institutes of Health and NSF 0933828.

7.7 References

(1) Burke, F. J. T.; Cheung, S. W.; Mjor, I. A.; Wilson, N. H. F. *Quintessence International* **1999,** *30,* 234-242.

(2) Labella, R.; Lambrechts, P.; Van Meerbeek, B.; Vanherle, G. *Dent Mater* **1999,** *15,* 128-137.

(3) Walls, A. W. G.; Mccabe, J. F.; Murray, J. J. *Journal of Dentistry* **1988,** *16,* 177-181.

(4) Carioscia, J. A.; Lu, H.; Stanbury, J. W.; Bowman, C. N. *Dent Mater* **2005,** *21,* 1137-1143.

(5) Lu, H.; Carioscia, J. A.; Stansbury, J. W.; Bowman, C. N. *Dent Mater* **2005,** *21,* 1129-1136.

(6) Cramer, N. B.; Couch, C. L.; Schreck, K. M.; Boulden, J. E.; Wydra, R.; Stansbury, J. W.; Bowman, C. N. *Dent Mater* **2010,** *26,* 799-806.

(7) Cramer, N. B.; Couch, C. L.; Schreck, K. M.; Carioscia, J. A.; Boulden, J. E.; Stansbury, J. W.; Bowman, C. N. *Dent Mater* **2010,** *26,* 21-28.

(8) Stansbury, J. W. *Polymers of Biological and Biomedical Significance* **1994,** *540,* 171-183.

(9) Ge, J. H.; Trujillo-Lemon, M.; Stansbury, J. W. *Macromolecules* **2006,** *39,* 8968-8976.

(10) Lee, T. Y.; Cramer, N. B.; Hoyle, C. E.; Stansbury, J. W.; Bowman, C. N. *J Polym Sci Pol Chem* **2009,** *47,* 2509-2517.

(11) Kloxin, C. J.; Scott, T. F.; Adzima, B. J.; Bowman, C. N. *Macromolecules* **2010,** *43,* 2643-2653.

(12) Kloxin, C. J.; Scott, T. F.; Bowman, C. N. *Macromolecules* **2009,** *42,* 2551-2556.

(13) Park, H. Y.; Kloxin, C. J.; Scott, T. F.; Bowman, C. N. *Dent Mater* **2010,** *26,* 1010-1016.

(14) Park, H. Y.; Kloxin, C. J.; Scott, T. F.; Bowman, C. N. *Macromelecules* **2010,** *43,* 10188-10190.

(15) Ganster, B.; Fischer, U. K.; Moszner, N.; Liska, R. *Macromolecules* **2008,** *41,* 2394-2400.

(16) Lu, H.; Stansbury, J. W.; Dickens, S. H.; Eichmiller, F. C.; Bowman, C. N. *Journal of Materials Science-Materials in Medicine* **2004,** *15,* 1097-1103.

(17) Ferrillo, R. G.; Achorn, P. J. *Journal of Applied Polymer Science* **1997,** *64,* 191-195.

(18) Li, G.; Lee-Sullivan, P.; Thring, R. W. *Journal of Thermal Analysis and Calorimetry* **2000,** *60,* 377-390.

(19) Flory, P. J. *Principles of Polymer Chemistry*; Cornell University Press, Ithaca, NY, 1953.

Chapter 8

Stress Relaxation of trithiocarbonate-Dimethacrylate-based Dental Composites

To reduce polymerization-induced shrinkage stress while maintaining mechanical properties, reversible addition-fragmentation chain transfer (RAFT) was incorporated in dimethacrylate-based dental composite. We hypothesized that the incorporation of the trithiocarbonate functional group within dimethacrylate monomers will lead to lower stress as compared with conventional dimethacrylates since undergoing RAFT will rearrange the molecular connectivity in the polymer networks and promote stress relaxation. A dimethacrylate monomer incorporating a trithiocarbonate functional group was formulated with the TEGDMA at 30 to 70 wt% and compared to a control resin comprised of a BisGMA-TEGDMA (bisphenylglycidyl dimethacrylate/triethylene glycol dimethacrylate) 70/30 wt% resin. Shrinkage stress and the methacrylate conversion were measured during polymerization. In addition, fracture toughness and elastic modulus were measured to compare the mechanical properties. All experiments were performed as the composites which include 75 wt% silica fillers. The trithiocarbonate-including composite demonstrated 65% stress reduction when compared with the standard BisGMA-TEGDMA composite. The reaction rate of the trithiocarbonate-based composite was slower than the control composite, presumably due to the RAFT reaction. Fracture toughness of the TTCDMA-based composite was not significantly different from the TEGDMA-based composite though the TTCDMA-based composite has much lower stress. Incorporation of the

trithiocarbonate-including monomer reduced the T_g (30^oC reduction) since the trithiocarbonate dimethacrylate has a lower T_g compared with the TEGDMA. Although incorporation of the trithiocarbonate dimethacrylate reduced T_g compared with the standard composite, RAFT of the trithiocarbonate functional group demonstrated an excellent stress relaxation effect while maintaining the elastic modulus and fracture toughness. It promises that this new RAFT-capable monomer will be the marvelous replaceable diluents for the BisGMA-based dental materials. Further study exploring ratio between methacrylates or changing chemical structure will enhance the stress relaxation effect of the trithiocarbonate to produce an excellent dental materials.

8.1 Introduction

There are many requirements for dental restorative materials such as being easy to manipulate and having desirable aesthetics, but the most important characteristic is the restoration of the original physical behavior of the native tooth structure. Though polymer-based composites have been improved, volume shrinking and the associated stress that evolve during curing remains a critical drawback since it leads to microcracking, microleakage, and secondary caries[1]. Particularly, during the polymerization of dimethacrylate resins which represent the primary polymerizable component of dental composites, a large stress arises due to the nature of the monomer-polymer densification process coupled with the chain-growth polymerization mechanism[2].

Other approaches to reduce stress such as thiol-ene[3,4] and thio-yne reactions[5], phase separation[6], and ring-opening polymerizations[7-8] have been reported as methodologies for minimizing the volume shrinkage and corresponding shrinkage stress. We have previously demonstrated that the incorporation of a reversible covalent bond which undergoes addition-fragmentation chain transfer (AFCT) into a polymerizable structure leads to significant stress reduction. Previously, AFCT of allyl sulfide-containing monomers, primarily in thiol-ene reactions, was demonstrated to relieve the shrinkage stress by allowing molecular rearrangement throughout the polymer network[9-10]. Previously, the allyl sulfide functional group was incorporated in thiol-ene[11] and thiol-yne reactions[12] to maximize its stress relaxation effect since the allyl sulfide undergoes fully *reversible* AFCT only in the presence of the thiyl radical (See Figure 8.1(A)).

Unfortunately, incorporation of the allyl sulfide into the methacrylate-based system exhibited a reduced stress relaxation effect relative to the amount of the methacrylate monomer in the system[13]. As the methacrylate content of the resin increases, the stress relaxation effect via AFCT decreased since the allyl sulfide group does not undergo a reversible AFCT reaction in the presence of the carbon-centered radical that is prevalent in methacrylate-rich polymerizations (See Figure 8.1(B)).

The trithiocarbonate functionality is frequently used as a reversible addition-fragmentation chain transfer (RAFT) agent to form polymers having low polydispersity and other characteristics of a controlled radical polymerization[14]. Unlike the allyl sulfide functional group, the trithiocarbonate functional group is capable of fully reversible AFCT, resulting in the conservation of molecular structures, when reacting with a carbon-centered radical such as those that are present in methacrylate polymerizations (Figure 8.1(C)). We hypothesize that the incorporation of the trithiocarbonate within the dimethacrylate monomer structure will result in lower stress when compared with conventional, analogous dimethacrylates. In this study, a dimethacrylate monomer including a trithiocarbonate functional group was designed and evaluated for its effects of stress reduction when it is used to replace TEGDMA in conventional BisGMA-TEGDMA (bisphenylglycidyl dimethacrylate/triethylene glycol dimethacrylate) resins. In addition, fracture toughness and elastic modulus were measured to compare the mechanical properties. All experiments were performed for composites which include 75 wt% silica fillers.

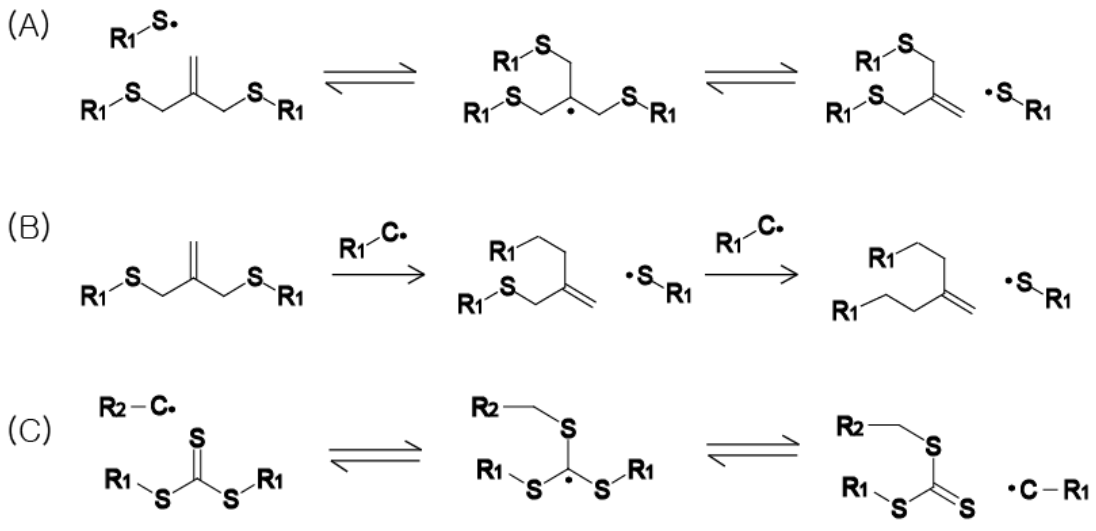

Figure 8.1. (A) Schematic of the allyl sulfide AFCT mechanism in the presence of a thiyl radical which results in a symmetrical chemical structure that promotes reversibility. (B) Schematic of the allyl sulfide AFCT mechanism in the presence of a carbon-centered radical which results in an asymmetrical chemical structure and irreversibility. (C) Schematic of the RAFT mechanism of a trithiocarbonate in the presence of a carbon radical which results in a symmetrical chemical structure and reversibility.

8.2 Materials & Methods

8.2.1 Materials

The monomers and photoinitiator used in this study are shown in Figure 8.2. S,S'-bis[α,α'-dimethyl-α''-(acetyloxy)ethyl 2-methyl-2-propenoate]-trithiocarbonate (TTCDMA, Trithio carbonate dimethacrylate) was synthesized from S,S'-bis(α,α'-dimethyl-α''-acetyl chloride)-trithiocarbonate and 2-hydroxyethyl methacrylate (HEMA) following the procedure in the literature[15]. To purify, the crude oil was dissolved in a 9:1 haxanes:ethyl acetate mixture and filtered to remove insoluble impurities, then column chromatography was performed with a 8:2 hexanes/ethyl acetate solution. S,S'-bis(α,α'-dimethyl-α''-acetyl chloride)-trithiocarbonate was made by the chlorination of the S,S'-bis(α,α'-dimethyl-α''-acetic acid)-trithiocarbonate with thionyl chloride [15]. S,S'-bis(α,α'-dimethyl-α''-acetic acid)-trithiocarbonate was prepared according to a previously published procedure [16]. Bisphenylglycidyl dimethacrylate (BisGMA, provided by Esstech) and triethylene glycol dimethacrylate (TEGDMA, provided by Esstech) were used as received. Resins were composed of 70 wt.% BisGMA and 30wt.% TEGDMA or TTCDMA. A phosphine oxide, phenyl bis(2,4,6-trimethyl benzoyl) (BAPO, Ciba Specialty Chemicals), , was utilized at 1.5 wt% in the resins as a visible light-active photoinitiator. 75 wt.% of silica filler (0.4μm, Confi-Dental) was used to comprise the composite.

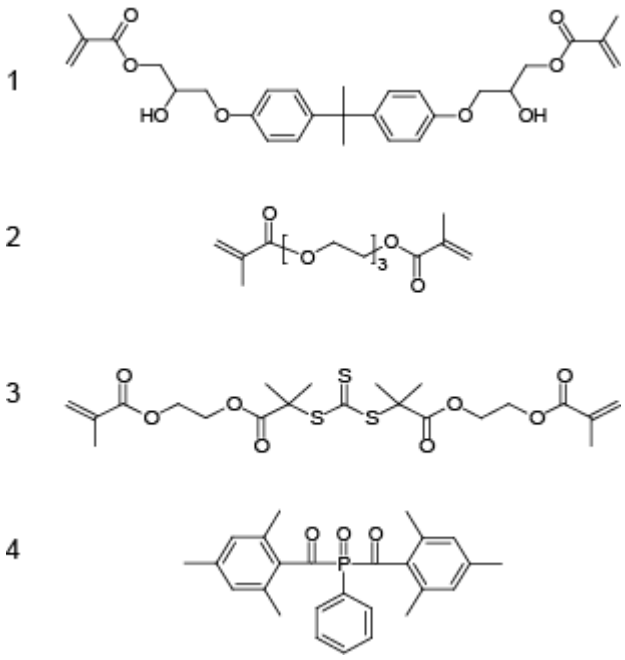

Figure 8.2. Materials used: (1) BisGMA (2) TEGDMA (3) TTCDMA (4) BAPO

8.2.2 Methods

Composite samples (2mm thickness) were irradiated at 70 mW/cm^2 intensity with 400-500 nm light (Acticure 4000) for 20 minute to observe the conversion of the methacrylate functional group during polymerization. The conversions of the methacrylate was determined by monitoring the infrared absorption peak centered at 6166 cm^{-1} (C=**C-H** stretching, overtone) using Fourier transform infrared (FTIR) spectroscopy (Nicolet 750). Fracture toughness was measured by using a Mechanical Test System (MTS, The 858 Mini Bionix II Test System) using a 3-point bending test procedure with 20mm span and 1mm/minute rate. The elastic moduli (E′)

and glass transition temperature (T_g) of polymerized samples were determined by dynamic mechanical analysis (DMA) (TA Instruments Q800). DMA experiments were performed at a strain and frequency of 0.1% and 1 Hz, respectively, and scanning the temperature twice at ramp rate of 2 ºC/minute. The T_g was assigned as the temperature at the tan delta peak maximum [17-18] of the second scan. This methodology does not necessarily measure the T_g of the as cured sample due to changes in conversion that occur during the first thermal scan. Rather, the measurement is indicative of the maximum T_g achieved under these conditions. [19-20] Specimens which are used for MTS and DMA experiments are prepared by sandwiching the uncured composite in a rectangular mold (2 mm gap) and irradiating under the same conditions which are used for the FTIR experiments. The shrinkage stress was monitored using tensometry (Paffenbarger Research Center, American Dental Association Health Foundation)[3, 21] during the photopolymerization of the composites. Uncured composite was injected between two glass rods which are positioned in a 9 cm beam length of the stainless steel beam. Samples were covered with a plastic sheath to prevent oxygen inhibition of the methacrylate during polymerization.

8.3 Results

Fracture toughness and DMA measurements of the BisGMA-TEGDMA and BisGMA-TTCDMA composites are presented in Figure 8.3. The elastic modulus of the TTCDMA-based composite was slightly lower than for the TEGDMA-based composite over the temperature range from 10°C to 100°C. The elastic modulus of the TTCDMA-based composite decreased rapidly from 100°C since the glass transition of the composite is lower than the BisGMA-TEGDMA composite. Although TTCDMA has a lower T_g than TEGDMA, the fracture toughness value of the as-cured sample was slightly higher though not significantly different as compared to the TEGDMA-based composite (Figure 8.3(A)).

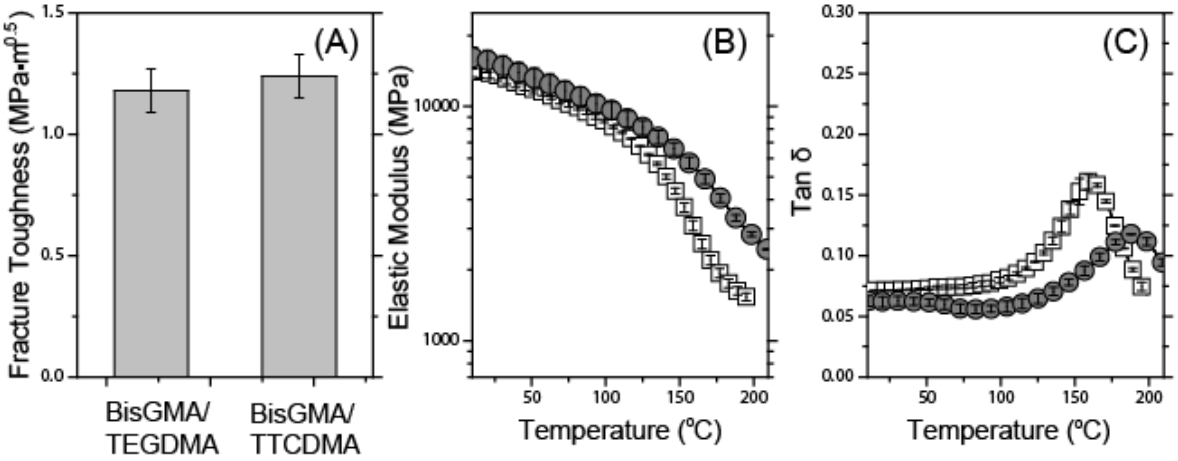

Figure 8.3. (A) Fracture toughness, (B) Elastic modulus, and (C) tangent δ of BisGMA-TEGDMA 70/30 wt% (●) and BisGMA-TTCDMA 70/30 wt% (□) composites. Resins contain 1.5 wt% BAPO, 75wt% of silica filter was loaded, irradiated at 70 mW/cm^2 using 400-500 nm light for 20 minutes.

Reaction kinetics for the BisGMA-TEGDMA and BisGMA-TTCDMA composites were monitored for 20 minutes during irradiation (Figure 8.4). The methacrylate conversion in the TTCDMA-based composite was lower initially; however, the final conversion was the same as the TEGDMA-based control system. The shrinkage stress of the TTCDMA-based composite evolves more slowly compared as compared with the stress of TEGDMA-based composite. While both composites exhibited similar final conversion values, the final shrinkage stress of the TTCDMA-based system was 65% lower than the stress level of the TEGDMA-based composite (Figure 8.5(A)).

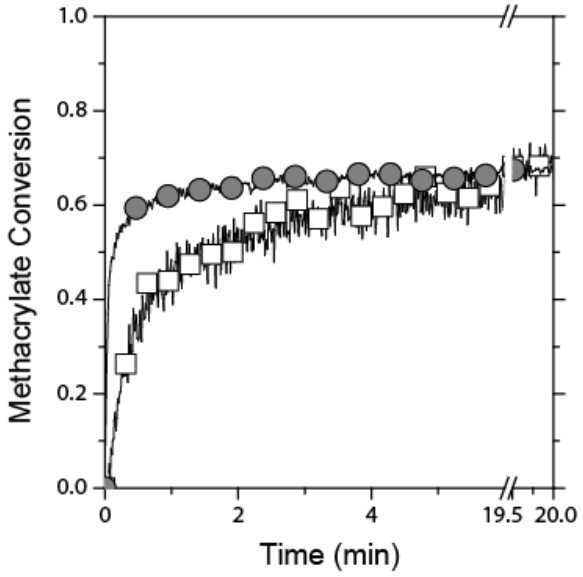

Figure 8.4. Reaction behavior of the methacrylate group in BisGMA-TEGDMA 70/30 wt% (●) and BisGMA-TTCDMA 70/30 wt% (□) composites. Resins contain 1.5wt% BAPO and were cured using 400-500nm light at 70 mW/cm^2 for 20 minutes.

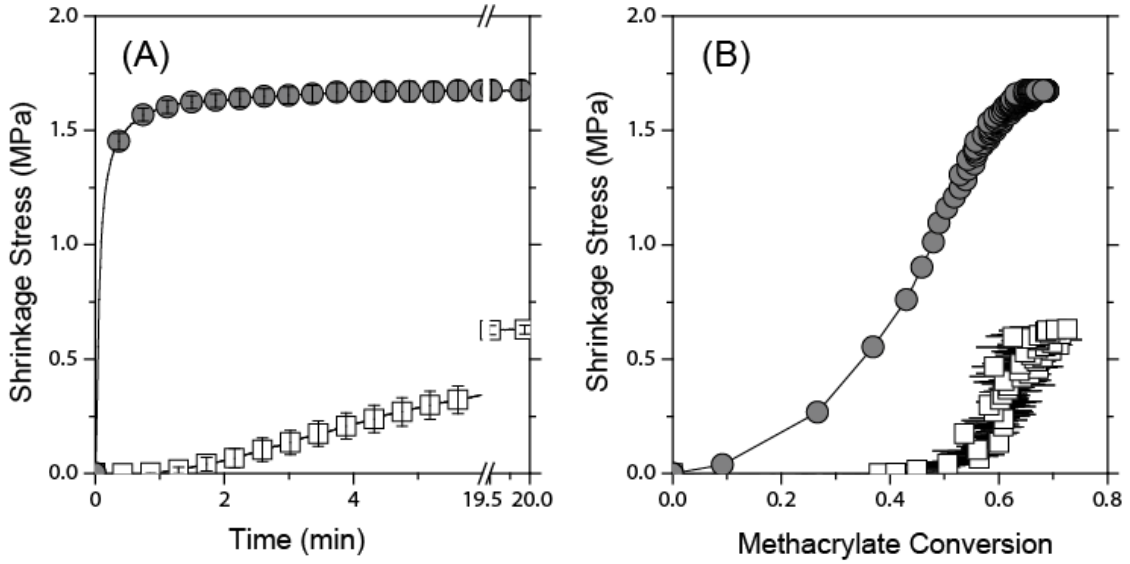

Figure 8.5. Polymerization shrinkage stress versus (A) time and (B) methacrylate conversion for BisGMA-TEGDMA 70/30 wt% (●) and BisGMA-TTCDMA 70/30 wt% (□) composites. Resins contain 1.5 wt% BAPO and 75wt% silica filter, and were irradiated at 70 mW/cm^2 using 400-500 nm light for 20 minutes.

Table 8.1. Summary of the methacrylate conversion, stress, T_g, elastic modulus (E'), and fracture toughness for BisGMA-TEGDMA 70/30 wt% and BisGMA-TTCDMA 70/30 wt% composites. The composite is formulated with 75wt% filler and 25wt% resin. Resins includes 1.5 wt% of BAPO as a visible light initiator and are exposed to 400-500nm light for 20 minutes.

Systems	Methacrylate conversion	Stress [MPa]	T_g [℃]	E' at 25℃ Before heating [Gpa]	Fracture Toughness [Mpa·m$^{0.5}$]
BisGMA-TEGDMA	0.67 ± 0.003	1.7 ± 0.04	184 ± 1	16 ± 3	1.18 ± 0.09
BisGMA-TTCDMA	0.68 ± 0.02	0.6 ± 0.02	155 ± 2	14 ± 2	1.24 ± 0.09

8.4 Discussion

The TTCDMA monomer was initially designed to have a similar molecular structure with TEGDMA, targeting its use as a reactive diluent to replace TEGDMA while simultaneously adding RAFT capability to promote stress relaxation. Since the RAFT reaction is more favorable when the leaving radical group is more stable, the TTCDMA core which replaces ethylene glycol was designed to have the adjacent dimethyl substituted carbon adjacent to the trithiocarbonate as the fragmentation of the carbon-sulfur bond (Figure 8.1(C)) generates a stable tertiary carbon radical [16]. This design made the molecular structure of the TTCDMA significantly larger than its analogue TEGDMA. As a result, TTCDMA-based composites, at equivalent conversions, have a very slight reduction in the crosslink density of the network as compared to TEGDMA analogue networks. Though the incorporation of the TTCDMA decreased the T_g compared with the control composite after the heating cycle, it did not affect to the fracture toughness of the materials (Figure 8.3(A)).

While having similar fracture toughness, the TTCDMA-based composite, despite containing only 30% of monomers with the RAFT core, exhibits a much lower stress as compared with the TEGDMA-based composite (Figure 8.5(A)). Reduced polymerization rate can lower the final conversion; however, here, the TTCDMA-based composite exhibited an equivalent methacrylate conversion as compared with the TEGDMA-based composite.

As shown in Figure 8.5(B), the origin of the stress is also significantly different in these two

systems due to the AFCT mechanism. In conventional dimethacrylate polymerizations, the stress level begins to rise at very low conversions; however, the stress in the TTCDMA-based composite begins to rise only after nearly 40 % conversion of methacrylate groups. This contrasts to the TEGDMA-based composite where the stress begins to increase before 10 % methacrylate conversion. It is clear that the incorporation of a RAFT-capable functional group, particularly one such as the trithiocarbonate that is capable of multiple reversible reactions with a methacrylate radical, into a dimethacrylate polymerization, even in low amounts, dramatically alters the stress evolution behavior in these systems. This outcome results in a new paradigm to consider in methacrylate-based dental restorative materials for preserving overall network mechanics while reducing stress levels.

8.5 Conclusions

BisGMA-TEGDMA and trithiocarbonate-containing BisGMA-TTCDMA-based composites were investigated to demonstrate stress relaxation via RAFT. The trithiocarbonate functional group was implemented to induce successfully RAFT which led to network rearrangement. Ultimately, the inclusion of this mechanism resulted in a 65 % stress reduction as compared to the standard BisGMA-TEGDMA composite. Fracture toughness of the TTCDMA-based composite was slightly higher though not significantly different than the TEGDMA-based composite even though the TTCDMA-based composite has dramatically reduced stress. In summary, the RAFT mechanism for stress relaxation via the inclusion of trithiocarbonates and

similar RAFT moieties has potential for replacing conventional dimethacrylate materials with nearly identical mechanical properties but stress levels that are a fraction of current composites.

8.6 Acknowledgements

This investigation was supported by NIDCR 2 R01 DE-010959-11 from the National Institutes of Health and NSF 0933828.

8.7 References

(1) Burke, F. J. T.; Cheung, S. W.; Mjor, I. A.; Wilson, N. H. F. *Quintessence International* **1999,** *30,* 234-242.

(2) Kleverlaan, C. J.; Feilzer, A. J. *Dent Mater* **2005,** *21,* 1150-1157.

(3) Lu, H.; Carioscia, J. A.; Stansbury, J. W.; Bowman, C. N. *Dent Mater* **2005,** *21,* 1129-1136.

(4) Carioscia, J. A.; Lu, H.; Stanbury, J. W.; Bowman, C. N. *Dent Mater* **2005,** *21,* 1137-1143.

(5) Chan, J. W.; Shin, J.; Hoyle, C. E.; Bowman, C. N.; Lowe, A. B. *Macromolecules* **2010,** *43,* 4937-4942.

(6) Lee, T. Y.; Cramer, N. B.; Hoyle, C. E.; Stansbury, J. W.; Bowman, C. N. *J Polym Sci Pol Chem* **2009,** *47,* 2509-2517.

(7) Ge, J. H.; Trujillo-Lemon, M.; Stansbury, J. W. *Macromolecules* **2006,** *39,* 8968-8976.

(8) Stansbury, J. W. *Polymers of Biological and Biomedical Significance* **1994,** *540,* 171-183.

(9) Scott, T. F.; Draughon, R. B.; Bowman, C. N. *Advanced Materials* **2006,** *18,* 2128-+.

(10) Scott, T. F.; Schneider, A. D.; Cook, W. D.; Bowman, C. N. *Science* **2005,** *308,* 1615-1617.

(11) Kloxin, C. J.; Scott, T. F.; Bowman, C. N. *Macromolecules* **2009,** *42,* 2551-2556.

(12) Park, H. Y.; Kloxin, C. J.; Scott, T. F.; Bowman, C. N. *Macromelecules* **2010,** *43,* 10188-10190.

(13) Park, H. Y.; Kloxin, C. J.; Scott, T. F.; Bowman, C. N. *Dent Mater* **2010,** *26,* 1010-1016.

(14) Mayadunne, R. T. A.; Rizzardo, E.; Chiefari, J.; Krstina, J.; Moad, G.; Postma, A.; Thang, S. H. *Macromolecules* **2000,** *33,* 243-245.

(15) Pavlovic, D.; Linhardt, J. G.; Kunzler, J. F.; Shipp, D. A. *J Polym Sci Pol Chem* **2008,** *46,* 7033-7048.

(16) Lai, J. T.; Filla, D.; Shea, R. *Macromolecules* **2002,** *35,* 6754-6756.

(17) Ferrillo, R. G.; Achorn, P. J. *Journal of Applied Polymer Science* **1997,** *64,* 191-195.

(18) Li, G.; Lee-Sullivan, P.; Thring, R. W. *Journal of Thermal Analysis and Calorimetry* **2000,** *60,* 377-390.

(19) Scott, T. F.; Cook, W. D.; Forsythe, J. S.; Bowman, C. N.; Berchtold, K. A. *Macromolecules* **2003,** *36,* 6066-6074.

(20) Zhu, S.; Tian, Y.; Hamielec, A. E.; Eaton, D. R. *Macromolecules* **1990,** *23,* 1144-1150.

(21) Lu, H.; Stansbury, J. W.; Dickens, S. H.; Eichmiller, F. C.; Bowman, C. N. *Journal of Materials Science-Materials in Medicine* **2004,** *15,* 1097-1103.

Chapter 9

Conclusions and Recommendations

Since polymer materials have come to dominate our life by replacing many other, more traditional materials, any endeavors to improve their performance have heightened importance. Here, we have strived to develop methodologies to reduce and understanding of the processes relevant to the origins of polymerization-induced shrinkage stress. In this thesis, addition-fragmentation chain transfer (AFCT) was utilized to create adaptable polymer networks with radical-mediated bond rearrangement that occurs throughout the polymerization. Addition-fragmentation chain transfer (AFCT) enables the relaxation of polymerization shrinkage-induced stress within a forming polymer network by promoting the rearrangement of the network connectivity without any associated reduction in the crosslink density or the mechanical properties of the ultimate materials. In previous studies, the presence of the allyl sulfide functional group was shown to reduce the final stress in thiol-ene resins via AFCT. Unfortunately, thiol-ene polymerizations often yield elastomeric materials with low glass transition temperatures (T_gs) that are ill-suited for structural applications.

To extend the utility of AFCT into structural applications, AFCT-capable monomers have been incorporated into many systems to achieve both low stress and excellent mechanical properties by designing chemical structure of monomers and by exploration of the polymerization and

relaxation mechanisms. In particular, incorporation of AFCT-capable monomers into conventional dental resins was investigated to generate novel low stress dental composites.

Based on the previous stress relaxation results of the ally sulfide functional group in thiol-ene systems, the effort to increase mechanical properties was first performed by including methacrylates in thiol-ene resins to form thiol-ene-methacrylate ternary networks. A dramatic reduction in stress was observed upon increasing the allyl sulfide-containing thiol-ene fraction of the resin; however, this reduction was accompanied by reduced mechanical properties (i.e., glass transition temperature and modulus). Nevertheless, this work demonstrated that allyl sulfide AFCT was capable of reducing the stress in glassy, methacrylate-based materials which is highly desirable for dental and other applications.

Since the stress relaxation effect was maximized in the thiol-ene system, allyl sulfide functional groups were incorporated into a highly crosslinked thiol-yne network to reduce the associated polymerization-induced shrinkage stress. Polymerization reactions utilizing thiol-yne functional groups have many of the advantageous attributes of the thiol-ene-based materials, such as possessing a delayed gel-point, being resistant to oxygen inhibition, and having rapid polymerization kinetics, while also possessing a high glass transition temperature. In this study, we found that the incorporation of allyl sulfide functional groups in the polymer backbone of a material possessing a super-ambient T_g reduces polymerization-induced shrinkage stress, owing to network connectivity rearrangement via the AFCT mechanism.

Towards development of low stress dental restorative materials, the allyl sulfide functional group

was incorporated in methacrylate-based systems. First, methacrylate monomer was incorporated in the propyl and allyl sulfide-based thiol-yne to increase the glass transition temperature in addition to investigating the stress relaxation by AFCT of the allyl sulfide functional group. Since it was demonstrated that the stress relaxation effect increased as the allyl sulfide concentration increased, it was hypothesized that the thiol-yne-methacrylate can possess both a high allyl sulfide concentration while having a higher glass transition temperature. As expected, the allyl sulfide-based thiol-yne-methacrylate system demonstrates stress relaxation up to 55% and T_g increase of up to 40^{o}C compared with the control AFCT-incapable thiol-yne-methacrylate. In addition, this ternary system demonstrates approximately 3 times lower stress compared with BisGMA-TEGDMA resins while possessing excellent mechanical properties.

Although BisGMA and its analog are the most commonly used resin for dental restorative composites, development of new monomers which can replace them is highly necessary because of not only the volume shrinkage and shrinkage stress also the concerns about the bisphenol A structure. Allyl sulfide functional groups were directly incorporated into methacrylate monomers to determine their effect on stress relaxation via addition-fragmentation chain transfer and create novel monomer which can replace the more conventional BisGMA/TEGDMA monomers for dental applications. However, the stress relaxation by AFCT was not effective due to the irreversible reaction between the carbon radical and the allyl sulfide when the allyl sulfide functional group was incorporated in the only methacrylate system undergoing exclusively chain growth polymerization. To overcome the non effectiveness owing to the irreversible reaction which consumes the allyl sulfide group in the methacrylate-based system, incorporation of allyl sulfides through a ring-opening polymerization mechanism in the

norbornene-methacrylate resin was performed. This allyl sulfide-based norbornene-methacrylate resin demonstrated almost zero shrinkage stress compared with conventional BisGMA/TEGDMA 70/30 wt% resin. Increasing the amount of the allyl sulfide-containing species in the resin formulation further reduces the final stress by as much as 50%. The mechanical properties of the allyl sulfide-based dental resins were improved by changing the molar ratio between the methacrylate and norbornene functional groups while maintaining a similar shrinkage stress level. These low stress resins exhibit excellent mechanical properties that promise to be a positive component as dental restorative materials.

Since direct incorporation of the allyl sulfide in methacrylate-based systems was not effective for stress relaxation with large amounts of methacrylate due to the nature of the allyl sulfide group and its limited capability for reversible reactions with methacrylic radicals, development of an additional AFCT-capable monomer was required. Trithiocarbonates were used in place of allyl sulfides in dimethacrylate monomers, where the trithiocarbonate enables reversible reactions with the methacrylic radicals. A dimethacrylate monomer including a trithiocarbonate functional group was designed and evaluated for the stress reduction when it was used to replace TEGDMA in a conventional BisGMA-TEGDMA composite. The trithiocarbonate dimethacrylate demonstrated 65 % stress reduction compared with the standard BisGMA-TEGDMA composite despite being present in only 30%. Fracture toughness of the TTCDMA-based composite was slightly higher than the TEGDMA-based composite even though the TTCDMA-based composite had a much lower stress value. Although incorporation of the TTCDMA reduced T_g by 30^{o}C compared with the standard composite, RAFT of the trithiocarbonate functional group demonstrated excellent stress relaxation, indicating that TTCDMA and related monomers

represent excellent candidates for reactive diluents in BisGMA-based dental materials.

In summary, this thesis has demonstrated the development and implementation of thiol-ene and thiol-yne based monomers that are capable of undergoing AFCT to reduce polymerization stress further in a glassy polymer and its application for the conventional glassy methacrylate-based dental resins. Additionally, novel monomers that undergo AFCT were developed and implemented in methacrylate-based resins that undergo propagation exclusively through chain growth mechanisms. The improved understanding of the trithiocarbonate functional group, which demonstrated excellent stress relaxation effect in the monomers undergo its propagation by chain growth polymerization, will broadly expand its utility for a wide range of applications such as coatings, microelectronics, photoresists, and dental materials. In particular, color elimination of the trithiocarbonate-containing monomer through better understanding of its chemical structure and optical properties (i.e. absorption of light) is industrially necessary. In addition, the stress relaxation ability of conventional RAFT agents needs to be evaluated in crosslinked polymer networks. If inclusion of a RAFT agent relaxes shrinkage stress effectively in polymer resins, the impact to the industry will be pronounced since adding a RAFT agent into an already established system is much more convenient as compared to incorporation of the RAFT functional group into monomers synthetically. These approaches can be further applied to develop self-healing materials or topographical corrugation in thin films.

Bibliography

(1) Ueberreiter, K.; Kanig, G. *Journal of Chemical Physics* **1950,** *18,* 399-406.

(2) Scott, T. F.; Draughon, R. B.; Bowman, C. N. *Advanced Materials* **2006,** *18,* 2128-+.

(3) Bowen, R. *The journal of the american dental asssociation* **1967,** *74,* 439.

(4) Alcoutlabi, M.; McKenna, G. B.; Simon, S. L. *Journal of Applied Polymer Science* **2003,** *88,* 227-244.

(5) Groenewoud, W. M. *Characterisation of Polymers by Thermal Analysis*; 1st ed.: ELSEVIER SCIENCE B.V., Amsterdam, 2001; p 13.

(6) Ferrillo, R. G.; Achorn, P. J. *Journal of Applied Polymer Science* **1997,** *64,* 191-195.

(7) Kloxin, C. J.; Scott, T. F.; Adzima, B. J.; Bowman, C. N. *Macromolecules* **2010,** *43,* 2643-2653.

(8) Park, H. Y.; Kloxin, C. J.; Scott, T. F.; Bowman, C. N. *Dent Mater* **2010,** *26,* 1010-1016.

(9) Nair, C. P. R.; Mathew, D.; Ninan, K. N. *New Polymerization Techniques and Synthetic Methodologies* **2001,** *155,* 1-99.

(10) Ahmed S. Abuelyaman, S. B. M., Kevin M. Lewandowski, David J. Plaut Dental compositions containing hybrid monomers. 2011.

(11) Lu, H.; Trujillo-Lemon, M.; Ge, J.; Stansbury, J. W. *Compend Contin Educ Dent* **2010,** *31 Spec No 2,* 1-4.

(12) Li, G.; Lee-Sullivan, P.; Thring, R. W. *Journal of Thermal Analysis and Calorimetry* **2000,** *60,* 377-390.

(13) Francis, L. F.; McCormick, A. V.; Vaessen, D. M.; Payne, J. A. *Journal of Materials Science* **2002,** *37,* 4717-4731.

(14) Trujillo-Lemon, M.; Ge, J. H.; Lu, H.; Tanaka, J.; Stansbury, J. W. *J Polym Sci Pol Chem* **2006,** *44,* 3921-3929.

(15) Kilambi, H.; Cramer, N. B.; Schneidewind, L. H.; Shah, P.; Stansbury, J. W.; Bowman, C. N. *Dent Mater* **2009,** *25,* 33-38.

(16) Evans, R. A.; Rizzardo, E. *J Polym Sci Pol Chem* **2001,** *39,* 202-215.

(17) Evans, R. A.; Rizzardo, E. *Macromolecules* **2000,** *33,* 6722-6731.

(18) Scott, T. F.; Cook, W. D.; Forsythe, J. S.; Bowman, C. N.; Berchtold, K. A. *Macromolecules* **2003,** *36,* 6066-6074.

(19) Lai, J. T.; Filla, D.; Shea, R. *Macromolecules* **2002,** *35,* 6754-6756.

(20) Govaerts, T. C.; Vogels, I. A.; Compernolle, F.; Hoornaert, G. J. *Tetrahedron* **2004,** *60,* 429-439.

(21) Cramer, N. B.; Reddy, S. K.; Cole, M.; Hoyle, C.; Bowman, C. N. *J Polym Sci Pol Chem* **2004,** *42,* 5817-5826.

(22) Young, R. J.; Lovell, P. A. *Introduction to Polymers*; Chapman & Hall, London, 1991; p 443.

(23) Cramer, N. B.; Couch, C. L.; Schreck, K. M.; Carioscia, J. A.; Boulden, J. E.; Stansbury, J. W.; Bowman, C. N. *Dent Mater* **2010,** *26,* 21-28.

(24) Lu, H.; Carioscia, J. A.; Stansbury, J. W.; Bowman, C. N. *Dent Mater* **2005,** *21,* 1129-1136.

(25) Mayadunne, R. T. A.; Rizzardo, E.; Chiefari, J.; Krstina, J.; Moad, G.; Postma, A.; Thang, S. H. *Macromolecules* **2000,** *33,* 243-245.

(26) Moad, G.; Rizzardo, E.; Thang, S. H. *Aust J Chem* **2005,** *58,* 379-410.

(27) Drury, C. J.; Mutsaers, C. M. J.; Hart, C. M.; Matters, M.; de Leeuw, D. M. *Applied Physics Letters* **1998,** *73,* 108-110.

(28) Cramer, N. B.; O'Brien, C. P.; Bowman, C. N. *Polymer* **2008,** *49,* 4756-4761.

(29) Ge, J. H.; Trujillo-Lemon, M.; Stansbury, J. W. *Macromolecules* **2006,** *39,* 8968-8976.

(30) Lee, T. Y.; Cramer, N. B.; Hoyle, C. E.; Stansbury, J. W.; Bowman, C. N. *J Polym Sci Pol Chem* **2009,** *47,* 2509-2517.

(31) Kloosterboer, J. G. *Advances in Polymer Science* **1988,** *84,* 1-61.

(32) Ganster, B.; Fischer, U. K.; Moszner, N.; Liska, R. *Macromolecules* **2008,** *41,* 2394-2400.

(33) Vasudevan, V. K.; Stansbury, E. E.; Brooks, C. R. *Journal of Metals* **1987,** *39,* A54-A54.

(34) Scott, T. F.; Schneider, A. D.; Cook, W. D.; Bowman, C. N. *Science* **2005,** *308,* 1615-1617.

(35) Chan, J. W.; Zhou, H.; Hoyle, C. E.; Lowe, A. B. *Chem Mater* **2009,** *21,* 1579-1585.

(36) Nair, D. P.; Cramer, N. B.; Scott, T. F.; Bowman, C. N.; Shandas, R. *Polymer* **2010,** *51,* 4383-4389.

(37) Boulden, J. E.; Cramer, N. B.; Bowman, C. N. *Abstr Pap Am Chem S* **2008,** *235,* -.

(38) Bowman, C. N.; Cramer, N. B.; Reddy, S. K.; Kilambi, H.; O'Brien, A. K.; Rydholm, A.; Anseth, K. S. *Abstr Pap Am Chem S* **2008,** *235,* -.

(39) Venhoven, B. A. M.; Degee, A. J.; Davidson, C. L. *Biomaterials* **1993,** *14,* 871-875.

(40) Walls, A. W. G.; Mccabe, J. F.; Murray, J. J. *Journal of Dentistry* **1988,** *16,* 177-181.

(41) Crawford, L. R.; Stansbury, J. W. *Abstr Pap Am Chem S* **2006,** *231,* -.

(42) Kleverlaan, C. J.; Feilzer, A. J. *Dent Mater* **2005,** *21,* 1150-1157.

(43) Labella, R.; Lambrechts, P.; Van Meerbeek, B.; Vanherle, G. *Dent Mater* **1999,** *15,* 128-137.

(44) Davidson, C. L.; Feilzer, A. J. *Journal of Dentistry* **1997,** *25,* 435-440.

(45) Patel, M. P.; Braden, M.; Davy, K. W. M. *Biomaterials* **1987,** *8,* 53-56.

(46) Meijs, G. F.; Rizzardo, E.; Thang, S. H. *Macromolecules* **1988,** *21,* 3122-3124.

(47) Kunert, P.; Schneider, W.; Flory, J. *Aesthetic Plastic Surgery* **1988,** *12,* 101-106.

(48) Flory, P. J. *Principles of Polymer Chemistry*; Cornell University Press, Ithaca, NY, 1953.

(49) Lu, H.; Stansbury, J. W.; Dickens, S. H.; Eichmiller, F. C.; Bowman, C. N. *Journal of Materials Science-Materials in Medicine* **2004,** *15,* 1097-1103.

(50) Cramer, N. B.; Couch, C. L.; Schreck, K. M.; Boulden, J. E.; Wydra, R.; Stansbury, J. W.; Bowman, C. N. *Dent Mater* **2010,** *26,* 799-806.

(51) Jacobine, A. F. *Radiation Curing in Polymer Science and Technology*; Elesvier Applied Science, London, 1993; Vol. 3, p 219-268.

(52) Zhu, S.; Tian, Y.; Hamielec, A. E.; Eaton, D. R. *Macromolecules* **1990,** *23,* 1144-1150.

(53) Berchtold, K. A.; Hacioglu, B.; Nie, J.; Cramer, N. B.; Stansbury, J. W.; Bowman, C. N. *Macromolecules* **2009,** *42,* 2433-2437.

(54) Cramer, N. B.; Stansbury, J. W.; Bowman, C. N. *J Dent Res* **2011,** *90,* 402-416.

(55) Ye, S.; Cramer, N. B.; Bowman, C. N. *Macromolecules* **2011,** *44,* 490-494.

(56) Peutzfeldt, A. *European Journal of Oral Sciences* **1997,** *105,* 97-116.

(57) Burke, F. J. T.; Cheung, S. W.; Mjor, I. A.; Wilson, N. H. F. *Quintessence International* **1999,** *30,* 234-242.

(58) Adzima, B. J.; Aguirre, H. A.; Kloxin, C. J.; Scott, T. F.; Bowman, C. N. *Macromolecules* **2008,** *41,* 9112-9117.

(59) Stansbury, J. W. *Polymers of Biological and Biomedical Significance* **1994,** *540,* 171-183.

(60) Yoffe, A. D. *Advances in Physics* **2001,** *50,* 1-208.

(61) Stansbury, J. W.; Bowman, C. N.; Newman, S. M. *Physics Today* **2008,** *61,* 82-83.

(62) Park, H. Y.; Kloxin, C. J.; Scott, T. F.; Bowman, C. N. *Macromelecules* **2010,** *43,* 10188-10190.

(63) Kloxin, C. J.; Scott, T. F.; Bowman, C. N. *Macromolecules* **2009,** *42,* 2551-2556.

(64) Dolman, S. J.; Hultzsch, K. C.; Pezet, F.; Teng, X.; Hoveyda, A. H.; Schrock, R. R. *J Am Chem Soc* **2004,** *126,* 10945-10953.

(65) Sanda, F.; Takata, T.; Endo, T. *Macromolecules* **1994,** *27,* 3986-3991.

(66) Pavlovic, D.; Linhardt, J. G.; Kunzler, J. F.; Shipp, D. A. *J Polym Sci Pol Chem* **2008,** *46,* 7033-7048.

(67) Chan, J. W.; Shin, J.; Hoyle, C. E.; Bowman, C. N.; Lowe, A. B. *Macromolecules* **2010,** *43,* 4937-4942.

(68) Cook, W. D. *Polymer* **1992,** *33,* 2152-2161.

(69) Lee, T. Y.; Carioscia, J.; Smith, Z.; Bowman, C. N. *Macromolecules* **2007,** *40,* 1473-1479.

(70) Lee, T. Y.; Smith, Z.; Reddy, S. K.; Cramer, N. B.; Bowman, C. N. *Macromolecules* **2007,** *40,* 1466-1472.

(71) Carioscia, J. A.; Lu, H.; Stanbury, J. W.; Bowman, C. N. *Dent Mater* **2005,** *21,* 1137-1143.

(72) Boulden, J. E.; Cramer, N. B.; Schreck, K. M.; Couch, C. L.; Bracho-Troconis, C.; Stansbury, J. W.; Bowman, C. N. *Dent Mater* **2011,** *27,* 267-272.

(73) Carioscia, J. A.; Schneidewind, L.; O'Brien, C.; Ely, R.; Feeser, C.; Cramer, N.; Bowman, C. N. *J Polym Sci Pol Chem* **2007,** *45,* 5686-5696.

(74) Szmant, H. H.; Mata, A. J.; Namis, A. J.; Panthananickal, A. M. *Tetrahedron* **1976,** *32,* 2665-2680.

(75) Lowe, A. B.; Hoyle, C. E.; Bowman, C. N. *Journal of Materials Chemistry* **2010,** *20,* 4745-4750.

(76) Fairbanks, B. D.; Scott, T. F.; Kloxin, C. J.; Anseth, K. S.; Bowman, C. N. *Macromolecules* **2009,** *42,* 211-217.

(77) Bowman, C. N.; Kloxin, C. J. *Aiche Journal* **2008,** *54,* 2775-2795.

(78) Sanda, F.; Takata, T.; Endo, T. *Macromolecules* **1994,** *27,* 1099-1111.

Appendix

NMR (Nuclear magnetic resonance) of synthesized monomers

1. 2-methylene-propane-1,3-di(thioethyl vinyl ether) (MDTVE)

^{1}H NMR (500 MHz, CDCl3, δ): 6.45 (dd, *J*) 6.8, 14.3, 2H), 5.04 (s, 2H), 4.19 (dd, *J*) 2.2, 14.3, 2H), 4.03 (dd, *J*) 2.2, 6.8, 2H), 3.83 (t, *J*) 6.7, 4H), 3.35 (s, 4H), 2.69 (t, *J*) 6.7, 4H)

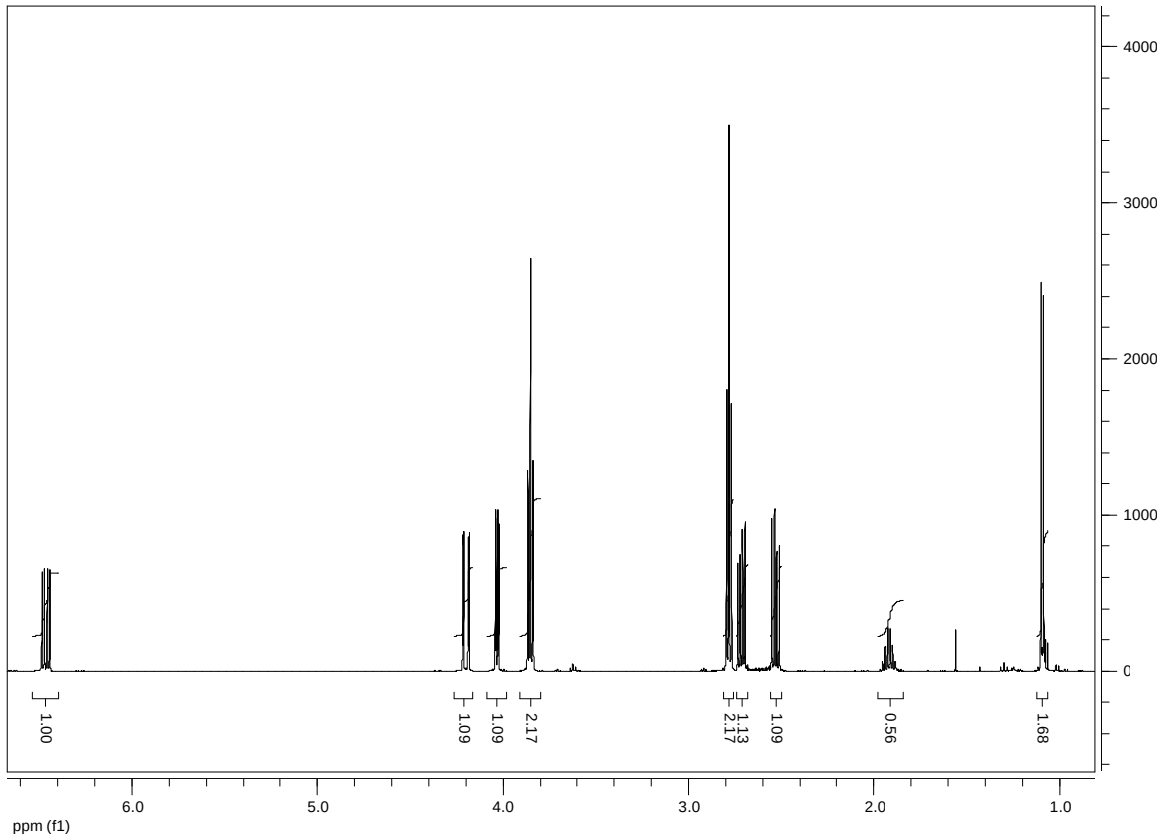

2. 2-methyl-propane-1,3-di(thioethyl vinyl ether) (MeDTVE)

^{1}H NMR (500 MHz, CDCl3, δ): 6.46 (dd, *J*) 6.8, 14.4, 2H), 4.19 (dd, *J*) 2.2, 14.3, 2H), 4.03 (dd, *J*) 2.2, 6.8, 2H), 3.85 (t, *J*) 6.7, 4H), 2.77 (t, *J*) 6.7, 4H), 2.62 (ddd, *J*) 6.5, 12.8, 92.4, 4H), 2.00-1.86 (m, 1H). 1.09 (d, *J*) 6.7, 3H)

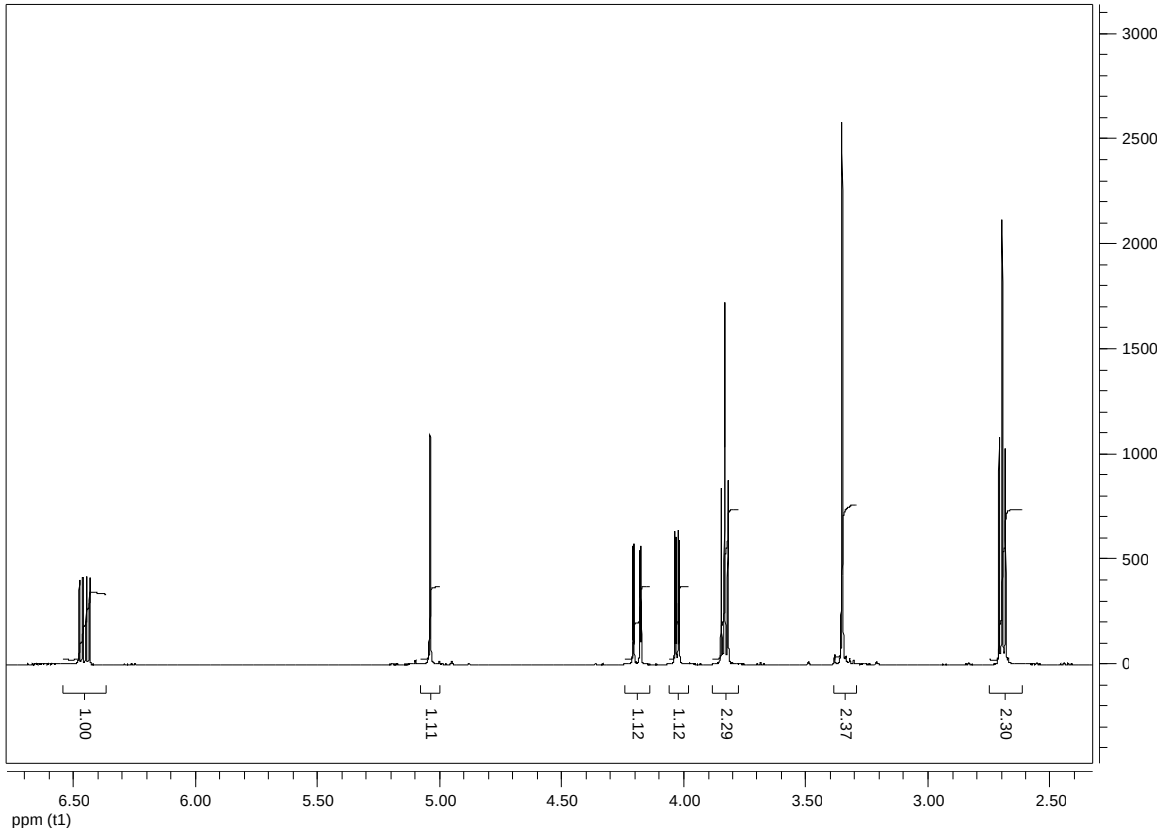

3. 2-methylene-propane-1,3-di(thiobut-1-yne) (MDTBY or DYAS)

^{1}H NMR (CDCl3) δ: 5.03 (s, 2H), 3.35 (s, 4H), 2.62-2.59 (t, 4H), 2.48-2.46 (t, 4H), 2.04-2.03 (t, 2H)

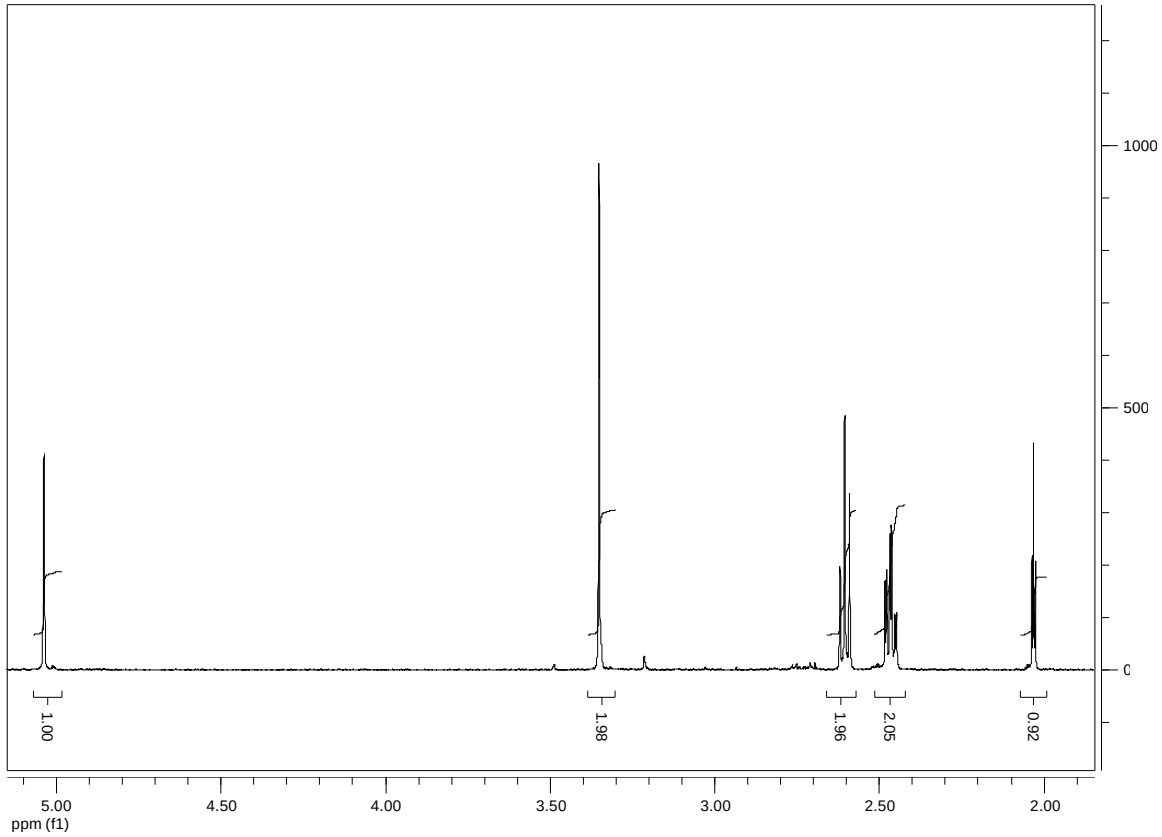

4. 2-methyl-propane-1,3-di(thiobut-1-yne) (MeDTBY or DYPS)

^{1}H NMR (CDCl3) δ: 2.72-2.68 (m, 6H), 2.54-2.47 (m, 6H), 2.05-2.04 (t, 2H), 1.95-1.88 (m, 1H), 1.09-1.08 (d, 3H)

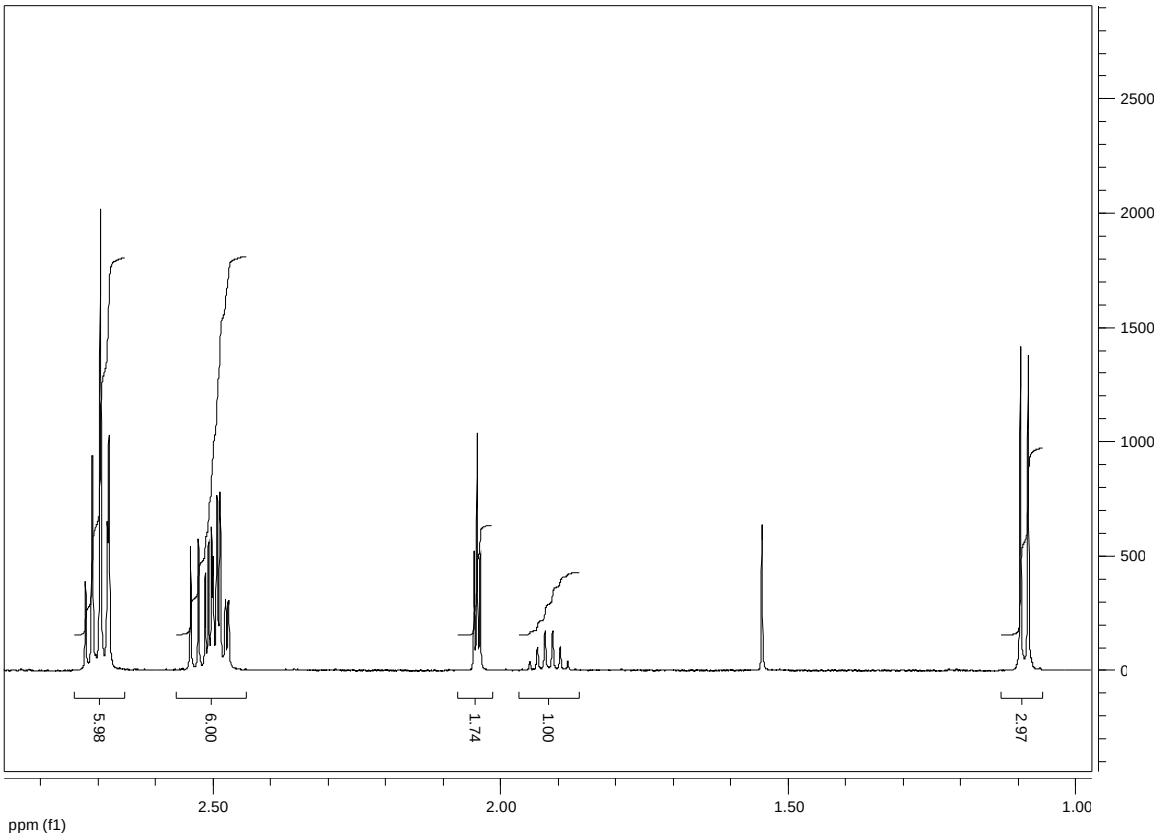

5. 1,9-bis[2-(methacryloyloxyethyl) succinyloxy]-3,7-dithia-5-methylene-nonane (SAS, Succinate Allyl Sulfide)

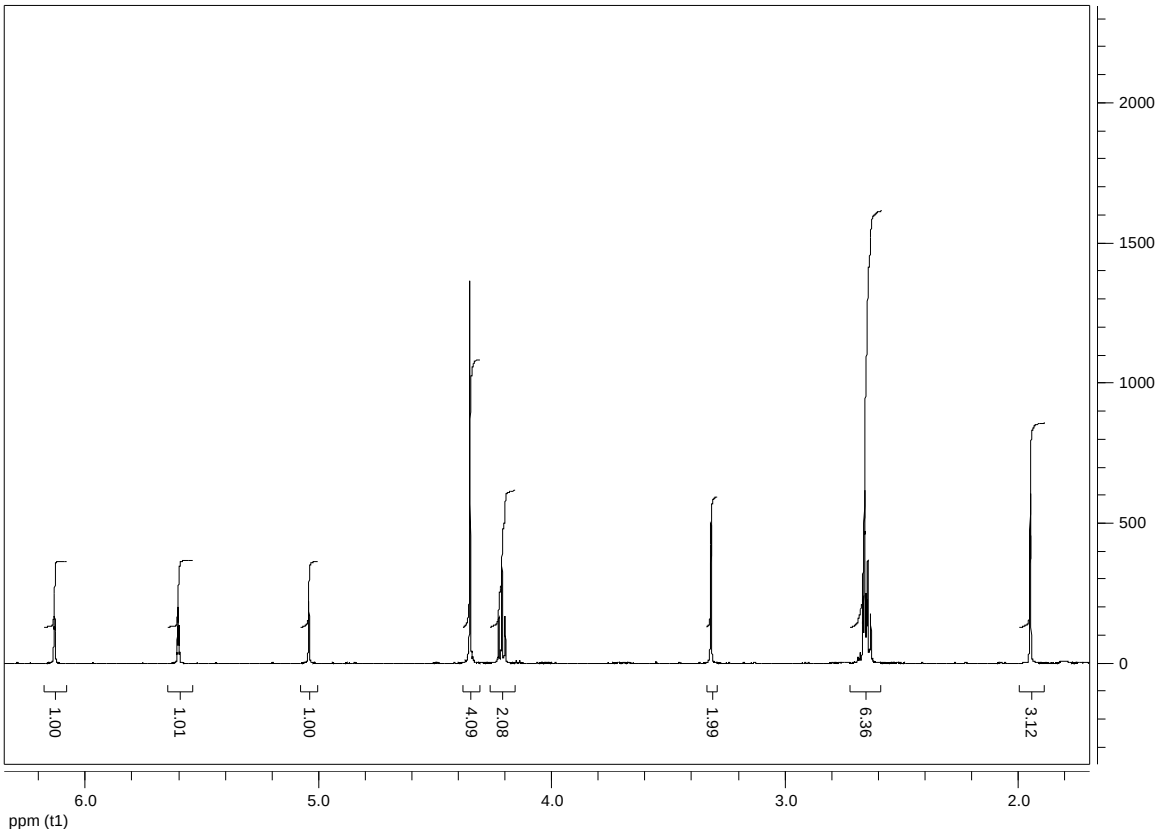

6. 2-(methacryloyloxyethyl) 7-methylene-1,5-dithiocan-3-yl phthalate (PAS, Phthalate Allyl Sulfide)

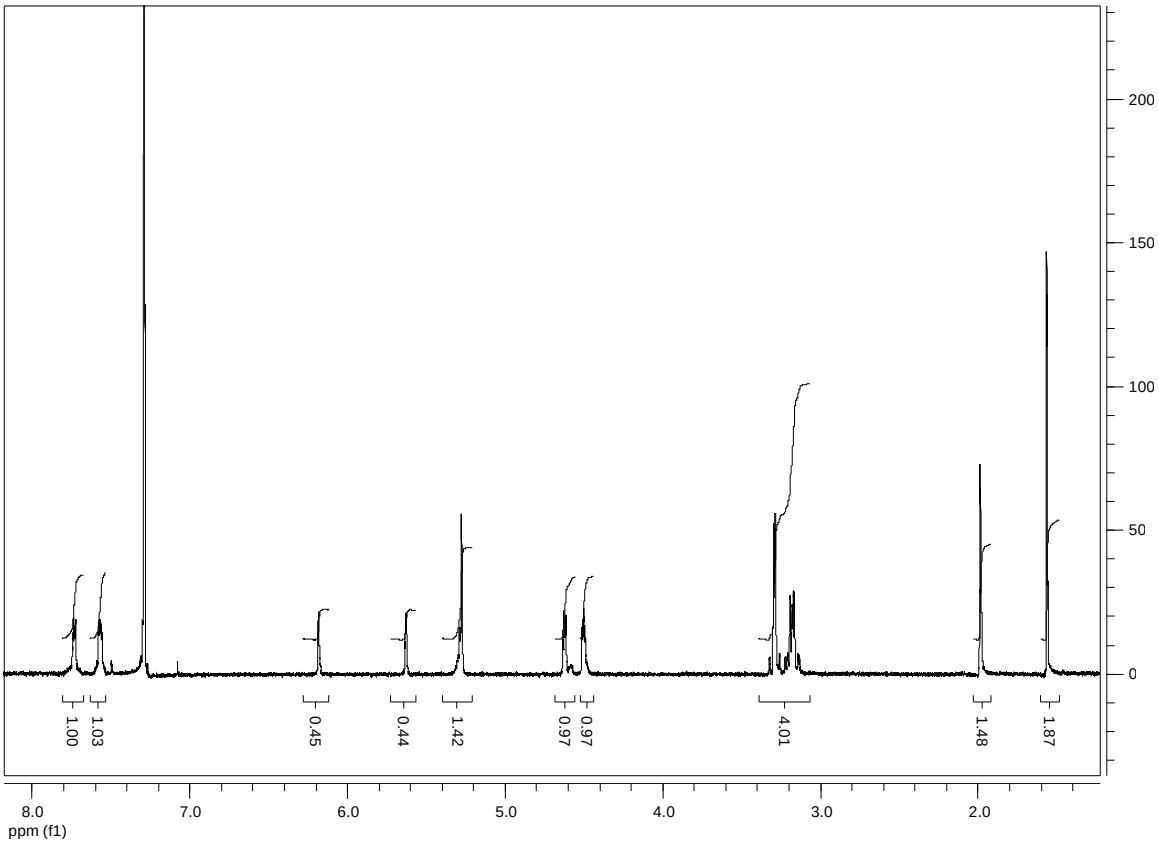

7. 1,9-bis[2-(methacryloyloxyethyl) succinyloxy]-3,7-dithia-5-methyl-nonane (SPS, Succinate Propyl Sulfide)

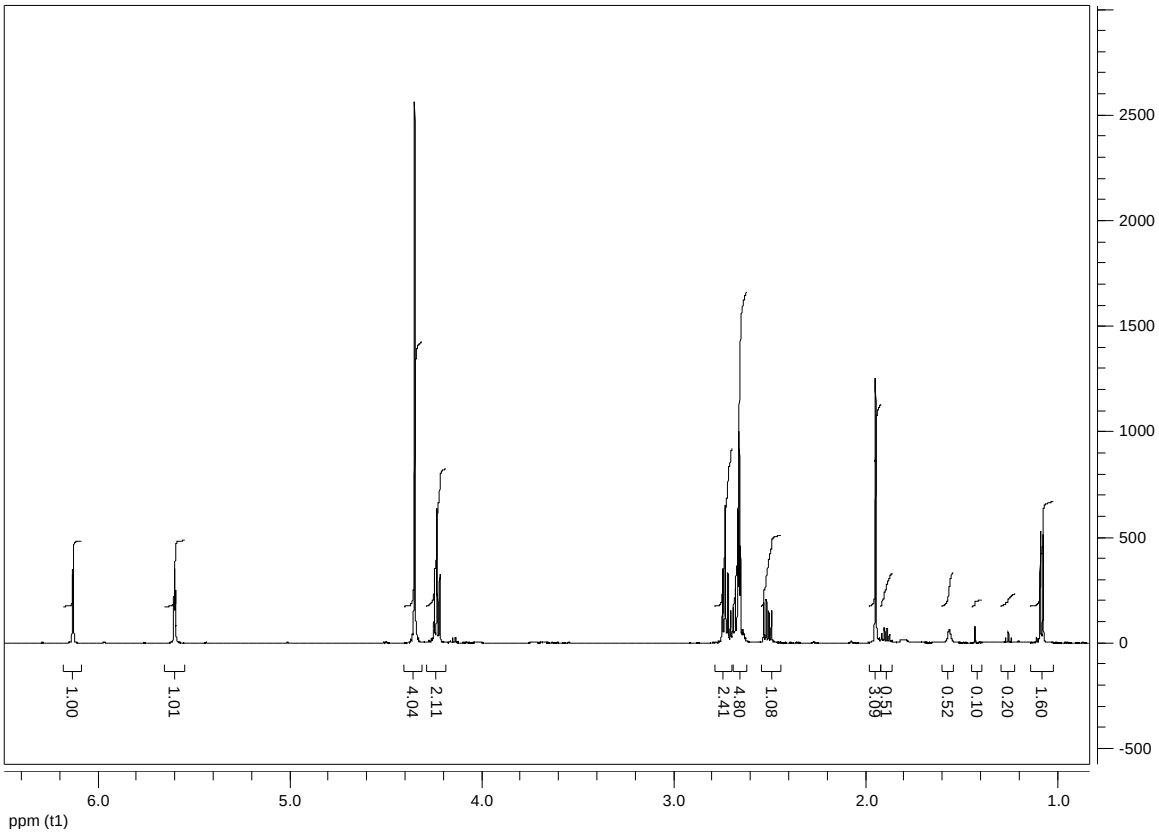

8. 2-(methacryloyloxyethyl) 7-methyl-1,5-dithiocan-3-yl phthalate (PES, Phthalate Ethyl Sulfide)

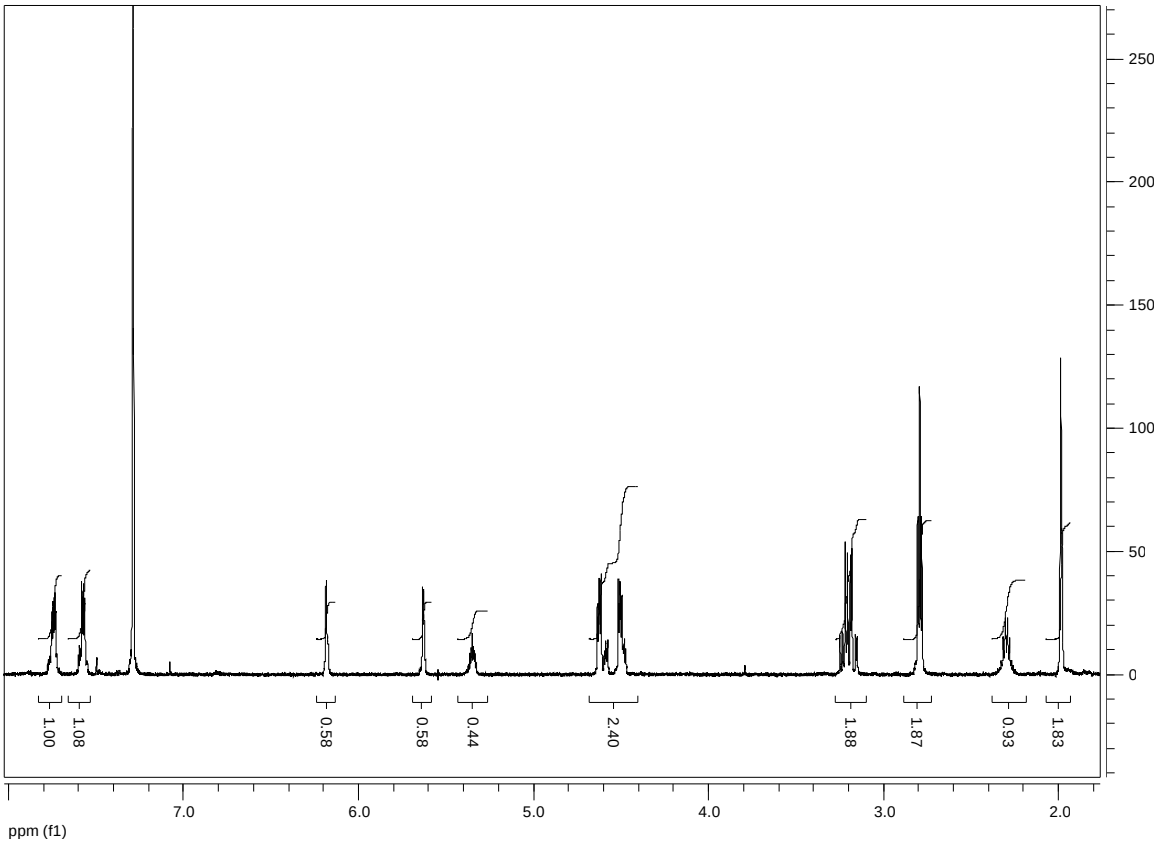

9. 2-Methylene-propane-1,3-di(norbornene sulfide) (NAS)

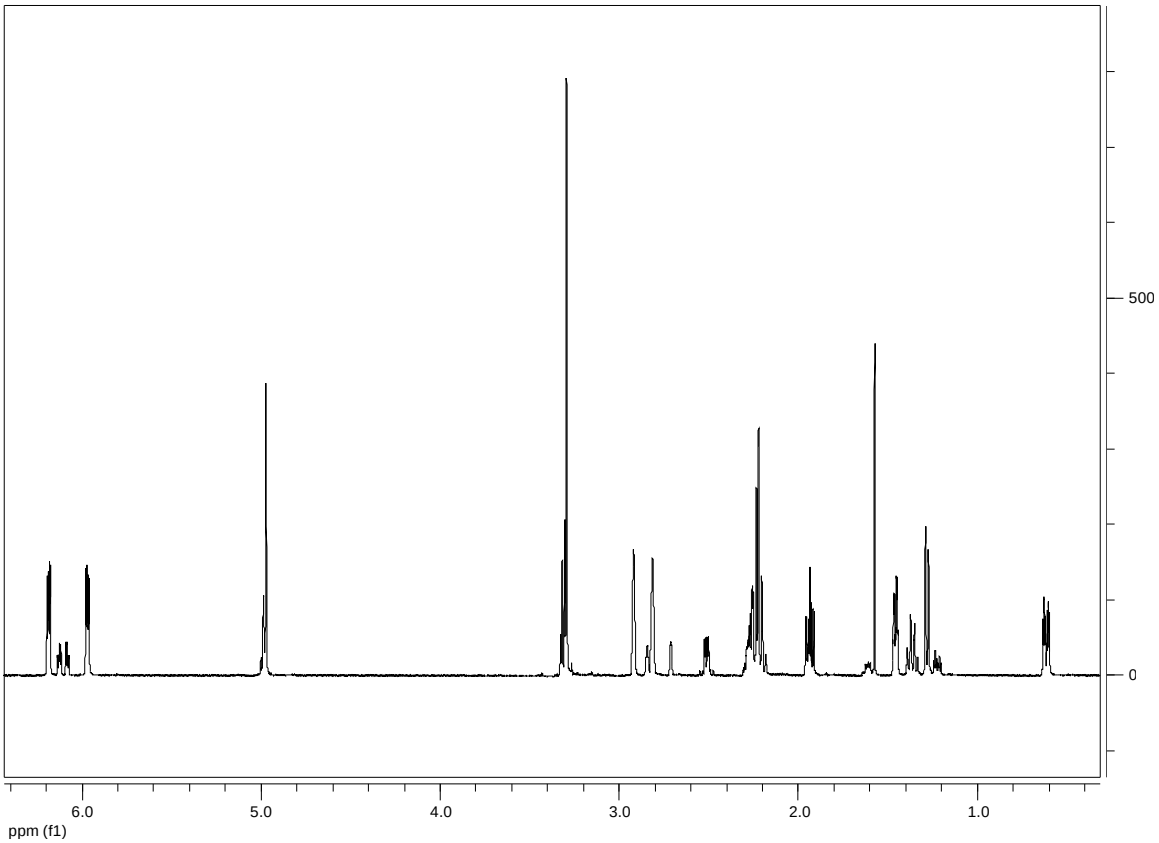

10. 2-Methyl-propane-1,3-di(norbornene sulfide) (NPS)

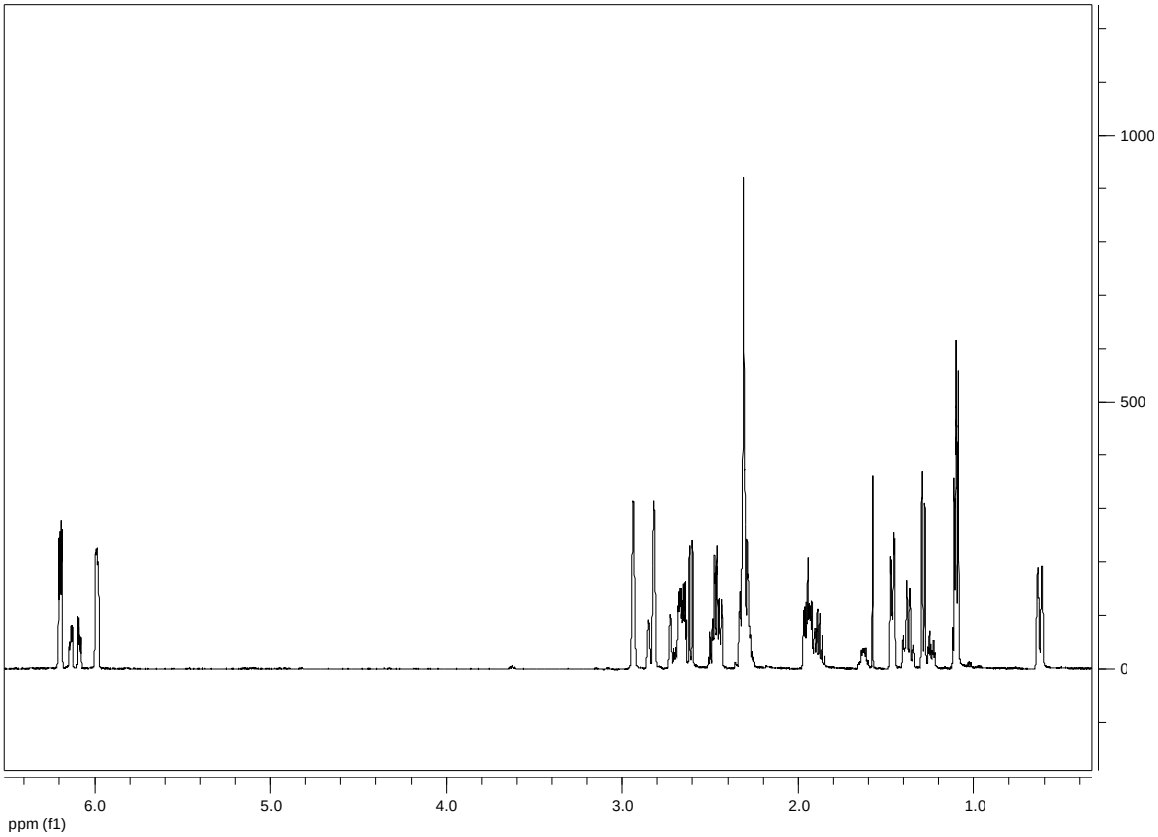

11. Ge-based photoinitiator (Dibenzoyl diethyl germane)

^{1}H NMR (CDCl3): δ (ppm): 7.73 (d, 4H, *J*) 6.64, Ar-H2,6,2′,6′), 7.39–7.51 (m, 8H, Ar-H3,3′,4,4′,5,5′), 1.50 (q, 4H, *J*) 7.89, -Ge-CH2-), 1.11 (t, 6H, *J*) 7.79, -Ge-CH2-*CH*3)

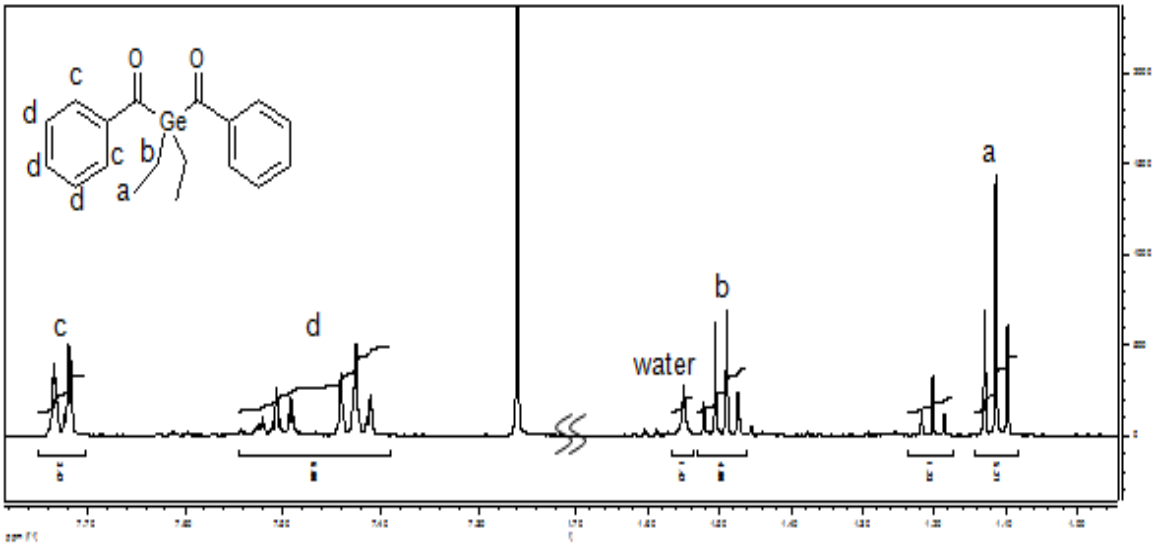

12. S,S'-bis[α,α'-dimethyl-α"-(acetyloxy)ethyl 2-methyl-2-propenoate]-trithiocarbonate (TTCDMA, Trithio carbonate dimethacrylate)

^{1}H NMR (CDCl3) δ: 6.17-6.07 (m, 2H), 5.62-5.54 (m, 2H), 4.33 (s, 8H), 1.97-1.90 (m, 6H), 1.64 (s,12H)